Developing remotely sensed indices for biodiversity studies across the conterminous US

By

Elena Razenkova

A dissertation submitted in partial fulfillment of the

requirements for the degree of

Doctor of Philosophy

(Forestry)

at the

UNIVERSITY OF WISCONSIN – MADISON

2023

Date of final oral examination: 05/04/2023

The dissertation is approved by the following members of the Final Oral Committee:

Volker C. Radeloff, Professor, Forest and Wildlife Ecology

Anna M. Pidgeon, Professor, Forest and Wildlife Ecology

Anthony Ives, Professor, Department of Integrative Biology

Benjamin Zuckerberg, Assistant Professor, Forest and Wildlife Ecology

Patrick Hostert, Professor, Department of Geography, Humboldt University, Berlin

Abstract

My dissertation focuses on developing remote sensing indices for understanding and monitoring biodiversity patterns at broad scales. Human activities cause major changes to the planet and greatly affect biodiversity. There is an urgent need for better assessments of the current status of biodiversity to understand and predict future changes, and to implement conservation actions that prevent or reduce biodiversity loss. However, monitoring biodiversity over large areas in the field is challenging. Remote sensing provides an opportunity to develop indices that are designed for biodiversity assessment, because satellite data are collected systematically across broad scales. Vegetation productivity patterns are important determinants of species richness and abundance. The Dynamic Habitat Indices (DHIs) derived from satellite data are three measures of annual vegetation productivity that have been specifically designed for biodiversity assessments. However, so far the DHIs have only been derived from coarse-resolution satellite imagery, which limits their value for management decisions. My goal was to develop the DHIs from medium spatial resolution Landsat data and evaluate the performance of the DHIs for modeling species richness and abundance across conterminous United States.

In my first chapter, I calculated the DHIs using 30-m Landsat and 250-m MODIS data and compared both datasets at three spatial extents. The main challenge in calculating the Landsat DHIs was low temporal resolution compared with MODIS. I also assessed where the Landsat DHIs provided advantages over MODIS DHIs in capturing spatial heterogeneity in vegetation productivity. Finally, I compared the Landsat DHIs calculated over different decades. Landsat and MODIS DHIs were highly correlated, indicating my approach in calculating Landsat DHIs worked well. The comparison Landsat DHIs for the 1990s and the 2010s showed strong changes.

In my second chapter, I evaluated the performance of the DHIs based on Landsat and MODIS in modeling species richness of overall species richness and twenty one bird guilds at four spatial extents. Overall, the predictive performance of DHIs based on Landsat and MODIS for the four spatial extents was very similar. However, Landsat DHI provided slightly higher predictive power in modeling some bird guilds including forest affiliates and specialists, grassland affiliates and specialists, and shrubland specialists. Landsat DHIs complemented topographic and land cover metrics in multivariate models.

In my third chapter, I tested the usefulness of the Landsat DHIs in modelling detection-corrected avian abundance for twenty bird species across Western United States. I found that models with the DHIs had lower AIC score than a null model, indicating that the DHIs captured important habitat characteristics for birds. Resident and migrant birds had stronger response to minimum and variation DHI. My results show the complexity of relationships between the DHIs and bird abundance that depend on species' life history and habitat preferences.

Acknowledgements

My PhD dissertation was made possible thanks to the many people who supported and helped me throughout my graduate school experience. First and foremost, I would like to express my gratitude to my academic supervisors, Drs. Volker Radeloff and Anna Pidgeon, for their guidance and support throughout the research process. Having Volker as remote sensing specialist and Anna as an ornithologist helped me to develop ideas and my research questions for this dissertation. Volker and Anna have always available for meetings, responsive, supportive, and inspiring. I am thankful to Volker for offering me research assistantship that supported this research.

I would also like to thank my committee members: Anthony Ives, Benjamin Zuckerberg, and Patrick Hostert for their expertise, great ideas, and insightful discussions. I especially appreciate Patrick's valuable comments on the manuscript, Benjamin's engaging classes, and Anthony's suggestions that shaped this research.

Thanks to both Volker and Anna for creating unique lab environment where I felt supported and valued member. I would like to extend my gratitude to all members of the SILVIS lab. I learned so much from you and enjoyed our time together on ski and canoe trips as well as our discussions during the weekly Google Earth Engine support group and lab lunches. Our trip to South Dakota for attending the Landsat science team meeting with Katarzyna Lewińska, He Yin, David Gudex-Cross, and Volker Radeloff was one of the interesting time. The last AGU meeting in Chicago was the best conference in my life because of our wonderful lab community. I am grateful to David Helmers, He Yin, Katarzyna Lewińska, Laura Farwell, Johanna Buchner,

Ashley Olah, Maia Persche, Evgenia Bragina, Afag Rizayeva, Natasha Rogova, and Eduarda Silviera for becoming my true friends and support group.

During my years as a graduate student, I had great opportunities to take unique seminars including Neotropical Birds seminar with Christian Estades, Land Abandonment with He Yin, Remote Sensing of Habitat with Laura Farwell, and wildlife seminar about Aldo Leopold with Curt Meine and Stanley Temple. I also had a great time playing basketball with folks from Pauli's, Peery's, Zuckerberg, and SILVIS labs. My heartfelt thanks to Evan Wilson and Yura Petrunenko for organizing our basketball games.

Most importantly, I want to acknowledge my family for their support. A special thanks to my husband Ilya Razenkov, and daughters, Katya and Julia. You are my constant motivation. I would love to thank my dear mother Lubov Zhalnina and sister Natalia Miroshnik for their daily prayers and faith in me.

Table of Contents

List of Figures

List of Tables

List of Appendices

Introductory

Biodiversity is declining globally, due to many threats including habitat loss from human activities, which modify ecosystems through land cover and land use change (Pimm et al. 2014, Ceballos et al. 2015). Conservation of biodiversity is critically important for the resilience and resistance of ecosystems to environmental change (Chapin et al. 2000). Moreover, biodiversity loss raises serious concerns about the services that humans receive from ecosystems (Sekercioglu 2006). Thus, there is an urgent need for accurate assessments of the current status of biodiversity to better understand key factors shaping large-scale biodiversity patterns and predict how species respond to environmental changes. Such assessments can allow timely implementation of conservation actions to prevent biodiversity loss. However, to obtain a spatially detailed map of species richness directly is difficult making remote sensing a valuable tool for biodiversity assessment (Nagendra 2001, Turner et al. 2003).

Satellite data can be used to characterize suitable habitat for each species, and predict species distributions (Nagendra 2001). Remotely sensed vegetation productivity is a key factors shaping species richness and abundance patterns (Myneni et al. 1995, Cohen and Goward 2004, Pettorelli et al. 2011). The challenge is to capture vegetation productivity patterns at the temporal and spatial scales that are most relevant for species. There is a trade-off between spatial and temporal resolution of satellite data. On the one hand, satellites with coarse spatial resolution have more observations over time, providing better estimations of annual vegetation productivity, but larger pixels can be too coarse for ecological studies and management applications. On the other hand, imagery with higher spatial resolution can provide more detailed information about spatial patterns of productivity, but temporal resolution is lower, especially for

historical data, which means that disturbances that affect biodiversity may be missed (Roxburgh et al. 2004, Ciais et al. 2005, Bigler et al. 2006).

The Dynamic Habitat Indices are remotely sensed estimates that summarize three aspects of annual vegetation productivity a) the cumulative productivity throughout the year, b) the minimum productivity, and c) the variation in productivity (Coops et al. 2008, Hobi et al. 2017, Radeloff et al. 2019). All three components of the DHIs are important for biodiversity because they are related to the available energy hypothesis (Wright 1983, Mittelbach et al. 2001, Hawkins et al. 2003, Bonn et al. 2004), the environmental stress hypothesis (Connell and Orias 1964, Currie et al. 2004), and the environmental stability hypothesis (Hurlbert and Haskell 2003, Williams and Middleton 2008), respectively (Radeloff et al. 2019). Indeed, numerous studies show that the DHIs derived form 1-km MODIS data are important predictors of species richness and of the abundance of individual species. For example, the DHIs effectively predict species richness for many taxa at national to global scales (Coops et al. 2009a, Zhang et al. 2016, Hobi et al. 2017, Radeloff et al. 2019), as well as abundance of mammals (Michaud et al. 2014, Razenkova et al. 2020, 2023). The DHIs were used in models of Andean condor habitat selection in Argentina and Chile (Perrig et al. 2020), of the geographic range of an enigmatic South American bamboo specialist, the Purple-winged Ground Dove (Lees et al. 2021), and of the distribution of bird species in California (Burns et al. 2020). For many of the species that have been modeled, 1-km DHIs are rather coarse though because the species are affected by habitat features at finer scales. Moreover, effective management applications often require maps with higher spatial resolution.

My overarching goal for the dissertation was to develop the Dynamic Habitat Indices (DHIs) with medium spatial resolution and to evaluate them in explaining avian species richness

and abundance across the conterminous United States. My study area is the 48 conterminous states of the USA (7.6 million km^2). This large area is suitable for my research questions because it includes a large range of ecoregions, climatic zones, and topography, resulting in large number of habitats and a wide range of the DHIs values. Moreover, two excellent datasets are available for bird richness and bird abundance for the conterminous United States and Western United States, respectively.

Chapter 1 Summary

Question 1: How well do the Dynamic Habitat Indices calculated from 30-m Landsat data capture the pattern of vegetation productivity over the conterminous United States compared with 250-m MODIS DHIs?

Biodiversity science requires effective tools to monitor patterns of species diversity at multiple temporal and spatial scales. Remote sensing provides measurements of key habitat factors, such as vegetation productivity that shape broad-scale patterns of biodiversity (Mittelbach et al. 2001, Hawkins et al. 2003, Bailey et al. 2004). However, a challenge is to capture vegetation productivity patterns at the temporal and spatial scales that are most relevant for species.

My goal was to develop the DHIs based on 30-m resolution Landsat data and compare them to 250-m resolution MODIS DHIs across the conterminous US. My objectives were to 1) develop and compare composite DHIs based on Landsat and MODIS imagery for five (2016-2020), ten (2011-2020), and twenty (2001-2020) years at three spatial extents, 2) evaluate how Landsat DHIs capture heterogeneity within MODIS pixels, and 3) assess changes in Landsat DHIs from 1990s to 2010s.

I calculated the DHIs based on either Landsat and MODIS for three time periods: for five (2016-2020), ten (2011-2020), or 20 years (2001-2020), and, in addition, I calculated the Landsat DHIs over ten years (1991-2000).

To compare the DHIs derived from Landsat and MODIS data, I ran Spearman correlation analysis at three spatial scales: 1) 85 Level III ecoregions, 2) 967 Level IV ecoregions, and 3) within the extent of each MODIS pixel. I found that patterns of DHIs based on Landsat and MODIS were generally similar, but Landsat DHIs captured more detailed information about landscapes. The main difference in spatial patterns between Landsat and MODIS occurred in forested areas and mountains. The Spearman correlation coefficients between the three DHIs for both datasets across the three periods and within Level III and Level IV ecoregions were high, indicating that Landsat DHIs were in good agreement with MODIS DHIs. My results show that Landsat DHIs captured unique information about landscapes compared with topographic and fragmentation metrics. When comparing Landsat DHIs from 1990s and 2010s, I found an increase in the cumulative DHI in the West Coast, in most of the mountain ranges, and in parts of the South and a decrease in Midwest and New England.

In summary, my results show that Landsat data are suitable for generating novel satellite data products designed for biodiversity applications. The newly developed DHIs based on Landsat have great potential for biodiversity monitoring at regional and local scales. The Landsat DHIs can help to advance our understanding of the importance of vegetation productivity in shaping patterns of species richness, abundances, and distribution of individual species.

Resulting paper (in review): Elena Razenkova, Katarzyna E. Lewińska, He Yin, Laura S. Farwell, Anna M. Pidgeon, Patrick Hostert, Nicholas C. Coops, and Volker C. Radeloff.

Medium-resolution Dynamic Habitat Indices from Landsat satellite imagery. *Remote Sensing of Environment*.

Chapter 2 Summary

Question 2: Do the Dynamic Habitat Indices calculated from 30-m Landsat and 250-m MODIS data provide comparable predictive power in models of bird richness across four spatial extents?

Biodiversity is declining due to many threats from human activities resulting in habitat loss, and climate change (Rockström et al. 2009, Butchart et al. 2010). It is important to understand the drivers of species richness patterns, to predict how species will respond to environment changes and ultimately design conservation actions that can prevent potential loss. Satellite data provide meaningful information about the biophysical characteristics of ecosystems (Turner et al. 2003, Cavender-Bares et al. 2022) and are suitable for monitoring biodiversity patterns at broad scales (Wright 1983, Gaston 2000, Mittelbach et al. 2001, Hawkins et al. 2003a, 2003b, Bonn et al. 2004). The DHIs calculated from 1-km MODIS data were successfully used in numerous studies (Coops et al. 2009b, Hobi et al. 2017, Radeloff et al. 2019). However, MODIS DHIs can be too coarse for some species. A key question is how much predictive power satellite data with medium spatial resolution can add to models compared with available coarse resolution data, knowing that the temporal resolution of medium spatial resolution satellite imagery is much lower.

My goal was to evaluate the predictive performance of the DHIs based on 30-m Landsat and 250-m MODIS in bird richness models. My objectives were: 1) compare the predictive performance the DHIs based on Landsat and MODIS in models of bird richness for four spatial extents and over heterogeneous landscapes, 2) evaluate the relative importance of Landsat DHIs

and other environmental predictors in bird richness models, and 3) test the Landsat DHIs calculated for 1991-2000 in model of species richness.

I expected that Landsat DHIs and MODIS provide similar predictive power, and that the Landsat DHIs outperform the MODIS DHIs in models of at least some bird guild and over heterogeneous landscapes. I expected there was no difference in predictive power of both DHIs for grassland species.

I conducted a linear regression analysis to examine the relationships between the DHIs and species richness. Building upon my first chapter, I used the DHIs derived from 30-m Landsat and 250-m MODIS data as predictors for species richness and summarized both datasets at four spatial extents that matched the four sets of bird data. I analyzed bird species richness of all bird species and of 19 functional bird guilds. In multivariate models combining Landsat DHIs with topography and land cover, I evaluated the relative importance of the Landsat DHIs.

My results show that Landsat and MODIS DHIs provided similar predictive power to most bird guilds for all four spatial extents. However, Landsat DHIs provided higher predictive power in models for overall species richness, forest affiliates and specialists, grassland affiliates, shrubland affiliates and specialists, and species with small body sizes. Similarly, in heterogeneous landscapes Landsat DHIs provided higher predictive power than MODIS DHIs. In multivariate models, Landsat DHIs complemented topographic and land-cover metrics and had a strong effect on species richness for most bird guilds. There was no substantial difference in performance of Landsat DHIs from the 1990s and the 2010s in models of species richness at any extents.

In summary, my results show that Landsat DHIs provided high predictive power in models of species richness. The relationship between the DHIs and species richness provide better understanding of importance of the higher resolution of the DHIs for predicting species richness.

Resulting paper (submitted): Elena Razenkova, Kathleen A. Carroll, Laura S. Farwell, Paul R. Elsen, Anna M. Pidgeon, Volker C. Radeloff. Explaining bird richness with the Dynamic Habitat Indices across the conterminous US. *Ecological Applications*.

Chapter 3 Summary

Question 3: Can the Dynamic Habitat Indices calculated based on 30-m Landsat predict bird abundances across the Western United States?

According to the North American Bird Conservation Initiative (NABCI), 37% of all bird species in North America are mostly at risk of extinction (NABCI 2016, Rosenberg et al. 2019). The global biodiversity crisis is fundamentally a problem of declining abundances of individual species. Thus there is an urgent need to identify factors that determine pattern of bird abundance over broad scales in order to inform effective conservation decisions. The DHIs were specifically developed for monitoring species richness, but may also provide valuable information when modeling individual species' abundance patterns. The More Individuals Hypothesis (MIH) explains heterogeneous pattern of species richness (Evans et al. 2005, 2006, Storch et al. 2018), but this hypothesis can also be directly applied to explain species abundance. More productive areas that have high biodiversity can support a higher number of individuals, because of abundant food resources (Srivastava and Lawton 1998, Storch et al. 2018, Razenkova et al.

2023). At same time, the relationship between available energy and abundance may be stronger for rare species than for common species (Evans et al. 2005, 2006), because where there is more available energy the extinction probability may be reduced, especially for rare species (Evans et al. 2005, 2006).

The main goal of my third chapter was to evaluate the utility of the Landsat DHIs in explaining bird abundance across the Western United States (US). My first objectives were 1) test if bird abundance is higher in areas with higher vegetation productivity, 2) compare the relationships between the DHIs and bird abundance for rare and common species, 3) assess whether bird groups based on migratory behavior exhibit different relationships to the DHIs.

I expected to find support for the MIH and to see higher numbers of individuals in more productive areas. I also expected that common species would show strong relationships with the DHIs, but rare species would have weaker relationships, because vegetation productivity is not the limiting factor for these species. Lastly, I expected that residents have a stronger relationship with minimum DHI, while long-distance migrants have a stronger relationship with variation DHI.

For bird data, I analyzed point count data obtained from the Integrated Monitoring in Bird Conservation Regions (IMBCR) Program for twenty bird species across the Western US. I used hierarchical distance-sampling abundance models to examine relationship between Landsat DHIs and avian abundance. I ran several possible abundance models for each species where Landsat DHIs from my first chapter were abundance covariates, and primary habitat, start time, and year were detection covariates, and calculated the AIC score.

I found that the DHIs were significant abundance covariates for 17 species, but the abundance was positively associated with higher productivity for five species. Contrary to my

predictions, I found that abundance of rare bird species had a stronger relationship with the DHIs than common species. Residents and long-distance migrants showed stronger associations with minimum DHI and variation DHI, while short distance migrants showed stronger relationships with cumulative DHI.

In conclusion, all three components of the DHIs captured important habitat characteristics for individual bird species and can be used in modeling avian abundance. Although my finding provided generally only weak support of MIH, I did find a strong relationship with vegetation productivity for rare species. My results highlight the complexity of relationships between the DHIs and bird abundance, which depend on life history and habitat preferences of the species.

Resulting paper (not submitted): Elena Razenkova, Maia E. Persche, Anna M. Pidgeon, Volker C. Radeloff. Explaining bird abundance with the Dynamic Habitat Indices across Western United States. *Journal of Applied Ecology*.

Significance

Identifying the factors driving species richness and abundance patterns across broad scales is crucial to understand the mechanisms influencing these patterns, and predict how species may respond to changing conditions. In order to safeguard biodiversity, better assessments of the current status of biodiversity are needed. However, biodiversity patterns are very complex, many factors matter for different regions and for different species. My research provide a better understanding of the relationship between vegetation productivity, avian species

richness and abundance of individual species across conterminous United States. My work contributes to science and conservation in three main ways.

Scientific contribution

My work contributes to avian **ecology** by improving the understanding of the factors shaping broad-scale patterns of species richness and abundance of individual species. While biodiversity patterns have been studied extensively, in most cases researchers used data that are either coarse or analyzed only limited geographical extents. My work was possible due to advancements in cloud computing technologies and open access to the full Landsat archive, which provide a great opportunity to generate novel products for biodiversity assessments (Kennedy et al. 2014, Wulder et al. 2019). My dissertation fill a gap by showing that satellite data with medium spatial resolution are suitable for calculating the Dynamic Habitat Indices for large areas. The DHIs capture patterns of vegetation productivity and reflect important habitat features. My research shows that Landsat DHIs are strong predictors for species richness and abundance.

In *chapter 1*, the comparison between Landsat and MODIS DHIs provides better understanding in which areas the increased spatial resolution afforded by Landsat was most important. In *chapter 2*, the relationship between the DHIs derived from medium (30-m) and coarse (250-m) spatial resolution satellite data and species richness provide deeper understating whether DHIs with medium resolution provide more advantages over DHIs with coarse resolution for which bird guilds and at what extents. I found that Landsat DHIs are strong predictors of bird richness, especially of those bird guilds that depend more on heterogeneous landscapes. The results of this chapter indicate that Landsat DHIs complement topographic and

land cover metrics and provide better understanding of the relative importance of these factors in shaping the patterns of species richness.

In chapter 3, my analyses of the relationship between Landsat DHIs and bird abundance increases knowledge how individual species respond to three DHIs. Results of this chapter highlight the complexity of the relationships between the DHIs and bird abundance of individual species indicating that the life history and habitat preferences of species play major roles in habitat selection. Importantly, the Landsat DHIs are effective to model abundance of rare species.

Methodological contribution

The main **methodological** contribution of this research is the development the Dynamic Habitat Indices based on 30-m Landsat data and testing in modeling avian species richness and abundance. The DHIs calculation became possible due to a cloud-based processing platform, Google Earth Engine (GEE), which allow to process satellite data over large areas and over long period of time effectively. My results show that satellite data with medium resolution are suitable to calculate composite DHIs both for recent years and even for historical times by incorporating several years of data (five years minimum) and filling data gaps with linear interpolation. My method is very promising for the calculation of Landsat DHIs and for further analysis of long-term changes in the DHIs, especially considering that my comparison between the Landsat DHIs for the 1990s and 2010s showed substantial changes. My GEE scripts to calculate the DHIs based on Landsat or MODIS are easily reproducible for other locations and can be calculated over different periods.

In *chapter 3*, I was the first to use Landsat DHIs in hierarchical distance-sampling abundance models for twenty bird with different IUCN statuses and population trends, migratory strategies, and habitat preferences across the Western United States. The DHIs can be valuable tool to capture habitat quality and foraging conditions that attract birds.

Conservation contribution

There is an urgent need for better assessment of current status of biodiversity to understand and predict future changes, and to implement conservation actions mitigating biodiversity loss. This dissertation contributes to **management and conservation science** by adding deeper understanding relationship between vegetation productivity and avian species richness and abundance.

First, I calculated the DHIs using Landsat data that are much higher resolution than available course-resolution MODIS DHIs. Landsat DHIs have great potential to quantify important characteristics of suitable habitat for many species and would be more relevant for fine-scale ecological studies and local management decisions. Second, 30-m resolution DHIs match the resolution of animal movement data, making Landsat data more suitable when assessing connectivity among habitat patches or movement corridors. Third, Landsat DHIs capture spatial heterogeneity much better than MODIS, and therefore are better for analyses in heterogeneous landscapes. My *chapters 2 and 3* provide examples how and where the Landsat DHIs can be used. The results of these chapters show that Landsat DHIs are useful for monitoring species richness and abundance patterns at broad scales. More specifically, Landsat DHIs predict species richness of all bird species and of 19 functional bird guilds well and provide higher predictive power for models over heterogeneous landscapes. In *chapter 3*,

incorporating knowledge of the relationship between Landsat DHIs and bird abundance helps to predict absolute abundances, suggesting that conservation managers can be used the DHIs as a tool for monitoring abundance for common and rare species.

References:

Bailey, S. A., M. C. Horner-Devine, G. Luck, L. A. Moore, K. M. Carney, S. Anderson, C. Betrus, and E. Fleishman. 2004. Primary productivity and species richness: Relationships among functional guilds, residency groups and vagility classes at multiple spatial scales. Ecography 27:207–217.

Bigler, C., O. U. Bräker, H. Bugmann, M. Dobbertin, and A. Rigling. 2006. Drought as an inciting mortality factor in scots pine stands of the Valais, Switzerland. Ecosystems 9:330–343.

Blakesley, J. A., and J. M. Timmer. 2019. Bird Conservancy of the Rockies available support for USFWS wildlife refuges participating in the Integrated Monitoring in Bird Conservation Regions (IMBCR) landbird monitoring program.

Bonn, A., D. Storch, and K. J. Gaston. 2004. Structure of the species-energy relationship. Proceedings of the Royal Society B: Biological Sciences 271:1685–1691.

Burns, P., M. Clark, L. Salas, S. Hancock, D. Leland, P. Jantz, R. Dubayah, and S. J. Goetz. 2020. Incorporating canopy structure from simulated GEDI lidar into bird species distribution models. Environmental Research Letters 15.

Butchart, S. H. M., M. Walpole, B. Collen, A. van Strien, J. P. W. Scharlemann, R. E. A. Almond, J. E. M. Baillie, B. Bomhard, C. Brown, J. Bruno, K. E. Carpenter, G. M. Carr, J. Chanson, A. M. Chenery, J. Csirke, N. C. Davidson, F. Dentener, M. Foster, A. Galli, J. N. Galloway, P. Genovesi, R. D. Gregory, M. Hockings, V. Kapos, J. F. Lamarque, F. Leverington, J. Loh, M. A. McGeoch, L. McRae, A. Minasyan, M. H. Morcillo, T. E. E. Oldfield, D. Pauly, S. Quader, C. Revenga, J. R. Sauer, B. Skolnik, D. Spear, D. Stanwell-Smith, S. N. Stuart, A. Symes, M. Tierney, T. D. Tyrrell, J. C. Vie, and R. Watson. 2010.

Global Biodiversity: Indicators of Recent Declines. Science 328:1164–1168.

Cavender-Bares, J., F. D. Schneider, M. J. Santos, A. Armstrong, A. Carnaval, K. M. Dahlin, L. Fatoyinbo, G. C. Hurtt, D. Schimel, P. A. Townsend, S. L. Ustin, Z. Wang, and A. M. Wilson. 2022. Integrating remote sensing with ecology and evolution to advance biodiversity conservation. Nature Ecology & Evolution 6:506–519.

Ceballos, G., P. R. Ehrlich, A. D. Barnosky, A. García, R. M. Pringle, and T. M. Palmer. 2015. Accelerated modern human-induced species losses: Entering the sixth mass extinction. Science Advances 1:9–13.

Chapin, F. S., E. S. Zavaleta, V. T. Eviner, R. L. Naylor, P. M. Vitousek, H. L. Reynolds, D. U. Hooper, S. Lavorel, O. E. Sala, S. E. Hobbie, M. C. Mack, and S. Díaz. 2000. Consequences of changing biodiversity. Nature 405:234–242.

Ciais, P., M. Reichstein, N. Viovy, A. Granier, J. Ogée, V. Allard, M. Aubinet, N. Buchmann, C. Bernhofer, A. Carrara, F. Chevallier, N. De Noblet, A. D. Friend, P. Friedlingstein, T. Grünwald, B. Heinesch, P. Keronen, A. Knohl, G. Krinner, D. Loustau, G. Manca, G. Matteucci, F. Miglietta, J. M. Ourcival, D. Papale, K. Pilegaard, S. Rambal, G. Seufert, J. F. Soussana, M. J. Sanz, E. D. Schulze, T. Vesala, and R. Valentini. 2005. Europe-wide reduction in primary productivity caused by the heat and drought in 2003. Nature 437:529–533.

Cohen, W. B., and S. N. Goward. 2004. Landsat ’ s Role in Ecological Applications of Remote Sensing. BioScience 54:535–545.

Connell, J. H., and E. Orias. 1964. The Ecological Regulation of Species Diversity. The American Naturalist 98:399–414.

Coops, N. C., R. H. Waring, M. A. Wulder, A. M. Pidgeon, and V. C. Radeloff. 2009a. Bird

diversity: a predictable function of satellite-derived estimates of seasonal variation in canopy light absorbance across the United States. Journal of Biogeography 36:905–918.

Coops, N. C., M. A. Wulder, D. C. Duro, T. Han, and S. Berry. 2008. The development of a Canadian dynamic habitat index using multi-temporal satellite estimates of canopy light absorbance. Ecological Indicators 8:754–766.

Coops, N. C., M. A. Wulder, and D. Iwanicka. 2009b. Exploring the relative importance of satellite-derived descriptors of production, topography and land cover for predicting breeding bird species richness over Ontario, Canada. Remote Sensing of Environment 113:668–679.

Currie, D. J., G. G. Mittelbach, H. V. Cornell, R. Field, J. F. Guegan, B. A. Hawkins, D. M. Kaufman, J. T. Kerr, T. Oberdorff, E. O'Brien, and J. R. G. Turner. 2004. Predictions and tests of climate-based hypotheses of broad-scale variation in taxonomic.pdf. Ecology Letters 7:1121–1134.

Evans, K. L., J. J. D. Greenwood, and K. J. Gaston. 2005. The roles of extinction and colonization in generating species-energy relationships. Journal of Animal Ecology 74:498–507.

Evans, K. L., N. A. James, and K. J. Gaston. 2006. Abundance, species richness and energy availability in the North American avifauna. Global Ecology and Biogeography 15:372–385.

Hawkins, B. A., R. Field, H. V. Cornell, D. J. Currie, J. F. Guegan, D. M. Kaufman, J. T. Kerr, G. G. Mittelbach, T. Oberdorff, E. M. O'Brien, E. E. Porter, and J. R. G. Turner. 2003. Energy, water, and broad-scale geographic patterns of species richness. Ecology 84:3105–3117.

Hobi, M. L., M. Dubinin, C. H. Graham, N. C. Coops, M. K. Clayton, A. M. Pidgeon, and V. C. Radeloff. 2017. A comparison of Dynamic Habitat Indices derived from different MODIS products as predictors of avian species richness. Remote Sensing of Environment 195:142–152.

Hurlbert, A. H., and J. P. Haskell. 2003. The effect of energy and seasonality on avian species richness and community composition. American Naturalist 161:83–97.

Kennedy, R. E., S. Andréfouët, W. B. Cohen, C. Gómez, P. Griffiths, M. Hais, S. P. Healey, E. H. Helmer, P. Hostert, M. B. Lyons, G. W. Meigs, D. Pflugmacher, S. R. Phinn, S. L. Powell, P. Scarth, S. Sen, T. A. Schroeder, A. Schneider, R. Sonnenschein, J. E. Vogelmann, M. A. Wulder, and Z. Zhu. 2014. Bringing an ecological view of change to landsat-based remote sensing. Frontiers in Ecology and the Environment 12:339–346.

Lees, A. C., C. Devenish, J. I. Areta, C. B. de Araújo, C. Keller, B. Phalan, and L. F. Silveira. 2021. Assessing the Extinction Probability of the Purple-winged Ground Dove, an Enigmatic Bamboo Specialist. Frontiers in Ecology and Evolution 9.

Michaud, J. S., N. C. Coops, M. E. Andrew, M. A. Wulder, G. S. Brown, and G. J. M. Rickbeil. 2014. Estimating moose (Alces alces) occurrence and abundance from remotely derived environmental indicators. Remote Sensing of Environment 152:190–201.

Mittelbach, G. G., C. F. Steiner, S. M. Scheiner, K. L. Gross, H. L. Reynolds, R. B. Waide, M. R. Willig, S. I. Dodson, and L. Gough. 2001. What is the observed relationship between species richness and productivity? Ecology 82:2381–2396.

Myneni, R. B., F. G. Hall, P. J. Sellers, and A. L. Marshak. 1995. Interpretation of spectral vegetation indexes. IEEE Transactions on Geoscience and Remote Sensing 33:481–486.

NABCI. 2016. North American Bird Conservation Initiative. 2016. The State of North America's

Birds 2016. Environment and Climate Change Canada: Ottawa, Ontario.

Nagendra, H. 2001. Using remote sensing to assess biodiversity. International Journal of Remote Sensing 22:2377–2400.

Perrig, P. L., S. A. Lambertucci, J. Cruz, P. A. E. Alarcón, P. I. Plaza, A. D. Middleton, G. Blanco, J. A. Sánchez-Zapata, J. A. Donázar, and J. N. Pauli. 2020. Identifying conservation priority areas for the Andean condor in southern South America. Biological Conservation 243:108494.

Pettorelli, N., S. Ryan, T. Mueller, N. Bunnefeld, B. Jedrzejewska, M. Lima, and K. Kausrud. 2011. The Normalized Difference Vegetation Index (NDVI): Unforeseen successes in animal ecology. Climate Research 46:15–27.

Pimm, S. L., C. N. Jenkins, R. Abell, T. M. Brooks, J. L. Gittleman, L. N. Joppa, P. H. Raven, C. M. Roberts, and J. O. Sexton. 2014. The biodiversity of species and their rates of extinction, distribution, and protection. Science 344.

Radeloff, V. C., M. Dubinin, N. C. Coops, A. M. Allen, T. M. Brooks, M. K. Clayton, G. C. Costa, C. H. Graham, D. P. Helmers, A. R. Ives, D. Kolesov, A. M. Pidgeon, G. Rapacciuolo, E. Razenkova, N. Suttidate, B. E. Young, L. Zhu, and M. L. Hobi. 2019. The Dynamic Habitat Indices (DHIs) from MODIS and global biodiversity. Remote Sensing of Environment 222:204–214.

Razenkova, E., M. Dubinin, A. M. Pidgeon, M. L. Hobi, L. Zhu, E. V. Bragina, A. M. Allen, M. K. Clayton, L. M. Baskin, N. C. Coops, and V. C. Radeloff. 2023. Abundance patterns of mammals across Russia explained by remotely sensed vegetation productivity and snow indices. Journal of Biogeography 50:932–946.

Razenkova, E., V. C. Radeloff, M. Dubinin, E. V Bragina, M. Allen, M. K. Clayton, A. M.

Pidgeon, L. M. Baskin, C. Nicholas, and M. L. Hobi. 2020. Vegetation productivity summarized by the Dynamic Habitat Indices explains patterns of moose abundance across Russia. Scientific Reports 10:1–12.

Rockström, J., W. Steffen, K. Noone, Å. Persson, F. S. Chapin, E. Lambin, T. M. Lenton, M. Scheffer, C. Folke, H. J. Schellnhuber, B. Nykvist, C. A. de Wit, T. Hughes, S. van der Leeuw, H. Rodhe, S. Sörlin, P. K. Snyder, R. Costanza, U. Svedin, M. Falkenmark, L. Karlberg, R. W. Corell, V. J. Fabry, J. Hansen, B. Walker, D. Liverman, K. Richardson, P. Crutzen, and J. Foley. 2009. A safe operating space for humanity. Nature 461:472–475.

Rosenberg, K. V., A. M. Dokter, P. J. Blancher, J. R. Sauer, A. C. Smith, P. A. Smith, J. C. Stanton, A. Panjabi, L. Helft, M. Parr, and P. P. Marra. 2019. Decline of the North American avifauna. Science 366:120–124.

Roxburgh, S. H., K. Shea, and J. B. Wilson. 2004. The intermediate disturbance hypothesis: Patch dynamics and mechanisms of species coexistence. Ecology 85:359–371.

Sekercioglu, C. H. 2006. Increasing awareness of avian ecological function. Trends in Ecology and Evolution 21:464–471.

Srivastava, D. S., and J. H. Lawton. 1998. Why more productive sites have more species: An experimental test of theory using tree-hole communities. American Naturalist 152:510–529.

Storch, D., E. Bohdalková, and J. Okie. 2018. The more-individuals hypothesis revisited: the role of community abundance in species richness regulation and the productivity–diversity relationship. Ecology Letters 21:920–937.

Turner, W., S. Spector, N. Gardiner, M. Fladeland, E. Sterling, and M. Steininger. 2003. Remote sensing for biodiversity science and conservation. Trends in Ecology and Evolution 18:306–314.

Williams, S. E., and J. Middleton. 2008. Climatic seasonality, resource bottlenecks, and abundance of rainforest birds: Implications for global climate change. Diversity and Distributions 14:69–77.

Wright, D. H. 1983. Species-energy theory: an extension of species–area theory. Oikos 41:496–506.

Wulder, M. A., T. R. Loveland, D. P. Roy, C. J. Crawford, J. G. Masek, C. E. Woodcock, R. G. Allen, M. C. Anderson, A. S. Belward, W. B. Cohen, J. Dwyer, A. Erb, F. Gao, P. Griffiths, D. Helder, T. Hermosilla, J. D. Hipple, P. Hostert, M. J. Hughes, J. Huntington, D. M. Johnson, R. Kennedy, A. Kilic, Z. Li, L. Lymburner, J. McCorkel, N. Pahlevan, T. A. Scambos, C. Schaaf, J. R. Schott, Y. Sheng, J. Storey, E. Vermote, J. Vogelmann, J. C. White, R. H. Wynne, and Z. Zhu. 2019. Current status of Landsat program, science, and applications. Remote Sensing of Environment 225:127–147.

Zhang, C., D. Cai, S. Guo, Y. Guan, K. Fraedrich, Y. Nie, X. Liu, and X. Bian. 2016. Spatial-Temporal Dynamics of China ' s Terrestrial Biodiversity: A Dynamic Habitat Index Diagnostic. Remote Sensing 8:1–18.

Chapter 1: Medium resolution Dynamic Habitat Indices from Landsat satellite imagery

Abstract

Biodiversity science requires effective tools to monitor patterns of species diversity at multiple temporal and spatial scales. Remote sensing provides measurements of key habitat factors, such as vegetation productivity that shape broad-scale patterns of biodiversity. The Dynamic Habitat Indices (DHIs) summarize aboveground vegetation productivity in a way that is ecologically relevant. The DHIs are well-grounded in ecological theories such as the species-

energy theory, which hypothesizes a strong connection between productivity and species richness. Existing DHIs were derived from MODIS at 1-km spatial resolution and are available after 2001 and predict species richness at broad scale well. That resolution is rather coarse relative to the scales at which many species perceive habitat though. Landsat data can capture key habitats at medium spatial resolution and has a longer temporal record. The challenge is that Landsat data is less frequently acquired than MODIS data, raising the question if the DHIs can be accurately calculated from Landsat data. Here, our main goals were to: a) develop, for the first time, the DHIs from 30-m Landsat data for the conterminous US, and b) compare these at different spatial and temporal scales with DHIs newly derived from 250-m resolution MODIS data. For both datasets, we calculated the DHIs from Normalized Difference Vegetation Index (NDVI) values for three time periods: of five (2016-2020), 10 (2011-2020), and 20 (2001-2020) years. We also compared Landsat and MODIS DHIs at three spatial extents: 1) Level III ecoregions (Environmental Protection Agency), 2) Level IV ecoregions, and 3) MODIS level (250-m). In addition, we took advantage of Landsat's long archive to calculate the DHIs for 1991-2000 and investigated how they changed by 2011-2020. We found that the Landsat and MODIS derived DHIs were highly correlated at ecoregion Levels III and IV extents for all time periods (Spearman correlation from 0.96 to 0.99 for mean and 0.6 to 0.98 for standard deviation), suggesting that our Landsat DHIs were accurate. However, at finer spatial scales the standard deviation of Landsat DHI and a difference map between and Landsat and MODIS DHIs highlight that the former captured spatial heterogeneity, especially in forested landscapes, much better. We also found considerable changes in Landsat DHIs from 1991-2000 to 2011-2020. For example, cumulative DHI increased along the West Coast, in mountain ranges, and in the South, but decreased in the Midwest. Our new DHIs at 30- and 250-m resolution for the conterminous

US have great potential for use in biodiversity science and conservation. All datasets are freely available.

Introduction

A key question in ecology is which environmental factors determine the patterns of biodiversity. The species-energy theory predicts that areas with higher amounts of plant biomass can support greater species richness of consumers due to availability of abundant food resources (Wright 1983, Currie et al. 1993, Hawkins et al. 2003a, 2003b). Remotely sensed indices capture the energy that is available in a system through photosynthesis, which is a proxy for vegetation productivity (Myneni et al. 1995, Cohen and Goward 2004, Pettorelli et al. 2011). However, a challenge is to capture vegetation productivity patterns at the temporal and spatial scales that are most relevant for species. On one hand, coarse resolution satellite sensors (e.g., > 250 m) provide more frequent observations thereby capturing more temporal variability in vegetation productivity. However their coarse resolution limits their utility over regional and local scales, especially where the environmental heterogeneity is high and local management decisions are required (Kennedy et al. 2014, Rose et al. 2015). Conversely medium- or high-resolution sensors (e.g., 10 - 30 m) provide more spatially detailed information (Wulder et al. 2008, 2019), but the frequency of observations is substantially lower, especially for historical data, thereby potentially missing disturbances that affect biodiversity (Roxburgh et al. 2004, Ciais et al. 2005, Bigler et al. 2006), and reducing the accuracy of derived metrics.

Remotely sensed measures of vegetation productivity dynamics can be used to understand factors that influence species richness. The Dynamic Habitat Indices (DHIs) summarize three measures of vegetation productivity over the course of a year based on three measures (Coops et al. 2008, Hobi et al. 2017, Radeloff et al. 2019). The first measure is

cumulative productivity: areas characterized by high cumulative productivity support more individuals (Srivastava and Lawton 1998, Hurlbert 2004) and tend to be more biodiverse (Wright 1983). The second measure is minimum productivity: areas with low minimum productivity may not have sufficient resources to support year-round resident species during seasons with lowest productivity. The third measure is coefficient of variation of vegetation productivity: areas with low seasonality tend to be more biodiverse. The DHIs are highly correlated with species richness across different taxa and have been successfully used for predicting species richness (Zhang et al. 2016, Radeloff et al. 2019), such as bird richness in Canada (Coops et al. 2009), US (Hobi et al. 2017), and Thailand (Suttidate et al. 2019); bird, mammal, and amphibian richness in China (Zhang et al. 2016, Zhu and Guo 2022), and across the globe (Coops et al. 2019, Radeloff et al. 2019). The DHIs also effectively predicted moose abundance in Canada (Michaud et al. 2014) and Russia (Razenkova et al. 2020).

So far, the DHIs have only been derived from coarse-resolution satellite data, such as from 8-km AVHRR and 1-km MODIS imagery. These data have proven to be highly valuable for biodiversity science already, for example, in models of Andean condor habitat selection in Argentina and Chile (Perrig et al. 2020), in models of geographic range of an enigmatic South American bamboo specialist, the Purple-winged Ground Dove (Lees et al. 2021), and in models of the distribution of bird species in California (Burns et al. 2020). For many of the species that have been modeled, 1-km DHIs are rather coarse though because the species are affected by habitat features at finer scales.

The DHIs at medium resolution would be much more relevant to finer-scale ecological studies and management decisions than coarse-resolution MODIS DHIs. Landsat DHIs can capture productivity dynamics within the territory of an individual bird (Leonard et al. 2008,

Jones 2011) or mammal (Oeser et al. 2020) and therefore reflect habitat better than coarser resolution imagery (Cohen and Goward 2004). Moreover, 30-m resolution metrics match the resolution of animal movement data, and therefore Landsat data are more suitable when assessing connectivity among habitat patches or movement corridors (Neumann et al. 2015, Bleyhl et al. 2017).

However, the challenge in calculating DHIs from Landsat data is the lower temporal resolution with a 16-day revisit cycle. These scarce observations are not sufficient to calculate the DHIs annually. One way to overcome this problem is to aggregate several years of imagery and calculate a composite metric. This also minimizes effects of erroneous observations in annual imagery. There is a trade-off though in that compositing data from many years will increase the number of observation, but changes in vegetation productivity caused by anthropogenic or natural disturbances can occur within the compositing period. The DHIs composited across many years may miss these changes. This trade-off raises the first question that is what aggregation period is optimal for the calculation of DHIs using Landsat imagery.

The second question is where the higher spatial resolution of Landsat DHIs, compared to MODIS DHIs, can capture spatial heterogeneity better, for example in more heterogeneous landscapes, such as those with complex terrain. Mountains are often hotspots for biodiversity (Badgley et al. 2017, Rahbek et al. 2019). Furthermore, strong gradients in temperature and environmental conditions provide more niches for different species than areas that are homogenous (Letten et al. 2013). For individual species, mountainous areas provide more refugia (Perrigo et al. 2020), and individual animals do not need to travel long distances to find suitable environmental and climatic conditions for survival and reproductive success (Elsen et al. 2020). Fragmentation of habitat due to land use change can be another source of heterogeneity

that might require the use of Landsat DHIs. Some species, such as habitat specialists, are negatively impacted by fragmentation (Henle et al. 2004), while other species benefit from it (Rybicki et al. 2020). Thus, there is a need for the DHIs that capture heterogeneity of vegetation productivity at medium spatial resolution.

Last but not least, many wildlife species are declining due to habitat loss and degradation (Butchart et al. 2010, Pimm et al. 2014). The long record of continuously acquired images of Landsat data provides a unique opportunity to monitor how the DHIs have changed since the 1990s (Wulder et al. 2019). This is critical to understand how habitat is changing over time and affecting species richness and abundance patterns.

Our primary goal was to develop the DHIs based on 30-m resolution Landsat data and compare them to 250-m resolution MODIS DHIs across the conterminous US. More specifically, our objectives were to:

- Calculate and compare composite DHIs based on Landsat and MODIS imagery for five (2016-2020), ten (2011-2020), and twenty (2001-2020) years at three spatial extents.
- Assess the ability of Landsat DHIs to capture heterogeneity within MODIS pixels in complex terrain and fragmented landscapes.
- Quantify changes in the Landsat DHIs for the 1990s to the 2010s.

Methods

Study area

Our study area was the conterminous US (7.6 million km2), which includes 85 Level III ecoregions and 967 Level IV ecoregions based on the Environmental Protection Agency (Omernik 1987).

Data

Calculating DHIs from Landsat data

We analyzed atmospherically corrected Surface Reflectance Tier 1 Collection 1 scenes obtained from Landsat-5 TM, Landsat-7 ETM+, and Landsat-8 OLI from 2001 to 2020 covering the conterminous US, in Google Earth Engine (access data 10-12-2018, Gorelick et al. 2017). We used only ETM+ data prior to the failure of the Scan Line Corrector to minimize stripes in our DHIs due to gaps in coverage (Markham et al. 2004). We removed pixels covered by clouds and cloud shadows with medium and high confidence based on the pixel quality assessment (QA) band from each Landsat image. Pixels were excluded based on pixel QA Bitmask as follows: bit 3, shadow; bits 6-7, cloud confidence where 2 was median confidence and 3 was high confidence; bit 8-9, cirrus confidence where 2 was median and 3 was high confidence. We also removed all pixels with negative reflectance values in any band. We replaced pixels identified as snow and ice based on the QA band with zeros because we assumed no photosynthetic activity. For the remaining pixels, we calculated the Normalized Difference Vegetation Index (NDVI) using bands 4 and 3 for TM, ETM+ and bands 5 and 4 for OLI. We selected NDVI because it is the most frequently used in remote sensing and ecology (Pettorelli 2013, Roy et al. 2016). Because OLI has narrower spectral bands than TM and ETM+, we applied a calibration correction (Roy et al. 2016). All negative NDVI values were replaced by zeros assuming that those were also snow and ice. To remove water pixels, we applied a mask of permanent water bodies derived from Landsat (Hansen et al. 2013).

For each pixel we calculated the median NDVI value for each month from all the observation for five (2016-2020), ten (2011-2020), or 20 years (2001-2020). In some months (mostly in winter) when there were no observations, we applied linear interpolation to fill in gaps

in the monthly median NDVI composite. Pixels that had missing data for more than four consecutive months were set to no-data. We selected to fill missing data up to four consecutive months because most pixels with missing data were from winter months and located in northern states when there was no photosynthetic activity during those months. From the interpolated NDVI composites, we calculate the three DHIs: 1) cumulative DHI (cum DHI), 2) minimum DHI (min DHI), and 3) seasonal DHI (var DHI). For objective 3, we also calculated the DHIs for 1991-2000, following the same protocol. During the 1990s, Landsat-4 and 5 TM, Landsat-7 ETM+ were in orbit. Data from Landsat-4 were very sparse during study period. Bands and wavelengths are similar across all three satellites therefore there was no need for additional calibration correction for NDVI calculation.

Data availability varied substantially for each time period (Table **1**). We used only OLI data for our five year period (2016-2020), OLI and TM data for our ten years (2011-2020), and OLI, TM and ETM+ four our twenty years (2001-2020). For each time period, we calculated the number of pixels with missing data and the percent of interpolated data.

Calculating DHIs from MODIS data

We analyzed MODIS Collection 6 16-day NDVI data at 250 m resolution (GEE Image collection MODIS/006/MOD13AQ1) to calculate DHIs. We followed established methods to calculate the MODIS DHIs (Hobi et al. 2017, Radeloff et al. 2019), but with minor changes. Similar to Hobi et al. (2017), we removed clouds and cloud shadow from each 16-day composite using the QA band. However, we replaced pixels flagged as snow and ice with zeros assuming no vegetative activity. We then calculated the median NDVI for each 16-days time step (23 observations in a year) for the same 5, 10 and 20 years.

Analysis for objective 1: Compare Landsat DHIs and MODIS DHIs

To compare the DHIs based on Landsat and MODIS, we ran Spearman correlation analyses at three spatial scales. We calculated mean and standard deviation for both types of DHIs over a) 85 Level III ecoregions (Figure **1**a), b) 967 Level IV ecoregions, and c) within the extent of each MODIS pixel. Ecoregions of Level III and IV are appropriate units for comparison of DHIs, because they are defined as areas that have similar ecosystems (Omernik and Griffith 2014). To compare the Landsat derived DHIs with corresponding MODIS pixels, we used a moving window of 8x8 pixels (240 m), which most closely matches the size of MODIS pixels (232 m). We calculated mean and standard deviation of Landsat-based cumulative DHI for each 8x8 pixel grid and resampled it to the MODIS data grid using the nearest neighbor rule. For comparison and visualization, we normalized data from 0 to 1 by dividing the DHI value of each pixel by the maximum value of the given mean cumulative DHI (Landsat or MODIS) hereafter referred to as "Landsat cumulative DHI and "MODIS cumulative DHI", respectively, and calculated the difference by subtracting Landsat from MODIS.

Ancillary environmental variables

We used five ancillary environmental variables including elevation, topography and land cover to model where Landsat DHIs varied the most within MODIS pixels. For elevation we used NASA Shuttle Radar Topography Mission (SRTM) elevation model with 30-m resolution (Farr et al. 2007). From the SRTM, we calculate the terrain ruggedness index (TRI) to characterize topographic heterogeneity (Riley 1999). For land cover, we analyzed the 2016 National Land Cover Database (NLCD) with 30-m resolution (Yang et al. 2018). We focused on three dominant land cover classes commonly used in ecological models: forest, shrubland, and grassland. Our forest class was the combination of NLCD classes 41-decidious forest, 42-

evegreen forest, 43-mixed forest. Our shrubland class included 51-dwarf scrub, and 52-shrub/scrub, and our grassland class only included 71-grassland/herbaceous. To quantify fragmentation, we applied the Morphological Spatial Pattern Analysis (MSPA) implemented in GUIDOS, a tool that classifies spatial patterns at the pixel level based on binary land-cover maps (Vogt et al. 2007, 2009). We calculated the percent of core and of edge area for each land cover class (forest, shrubland, and grassland), as two key metrics of fragmentation (Batáry and Báldi 2004, Vogt et al. 2007).

Analysis for objective 2: Assess the ability of Landsat DHIs to capture heterogeneity and fragmentation within individual MODIS pixels

To evaluate how Landsat DHIs relate to commonly used metrics of heterogeneity and fragmentation, we modeled relationships between the Landsat DHIs and topographic and landscape metrics. We sought to understand if variability in the DHIs captured by Landsat within MODIS pixels is associated with elevation, topography, or landscape metrics. To do so we randomly selected 10,000 MODIS pixels separated by at least 10 km to minimize spatial autocorrelation. We calculated the standard deviation of Landsat cumulative DHIs within MODIS pixels as the dependent variable, and mean and standard deviation of elevation and terrain ruggedness, plus percent core and edge area for forest, shrubland, and grassland as explanatory variables. Prior to modeling, we checked for collinearity among our explanatory variables and examined their scatter plots to check for nonlinear patterns. To meet the assumptions of linear regression we applied log transformation of the dependent variable that is the standard deviation of Landsat DHIs within MODIS pixels. First, we fitted univariate linear regression models and used the adjusted R2 to evaluate the total explanatory power of each model. Second, we fitted multivariate models with all possible subsets of the ten explanatory

variables, and used best subsets regression to identify the most important explanatory variables based on how often variables appeared in the top models as ranked based on the Bayesian Information Criterion (BIC) (Schwarz 1978). We assessed multicollinearity of the top model by examining the variance inflation factor (VIF) for each variable, applying a threshold of VIF <10 (O'Brien 2007).

Analysis for objective 3: Compare Landsat DHIs over 1991-2000 versus 2011-2020

We quantified changes in the Landsat DHIs for the 1990s with those for the 2010s. We asked first, how strongly the DHIs for both decades are correlated and, second, how their spatial patterns differed. For our first comparison we randomly selected 10,000 Landsat pixels each separated by 10-km to avoid spatial autocorrelation, and calculated Spearman correlation coefficients between the DHIs for the two decades. For our second comparison and for visualization, we normalized both sets of DHIs from 0 to 1 by dividing each DHI pixel value by the maximum value of the given DHI and made difference maps by subtracting the 1990s DHIs from the 2010s DHIs.

We performed all statistical analyses in R version 4.0.3 (R Core Team 2016), using the 'psych' package (Revelle 2017) to calculate correlation matrices, the 'leaps' package (Lumley 2009) to perform best subsets selection, and the 'car' package to calculate VIF for explanatory variables (Fox and Weisberg 2016).

Results

The DHIs calculated from Landsat

We calculated a monthly NDVI composite based on Landsat data for five (2016-2020), ten (1991-2000 and 2011-2020), and twenty years (2001-2020). We successfully generated

Landsat DHI even for a relatively short five year period (2016-2020), as well as for the 1990s (1991-2000), with much fewer observations. The DHIs based on Landsat reflected patterns of vegetation productivity across the conterminous US (Figure **1**). For example, cumulative DHI had the highest values in the east and southeast of the conterminous US, in the west along the coastline, and in forested areas of the Midwest. Minimum DHI values were also high in southeast and along the west coast and were low in the northern Midwest and West. In contrast, the variation DHI had high values in the north and in mountain areas, and low values in the south and along the west coast.

For each time period we had pixels with missing data that were located mostly in northern states (Appendix **1**) for single months and for consecutive months. Winter months had the highest number of pixels with missing data with the peak in January (Figure **2**, Appendix **1**). We found there were fewer missing data as we increased compositing period from five years to 20 years. In total, interpolated data made up 29.4% (1991-2000), 17.5% (2016-2020), 6.7% (2011-2020), and 1.7% (2001-2020) of total available data (Table **1**). In addition, we calculated the percent of pixels that were set as no-data due to use of our threshold of interpolation of four months and made up 0.002% (2016-2020), 0.001% (2011-2020), and 0.00004% (2001-2020).

Results for objective 1: MODIS DHIs versus Landsat DHIs

As expected, broad-scale patterns of DHIs based on Landsat and MODIS were generally very similar, but Landsat DHIs captured more detailed landscape patterns, especially in forested areas (Figure **3**). The Spearman correlation coefficients between means of the three DHIs based on Landsat and MODIS across three periods were 0.98-0.99 within Level III ecoregions, while the standard deviation ranged from 0.6 to 0.94. The Spearman correlation coefficients between mean

DHIs based on Landsat and MODIS were also high for Level IV ecoregions and ranged from 0.96 to 0.99, while standard deviations ranged from 0.63 to 0.89 (Table **2**).

The standard deviation of cumulative DHI based on Landsat imagery calculated across all MODIS pixels were higher in places dominated by forest (Figure **4**a). The difference map between MODIS cumulative DHI and Landsat cumulative DHI (i.e. MODIS minus Landsat) indicated that Landsat DHI was higher in some mountains such as the Sierra Nevada, the Cascade Range, the northern Rocky Mountains, and some states including Minnesota, Wisconsin and Michigan where forest is a dominant land cover (Figure **4**b).

Results for objective 2: Landsat DHIs within the footprint of MODIS pixels

First, we calculated the Pearson correlation values between the standard deviation of cumulative DHI based on Landsat and our various environmental variables including mean and standard deviation of elevation and terrain ruggedness, percent core and edge area in forest, shrubland, and grassland for randomly selected 10,000 MODIS pixels. Pearson correlation coefficients among all ancillary variables were low, except for mean and standard deviation of terrain ruggedness index, indicating that collinearity was generally not an issue ($r = 0.85$, Supplementary materials Appendix **2**). The correlation between standard deviation of cumulative DHI based on Landsat and percent of forest edge was the highest among all explanatory variables ($r = 0.46$). Second, we ran a series of univariate models in which the standard deviation of Landsat cumulative DHIs within MODIS pixels is the dependent variable, and all ancillary environmental variables were explanatory variables. In univariate models, individual variables explained only 2-15% of the variance in standard deviation of cumulative DHI (Table **3**). We found a positive relationship between standard deviation of cumulative DHI and forest habitat, and a negative relationship with grassland and shrubland habitat (Table **3**). Finally, we fitted

multivariate models. The adjusted R2 slightly increased for models incorporating multiple variables, explaining 26% of the variation in standard deviation of cumulative DHI (Table **3**). The best model included percent of forest edge, percent of grassland core area, and percent of shrubland core area. There was no multicollinearity between explanatory variables in the top selected models, as indicated by a VIF of less than 1.5.

Results for objective 3: Change in the Landsat DHIs from 1991-2000 to 2011-2020

The patterns of the DHIs were similar for both periods, but our difference maps also showed striking regional patterns (Figure **5**). Most notable, we found an increase in the cumulative DHI calculated in the West Coast, in most of the mountain ranges, and in parts of the South. However, cumulative DHI calculated over 1991-2000 was higher in the Midwest and New England. Minimum DHI decreased in the northern part of the US by the 2010s while variation DHI increased, especially in the Midwest.

Discussion

Our main goals were to develop the DHIs based on Landsat imagery, compare them with the DHIs derived from MODIS, and understand where the increased spatial resolution afforded by Landsat was most important. We successfully developed the Landsat DHIs for five (2016-2020), ten (2011-2020), and twenty years (2001-2020), and at broad scales, the spatial patterns of the DHIs based on Landsat and MODIS were similar. Indeed, the correlations between the Landsat and MODIS DHIs for 2016-2020, 2011-2020, and 2001-2020 were all high (0.96-0.99), indicating that we could derive composite Landsat DHIs for as few as five year periods. However, there were areas where Landsat DHIs clearly captured landscape heterogeneity better, and hence were quite different from MODIS DHIs, especially in mountains and forested areas.

The DHIs captured unique information about landscapes that differed from commonly used metrics characterizing environmental heterogeneity. Specifically, we found weak relationship between the standard deviation of the Landsat cumulative DHI and environmental heterogeneity as captured by topographic metrics. This finding matches prior results for 1-km MODIS DHIs, which have low correlation with climate variables, suggesting that the DHIs capture unique information and can complement other environmental variables (Radeloff et al. 2019, Suttidate et al. 2019). We also found weak relationships between the standard deviation of the cumulative DHI and fragmentation metrics. This might be because the DHIs were calculated based on NDVI, and NDVI can be similar for different land cover classes (e.g., forest and agricultural fields), while fragmentation metrics are based on land cover maps such that forest and cultivated field are discrete classes (Yang et al. 2018). In addition, the DHIs can vary notably within the same land cover class, which is feature that land cover classifications miss. Therefore, the DHIs can measure aspects of landcover distinct from fragmentation and topographic heterogeneity and can complement these variables in ecological models.

Another advantage of Landsat is the long record of data that allows detection of environmental changes over time (Kerr and Ostrovsky 2003). Our results show that we can calculate the DHIs for historical periods when observations are limited for some areas. The high correlation between the Landsat DHI for the 1990s and 2010s indicates that our approach for the DHIs calculation works well. We found substantial changes in all three DHIs over last thirty years, and the pattern of these changes is striking. Based on the difference map between the Landsat DHIs, we see generally increased vegetation productivity in forested areas but a decrease in in the forests of the northern Midwest. In general, changes in cumulative DHI indicate overall changes in vegetation productivity, while minimum DHI may also indicate

changes in snow cover pattern for northern states and places with high altitude. A previous study captured changes in ecozone composition over shorter time periods (6 years) by comparing annual MODIS DHIs from multiple years with average DHIs (Coops et al. 2008). Having DHIs from multiple years offers an opportunity to examine trends and how changes in DHIs affect biodiversity (Hobi et al. 2021).

Caveats and considerations

The main challenge of working with Landsat is the relatively low number of scenes available for a given time period, due to the return interval of overpasses, which is further reduced by the presence of clouds. We used Landsat data to generate a monthly NDVI composite (versus 16-day MODIS data) over five, 10, and 20 years, and for each of those time periods, there were pixels with no observations for some months. These missing months affected especially the cumulative and variation DHIs. To provide a consistent product we used linear interpolation to fill missing months before calculating our composite DHIs. We interpolated data up to four consecutive months, however, phenology curves are nonlinear, and we may have introduced erroneous higher values for winter or lower values for summer months. Most of the missing data occurred in winter when vegetation productivity is low, so our interpolations like affected the minimum DHI the most. We decided to interpolate data based on monthly median NDVI values for all years, instead of annually, because there is not enough cloud-free Landsat data in many parts of the US to do so reliably (Baumann et al. 2017).

Another limitation of our work is that we did not use the Point Spread Function (PSF) while aggregating Landsat DHIs to the nominal resolution of 250-m MODIS. This simplification excludes up to 25-30% of the signal of each MODIS pixel (Huang et al. 2019). However, we are confident our rescaling approach provided robust results, because of high values of the standard

deviation of Landsat-based dataset. Another caveat is that the wide swath of MODIS and the gridded sampling process causes mismatch between signal and ground source, introducing error in the MODIS product, especially in complex terrain which is not overcome completely even after preprocessing (Tan et al. 2006, Feng et al. 2012, Peng et al. 2015).

Regarding the trade-off between longer compositing periods, which provide more observations, but also increase the likelihood that land cover changed during the compositing period, and shorter periods, which are more likely to be similar across the period, but lack observations, we suggest that ten years is a good compromise for most applications. However, Landsat coverage is better in the US, than in other parts of the world. Therefore, the period used for calculating DHIs may need to be longer in other parts of the world. On the other hand, the recently launched Landsat 9 provides a great opportunity to investigate long-term trends in the DHIs, and when combined with Sentinel-2 would greatly reduce the need for interpolation for more recent years. We opted against including Sentinel-2 data, however, to focus on the comparisons of different time periods from one sensor, and the changes from the 1990s to the 2010s.

Advancements in cloud computing technologies and open access to the full Landsat archive provide a great opportunity to generate novel products that are relevant for biodiversity assessments (Kennedy et al. 2014, Wulder et al. 2019). Previously, only coarse resolution data at global or continental scales were available, however now data with medium resolution are also available over large areas (Gergely et al. 2019) and can be efficiently processed (Gorelick et al. 2017). Our newly developed DHIs based on Landsat have great potential for biodiversity monitoring at regional and local scales, for example, correlations with species richness as well as occurrence and abundance data. Thereby the Landsat DHIs can help to advance understanding of

the importance of proxies of productivity for species richness, distributions, and abundances. Such analyses can provide valuable information about habitat quality for managers striving to identify and protect critical habitat of species of concern. Lastly, we found that the long record of Landsat data captures long-term changes, and that opens great opportunities to investigate how these changes are affecting biodiversity. The 30-m Landsat and 250-m MODIS DHIs for the conterminous US, and global 1-km MODIS DHIs are freely available at http://silvis.forest.wisc.edu/data/dhis/.

References

Badgley, C., T. M. Smiley, R. Terry, E. B. Davis, L. R. G. DeSantis, D. L. Fox, S. S. B. Hopkins, T. Jezkova, M. D. Matocq, N. Matzke, J. L. McGuire, A. Mulch, B. R. Riddle, V. L. Roth, J. X. Samuels, C. A. E. Strömberg, and B. J. Yanites. 2017. Biodiversity and Topographic Complexity: Modern and Geohistorical Perspectives. Trends in Ecology and Evolution 32:211–226.

Batáry, P., and A. Báldi. 2004. Evidence of an edge effect on avian nest success. Conservation Biology 18:389–400.

Baumann, M., M. Ozdogan, A. D. Richardson, and V. C. Radeloff. 2017. Phenology from Landsat when data is scarce: Using MODIS and Dynamic Time-Warping to combine multi-year Landsat imagery to derive annual phenology curves. International Journal of Applied Earth Observation and Geoinformation 54:72–83.

Bigler, C., O. U. Bräker, H. Bugmann, M. Dobbertin, and A. Rigling. 2006. Drought as an inciting mortality factor in scots pine stands of the Valais, Switzerland. Ecosystems 9:330–343.

Bleyhl, B., M. Baumann, P. Griffiths, A. Heidelberg, K. Manvelyan, V. C. Radeloff, N. Zazanashvili, and T. Kuemmerle. 2017. Assessing landscape connectivity for large mammals in the Caucasus using Landsat 8 seasonal image composites. Remote Sensing of Environment 193:193–203.

Burns, P., M. Clark, L. Salas, S. Hancock, D. Leland, P. Jantz, R. Dubayah, and S. J. Goetz. 2020. Incorporating canopy structure from simulated GEDI lidar into bird species distribution models. Environmental Research Letters 15.

Butchart, S. H. M., M. Walpole, B. Collen, A. van Strien, J. P. W. Scharlemann, R. E. A. Almond, J. E. M. Baillie, B. Bomhard, C. Brown, J. Bruno, K. E. Carpenter, G. M. Carr, J. Chanson, A. M. Chenery, J. Csirke, N. C. Davidson, F. Dentener, M. Foster, A. Galli, J. N. Galloway, P. Genovesi, R. D. Gregory, M. Hockings, V. Kapos, J. F. Lamarque, F. Leverington, J. Loh, M. A. McGeoch, L. McRae, A. Minasyan, M. H. Morcillo, T. E. E. Oldfield, D. Pauly, S. Quader, C. Revenga, J. R. Sauer, B. Skolnik, D. Spear, D. Stanwell-Smith, S. N. Stuart, A. Symes, M. Tierney, T. D. Tyrrell, J. C. Vie, and R. Watson. 2010. Global Biodiversity: Indicators of Recent Declines. Science 328:1164–1168.

Ciais, P., M. Reichstein, N. Viovy, A. Granier, J. Ogée, V. Allard, M. Aubinet, N. Buchmann, C. Bernhofer, A. Carrara, F. Chevallier, N. De Noblet, A. D. Friend, P. Friedlingstein, T. Grünwald, B. Heinesch, P. Keronen, A. Knohl, G. Krinner, D. Loustau, G. Manca, G. Matteucci, F. Miglietta, J. M. Ourcival, D. Papale, K. Pilegaard, S. Rambal, G. Seufert, J. F. Soussana, M. J. Sanz, E. D. Schulze, T. Vesala, and R. Valentini. 2005. Europe-wide reduction in primary productivity caused by the heat and drought in 2003. Nature 437:529–533.

Cohen, W. B., and S. N. Goward. 2004. Landsat ’ s Role in Ecological Applications of Remote Sensing. BioScience 54:535–545.

Coops, N. C., D. K. Bolton, M. L. Hobi, and V. C. Radeloff. 2019. Untangling multiple species richness hypothesis globally using remote sensing habitat indices. Ecological Indicators 107.

Coops, N. C., R. H. Waring, M. A. Wulder, A. M. Pidgeon, and V. C. Radeloff. 2009. Bird diversity: a predictable function of satellite-derived estimates of seasonal variation in canopy light absorbance across the United States. Journal of Biogeography 36:905–918.

Coops, N. C., M. A. Wulder, D. C. Duro, T. Han, and S. Berry. 2008. The development of a Canadian dynamic habitat index using multi-temporal satellite estimates of canopy light absorbance. Ecological Indicators 8:754–766.

Currie, D. J., J. T. Fritz, D. J. Currie, J. T. Fritz, and J. T. Global. 1993. Global Patterns of Animal Abundance and Species Energy Use. Nordic Society Oikos 67:56–68.

Elsen, P. R., W. B. Monahan, and A. M. Merenlender. 2020. Topography and human pressure in mountain ranges alter expected species responses to climate change. Nature Communications 11:1–10.

Farr, T. G., P. A. Rosen, E. Caro, R. Crippen, R. Duren, S. Hensley, M. Kobrick, M. Paller, E. Rodriguez, L. Roth, D. Seal, S. Shaffer, J. Shimada, J. Umland, M. Werner, M. Oskin, D. Burbank, and D. E. and Alsdorf. 2007. The shuttle radar topography mission. Reviews of Geophysics 45:1–33.

Feng, M., C. Huang, S. Channan, E. F. Vermote, J. G. Masek, and J. R. Townshend. 2012. Quality assessment of Landsat surface reflectance products using MODIS data. Computers and Geosciences 38:9–22.

Fox, J., and S. Weisberg. 2016. Companion to Applied Regression.

Gergely, K. J., K. G. Boykin, A. J. McKerrow, M. J. Rubino, N. M. Tarr, and S. G. Williams. 2019. Gap Analysis Project (GAP) Terrestrial Vertebrate Species Richness Maps for the Conterminous U.S.: U.S. Geological Survey Scientific Investigations Report 2019–5034.

Gorelick, N., M. Hancher, M. Dixon, S. Ilyushchenko, D. Thau, and R. Moore. 2017. Google Earth Engine: Planetary-scale geospatial analysis for everyone. Remote Sensing of Environment 202:18–27.

Hansen, M. C., P. V. Potapov, R. Moore, M. Hancher, S. A. Turubanova, A. Tyukavina, D. Thau, S. V. Stehman, S. J. Goetz, T. R. Loveland, A. Kommareddy, A. Egorov, L. Chini, C. O. Justice, and J. R. G. Townshend. 2013. High-Resolution Global Maps of 21st-Century Forest Cover Change. Science 342:850–853.

Hawkins, B. A., R. Field, H. V. Cornell, D. J. Currie, J. F. Guegan, D. M. Kaufman, J. T. Kerr, G. G. Mittelbach, T. Oberdorff, E. M. O'Brien, E. E. Porter, and J. R. G. Turner. 2003a. Energy, water, and broad-scale geographic patterns of species richness. Ecology 84:3105–3117.

Hawkins, B. A., E. E. Porter, and J. A. F. Diniz-Filho. 2003b. Productivity and history as predictors of the latitudinal diversity gradient of terrestrial birds. Ecology 84:1608–1623.

Henle, K., K. F. Davies, M. Kleyer, C. Margules, and J. Settele. 2004. Predictors of species sensitivity to fragmentation. Biodiversity and Conservation 13:207–251.

Hobi, M. L., M. Dubinin, C. H. Graham, N. C. Coops, M. K. Clayton, A. M. Pidgeon, and V. C. Radeloff. 2017. A comparison of Dynamic Habitat Indices derived from different MODIS products as predictors of avian species richness. Remote Sensing of Environment 195:142–152.

Hobi, M. L., L. S. Farwell, M. Dubinin, D. Kolesov, A. M. Pidgeon, N. C. Coops, and V. C. Radeloff. 2021. Patterns of bird species richness explained by annual variation in remotely sensed Dynamic Habitat Indices. Ecological Indicators 127:107774.

Huang, M., S. Piao, P. Ciais, J. Peñuelas, X. Wang, T. F. Keenan, S. Peng, J. A. Berry, K. Wang, J. Mao, R. Alkama, A. Cescatti, M. Cuntz, H. De Deurwaerder, M. Gao, Y. He, Y. Liu, Y. Luo, R. B. Myneni, S. Niu, X. Shi, W. Yuan, H. Verbeeck, T. Wang, J. Wu, and I. A. Janssens. 2019. Air temperature optima of vegetation productivity across global biomes. Nature Ecology & Evolution.

Hurlbert, A. H. 2004. Species-energy relationships and habitat complexity in bird communities. Ecology Letters 7:714–720.

Jones, S. L. 2011. Territory size in mixed-grass prairie songbirds. Canadian Field-Naturalist 125:12–15.

Kennedy, R. E., S. Andréfouët, W. B. Cohen, C. Gómez, P. Griffiths, M. Hais, S. P. Healey, E. H. Helmer, P. Hostert, M. B. Lyons, G. W. Meigs, D. Pflugmacher, S. R. Phinn, S. L. Powell, P. Scarth, S. Sen, T. A. Schroeder, A. Schneider, R. Sonnenschein, J. E. Vogelmann, M. A. Wulder, and Z. Zhu. 2014. Bringing an ecological view of change to landsat-based remote sensing. Frontiers in Ecology and the Environment 12:339–346.

Kerr, J. T., and M. Ostrovsky. 2003. From space to species: ecological applications for remote sensing. Trends in Ecology & Evolution 18:299–305.

Lees, A. C., C. Devenish, J. I. Areta, C. B. de Araújo, C. Keller, B. Phalan, and L. F. Silveira. 2021. Assessing the Extinction Probability of the Purple-winged Ground Dove, an Enigmatic Bamboo Specialist. Frontiers in Ecology and Evolution 9.

Leonard, T. D., P. D. Taylor, and I. G. Warkentin. 2008. Landscape structure and spatial scale affect space use by songbirds in naturally patchy and harvested boreal forests. Condor 110:467–481.

Letten, A. D., M. B. Ashcroft, D. A. Keith, J. R. Gollan, and D. Ramp. 2013. The importance of temporal climate variability for spatial patterns in plant diversity. Ecography 36:1341–1349.

Lumley, T. 2009. Regression subset selection. R package version 2.9.

Markham, B. L., J. C. Storey, D. L. Williams, and J. R. Irons. 2004. Landsat sensor performance: History and current status. IEEE Transactions on Geoscience and Remote Sensing 42:2691–2694.

Michaud, J. S., N. C. Coops, M. E. Andrew, M. A. Wulder, G. S. Brown, and G. J. M. Rickbeil. 2014. Estimating moose (Alces alces) occurrence and abundance from remotely derived environmental indicators. Remote Sensing of Environment 152:190–201.

Myneni, R. B., F. G. Hall, P. J. Sellers, and A. L. Marshak. 1995. Interpretation of spectral vegetation indexes. IEEE Transactions on Geoscience and Remote Sensing 33:481–486.

Neumann, W., S. Martinuzzi, A. B. Estes, A. M. Pidgeon, H. Dettki, G. Ericsson, and V. C. Radeloff. 2015. Opportunities for the application of advanced remotely-sensed data in ecological studies of terrestrial animal movement. Movement Ecology 3:1–13.

O'Brien, R. M. 2007. A caution regarding rules of thumb for variance inflation factors. Quality and Quantity 41:673–690.

Oeser, J., M. Heurich, C. Senf, D. Pflugmacher, E. Belotti, and T. Kuemmerle. 2020. Habitat metrics based on multi-temporal Landsat imagery for mapping large mammal. Remote Sensing in Ecology and Conservation 6:52–69.

Omernik, J. M. 1987. Ecoregions of the Conterminous United (map supplement). Annals of the Association of American Geographers 77:118–125.

Omernik, J. M., and G. E. Griffith. 2014. Ecoregions of the Conterminous United States: Evolution of a Hierarchical Spatial Framework. Environmental Management 54:1249–1266.

Peng, J., Q. Liu, L. Wang, Q. Liu, W. Fan, M. Lu, and J. Wen. 2015. Characterizing the pixel footprint of satellite albedo products derived from MODIS reflectance in the Heihe River Basin, China. Remote Sensing 7:6886–6907.

Perrig, P. L., S. A. Lambertucci, J. Cruz, P. A. E. Alarcón, P. I. Plaza, A. D. Middleton, G. Blanco, J. A. Sánchez-Zapata, J. A. Donázar, and J. N. Pauli. 2020. Identifying conservation priority areas for the Andean condor in southern South America. Biological Conservation 243:108494.

Perrigo, A., C. Hoorn, and A. Antonelli. 2020. Why mountains matter for biodiversity. Journal of Biogeography 47:315–325.

Pettorelli, N. 2013. The Normalized Difference Vegetation Index. Oxford University Press, Oxford, UK.

Pettorelli, N., S. Ryan, T. Mueller, N. Bunnefeld, B. Jedrzejewska, M. Lima, and K. Kausrud. 2011. The Normalized Difference Vegetation Index (NDVI): Unforeseen successes in animal ecology. Climate Research 46:15–27.

Pimm, S. L., C. N. Jenkins, R. Abell, T. M. Brooks, J. L. Gittleman, L. N. Joppa, P. H. Raven, C. M. Roberts, and J. O. Sexton. 2014. The biodiversity of species and their rates of extinction, distribution, and protection. Science 344.

R Core Team. 2016. R: A language and environment for statistical computing. R Foundation for Statistical Computing, Vienna, Austria. URL https://www.R-project.org/.

Radeloff, V. C., M. Dubinin, N. C. Coops, A. M. Allen, T. M. Brooks, M. K. Clayton, G. C. Costa, C. H. Graham, D. P. Helmers, A. R. Ives, D. Kolesov, A. M. Pidgeon, G. Rapacciuolo, E. Razenkova, N. Suttidate, B. E. Young, L. Zhu, and M. L. Hobi. 2019. The Dynamic Habitat Indices (DHIs) from MODIS and global biodiversity. Remote Sensing of Environment 222:204–214.

Rahbek, C., M. K. Borregaard, R. K. Colwell, B. Dalsgaard, B. G. Holt, N. Morueta-Holme, D. Nogues-Bravo, R. J. Whittaker, and J. Fjeldså. 2019. Humboldt's enigma: What causes global patterns of mountain biodiversity? Science 365:1108–1113.

Razenkova, E., V. C. Radeloff, M. Dubinin, E. V Bragina, M. Allen, M. K. Clayton, A. M. Pidgeon, L. M. Baskin, C. Nicholas, and M. L. Hobi. 2020. Vegetation productivity summarized by the Dynamic Habitat Indices explains patterns of moose abundance across Russia. Scientific Reports 10:1–12.

Revelle, W. 2017. Procedures for Psychological, Psychometric, and Personality Research.

Rose, R. A., D. Byler, J. R. Eastman, E. Fleishman, G. Geller, S. Goetz, L. Guild, H. Hamilton, M. Hansen, R. Headley, J. Hewson, N. Horning, B. A. Kaplin, N. Laporte, A. Leidner, P. Leimgruber, J. Morisette, J. Musinsky, L. Pintea, A. Prados, V. C. Radeloff, M. Rowen, S. Saatchi, S. Schill, K. Tabor, W. Turner, A. Vodacek, J. Vogelmann, M. Wegmann, D. Wilkie, and C. Wilson. 2015. Ten ways remote sensing can contribute to conservation. Conservation Biology 29:350–359.

Roxburgh, S. H., K. Shea, and J. B. Wilson. 2004. The intermediate disturbance hypothesis: Patch dynamics and mechanisms of species coexistence. Ecology 85:359–371.

Roy, D. P., V. Kovalskyy, H. K. Zhang, E. F. Vermote, L. Yan, S. S. Kumar, and A. Egorov. 2016. Characterization of Landsat-7 to Landsat-8 reflective wavelength and normalized difference vegetation index continuity. Remote Sensing of Environment 185:57–70.

Rybicki, J., N. Abrego, and O. Ovaskainen. 2020. Habitat fragmentation and species diversity in competitive communities. Ecology Letters 23:506–517.

Schwarz, G. 1978. Estimating the Dimension of a Model. The Annals of Statistics 6:461–464.

Srivastava, D. S., and J. H. Lawton. 1998. Why more productive sites have more species: An experimental test of theory using tree-hole communities. American Naturalist 152:510–529.

Suttidate, N., M. L. Hobi, A. M. Pidgeon, P. D. Round, N. C. Coops, D. P. Helmers, N. S. Keuler, M. Dubinin, B. L. Bateman, and V. C. Radeloff. 2019. Tropical bird species richness is strongly associated with patterns of primary productivity captured by the Dynamic Habitat Indices. Remote Sensing of Environment 232:1–10.

Tan, B., C. E. Woodcock, J. Hu, P. Zhang, M. Ozdogan, D. Huang, W. Yang, Y. Knyazikhin, and R. B. Myneni. 2006. The impact of gridding artifacts on the local spatial properties of MODIS data: Implications for validation, compositing, and band-to-band registration across resolutions. Remote Sensing of Environment 105:98–114.

Vogt, P., J. R. Ferrari, T. R. Lookingbill, R. H. Gardner, K. H. Riitters, and K. Ostapowicz. 2009. Mapping functional connectivity. Ecological Indicators 9:64–71.

Vogt, P., K. H. Riitters, C. Estreguil, J. Kozak, T. G. Wade, and J. D. Wickham. 2007. Mapping spatial patterns with morphological image processing. Landscape Ecology 22:171–177.

Wright, D. H. 1983. Species-energy theory: an extension of species–area theory. Oikos 41:496–506.

Wulder, M. A., T. R. Loveland, D. P. Roy, C. J. Crawford, J. G. Masek, C. E. Woodcock, R. G. Allen, M. C. Anderson, A. S. Belward, W. B. Cohen, J. Dwyer, A. Erb, F. Gao, P. Griffiths, D. Helder, T. Hermosilla, J. D. Hipple, P. Hostert, M. J. Hughes, J. Huntington, D. M. Johnson, R. Kennedy, A. Kilic, Z. Li, L. Lymburner, J. McCorkel, N. Pahlevan, T. A. Scambos, C. Schaaf, J. R. Schott, Y. Sheng, J. Storey, E. Vermote, J. Vogelmann, J. C. White, R. H. Wynne, and Z. Zhu. 2019. Current status of Landsat program, science, and applications. Remote Sensing of Environment 225:127–147.

Wulder, M. A., J. C. White, S. N. Goward, J. G. Masek, J. R. Irons, M. Herold, W. B. Cohen, T. R. Loveland, and C. E. Woodcock. 2008. Landsat continuity: Issues and opportunities for land cover monitoring. Remote Sensing of Environment 112:955–969.

Yang, L., S. Jin, P. Danielson, C. Homer, L. Gass, S. M. Bender, A. Case, C. Costello, J. Dewitz, J. Fry, M. Funk, B. Granneman, G. C. Liknes, M. Rigge, and G. Xian. 2018. A new generation of the United States National Land Cover Database: Requirements, research priorities, design, and implementation strategies. ISPRS Journal of Photogrammetry and Remote Sensing 146:108–123.

Zhang, C., D. Cai, S. Guo, Y. Guan, K. Fraedrich, Y. Nie, X. Liu, and X. Bian. 2016. Spatial-Temporal Dynamics of China ' s Terrestrial Biodiversity: A Dynamic Habitat Index Diagnostic. Remote Sensing 8:1–18.

Zhu, L., and Y. Guo. 2022. Remotely Sensed Winter Habitat Indices Improve the Explanation of Broad-Scale Patterns of Mammal and Bird Species Richness in China. Remote Sensing 14.

Table 1. The time periods for which we calculate the DHIs, operational times of the different satellite, number of scenes that we analyzed, and percent interpolated data.

Period	L4 TM 07/1982 – 12/1993	L5 TM 03/1984-11/2011	L7 ETM+ 04/1999 – 05/2003	L8 OLI 02/2013 – 12/2020	Interpolated time steps (%)
1991-2000	302	70,354	12,521	No data	29.36%
2001-2020	No data	80,663	18,825	66,231	1.71%
2011-2020	No data	7,023	No data	66,231	6.75%
2016-2020	No data	No data	No data	42,662	17.5%

Table 2: Spearman correlation coefficients for the relationships of the three Landsat and MODIS DHIs for Level III (larger, n = 85), and IV (smaller, n = 967) ecoregions, and for the three time periods for which MODIS data were available.

		Ecoregion level III			Ecoregion level IV		
	Time period	Cumulative DHI	Minimum DHI	Variation DHI	Cumulative DHI	Minimum DHI	Variation DHI
Mean	2016-2020	0.99	0.98	0.98	0.99	0.96	0.96
	2011-2020	0.99	0.98	0.99	0.99	0.97	0.97
	2001-2020	0.99	0.98	0.99	0.99	0.97	0.98
Standard Deviation	2016-2020	0.94	0.83	0.60	0.88	0.74	0.63
	2011-2020	0.93	0.86	0.61	0.88	0.79	0.63
	2001-2020	0.94	0.81	0.65	0.89	0.76	0.63

Table 3: Results of linear regression relating the standard deviation of the mean cumulative DHI based on Landsat, within 10,000 randomly selected MODIS pixels, with predictor variables characterizing topography and fragmentation for 2016-2020, 2011-2020, and 2001-2020. Notes: Coefficient estimates (Est.) of variables are shown for univariate linear regression models. Adjusted R^2 are shown for all models, with the highest adjusted R^2 in bold. Significant relationship: *p<0.05, **p<0.01, ***p<0.001, NS not significant. Predictors are elevation, terrain ruggedness index (TRI), percent core and edge area for forest, grassland, and shrubland.

Variables:	2016-2020		2011-2020		2001-2020	
	Est.	adjR^2	Est.	adjR^2	Est.	adjR^2
Univariate models:						
Elevation mean	0.00	0.05***	0.00	0.05***	0.00	0.06***
Elevation std.dev.	0.01	0.02***	0.01	0.02***	0.01	0.02***
TRI mean	0.00	0.00NS	0.00	0.00NS	0.00	0.00NS
TRI std.dev.	0.00	0.00NS	0.00	0.00NS	0.00	0.00NS
Core forest	0.09	0.00***	0.09	0.00***	0.09	0.00***
Edge forest	0.54	**0.14*****	0.56	**0.15**	0.57	**0.15*****
Core grassland	-0.31	0.04***	-0.30	0.03	-0.30	0.03***
Edge grassland	-0.01	0.00NS	-0.01	0.00NS	-0.04	0.00NS
Core shrubland	-0.45	**0.13*****	-0.45	**0.13**	-0.48	**0.15*****
Edge shrubland	-0.09	0.00***	-0.07	0.00***	-0.12	0.00***
Multiple regression model:						
Elevation mean+Edge forest+Core grassland+Core shrubland		0.26				
Edge forest+Core grassland+Core shrubland				0.25		0.26

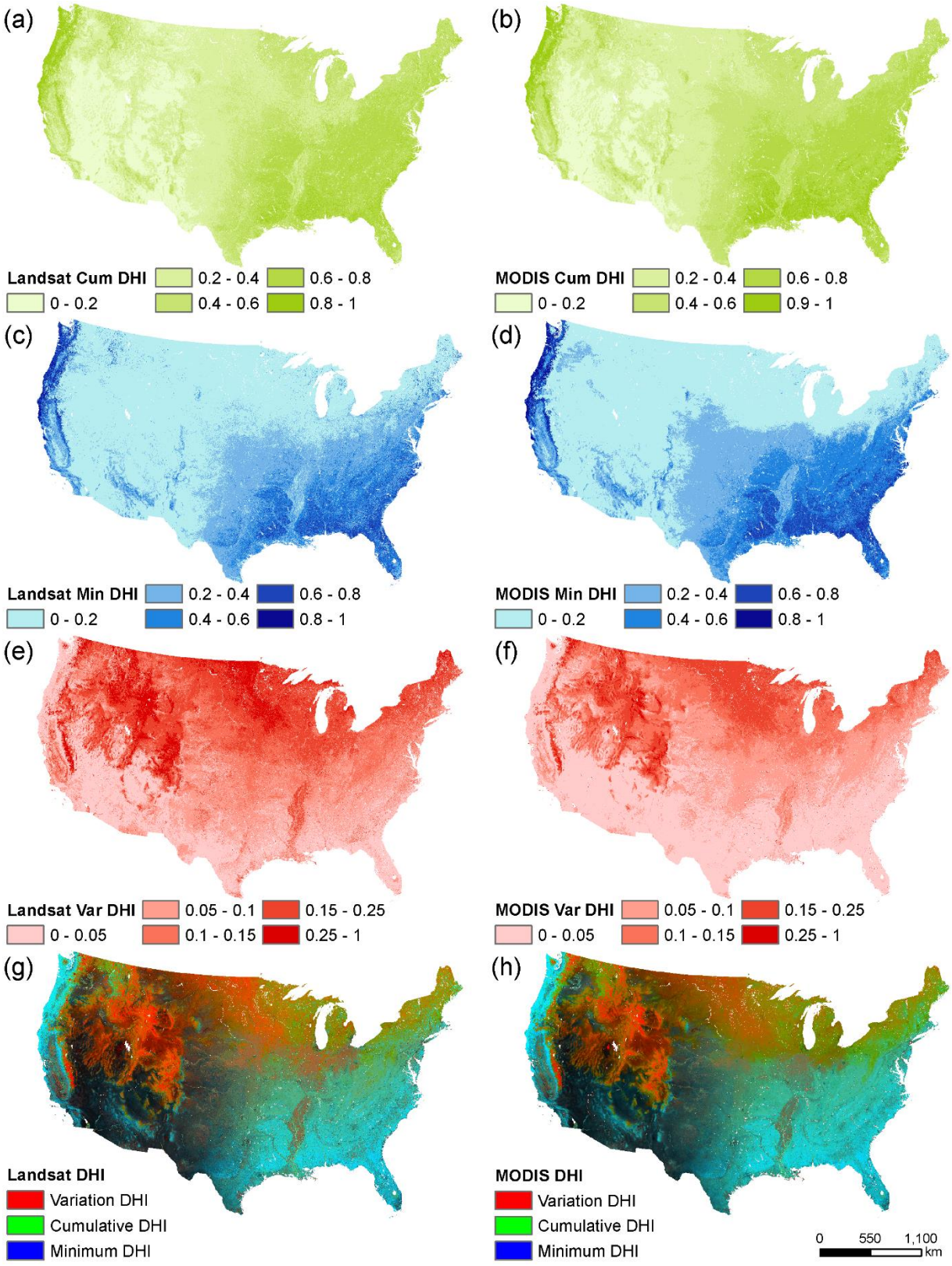
(a)
Landsat Cum DHI
0 - 0.2
0.2 - 0.4
0.4 - 0.6
0.6 - 0.8
0.8 - 1
(b)
MODIS Cum DHI
0 - 0.2
0.2 - 0.4
0.4 - 0.6
0.6 - 0.8
0.9 - 1
(c)
Landsat Min DHI
0 - 0.2
0.2 - 0.4
0.4 - 0.6
0.6 - 0.8
0.8 - 1
(d)
MODIS Min DHI
0 - 0.2
0.2 - 0.4
0.4 - 0.6
0.6 - 0.8
0.8 - 1
(e)
Landsat Var DHI
0 - 0.05
0.05 - 0.1
0.1 - 0.15
0.15 - 0.25
0.25 - 1
(f)
MODIS Var DHI
0 - 0.05
0.05 - 0.1
0.1 - 0.15
0.15 - 0.25
0.25 - 1
(g)
Landsat DHI
Variation DHI
Cumulative DHI
Minimum DHI
(h)
MODIS DHI
Variation DHI
Cumulative DHI
Minimum DHI
0
550
1,100
km

Figure 1. The DHIs based on Landsat and MODIS calculated over 20 years (2001-2020): (a) cumulative DHI based on Landsat, (b) cumulative DHI based on MODIS, (c) minimum DHI based on Landsat, (d) minimum DHI based on MODIS, (e) variation DHI based on Landsat, (f) variation DHI based on MODIS, (g) Landsat DHIs are shown in RGB where red = variation DHI, green = cumulative DHI, blue = minimum DHI, (h) MODIS DHIs are shown in RGB where red = variation DHI, green = cumulative DHI, blue = minimum DHI.

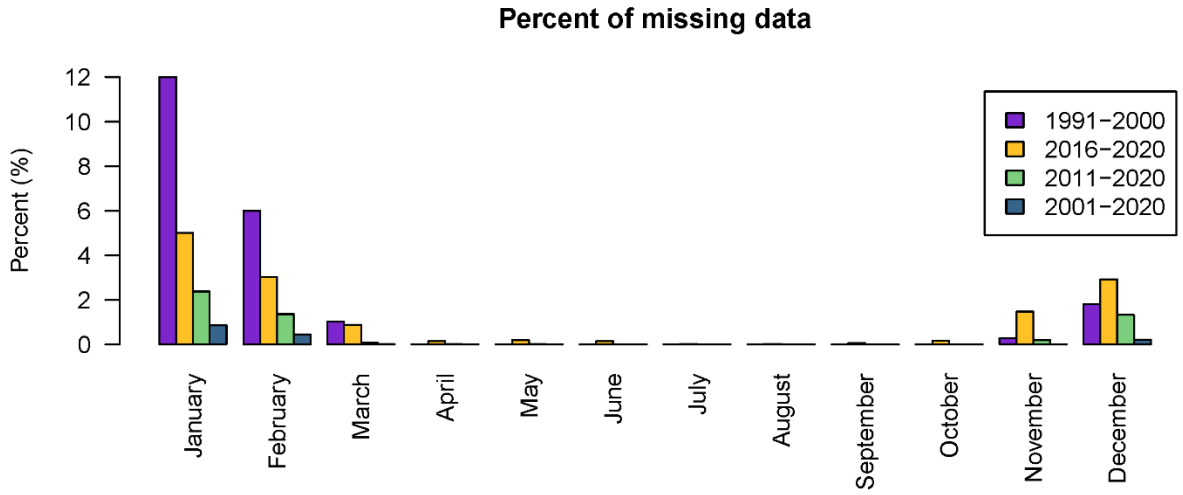

Figure 2: Percent of missing Landsat data for each month for our four time periods. Interpolation was for the most part only necessary in winter months, when productivity is zero in most of the conterminous U.S.

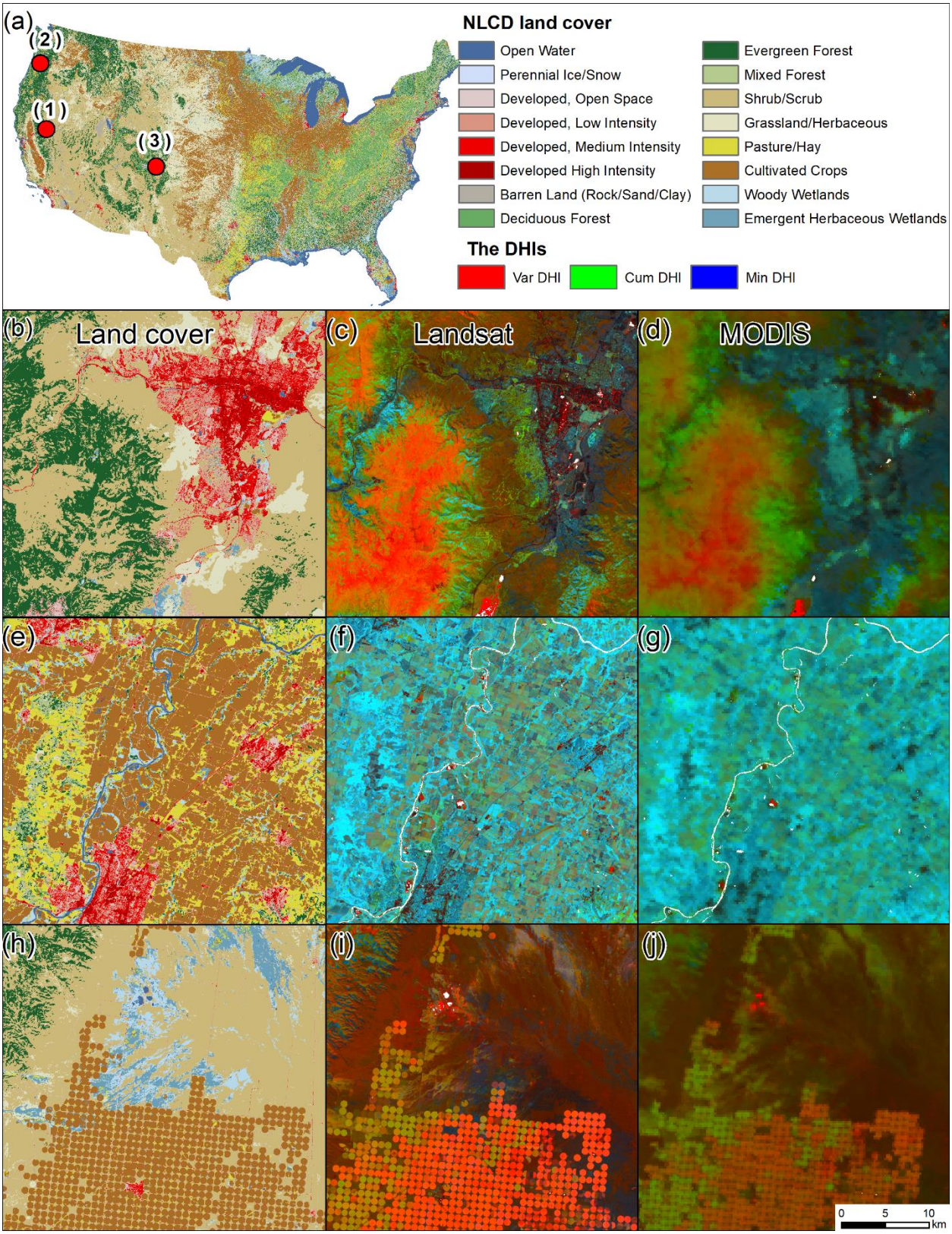
(a)
(2)
(1)
(3)
NLCD land cover
Open Water
Perennial Ice/Snow
Developed, Open Space
Developed, Low Intensity
Developed, Medium Intensity
Developed High Intensity
Barren Land (Rock/Sand/Clay)
Deciduous Forest
Evergreen Forest
Mixed Forest
Shrub/Scrub
Grassland/Herbaceous
Pasture/Hay
Cultivated Crops
Woody Wetlands
Emergent Herbaceous Wetlands
The DHIs
Var DHI
Cum DHI
Min DHI
(b) Land cover
(c) Landsat
(d) MODIS
(e)
(f)
(g)
(h)
(i)
(j)
0 5 10
km

Figure 3: Data layers corresponding to three sampled landscapes (a, b, e, h). First column: the 2016 version of Landsat-based National Land Cover Database (NLCD); second column: the DHIs based on Landsat; third column: the DHIs based on MODIS (2016-2020). The DHIs are shown in RGB where red is the variation DHI, green the cumulative DHI, and blue the minimum DHI.

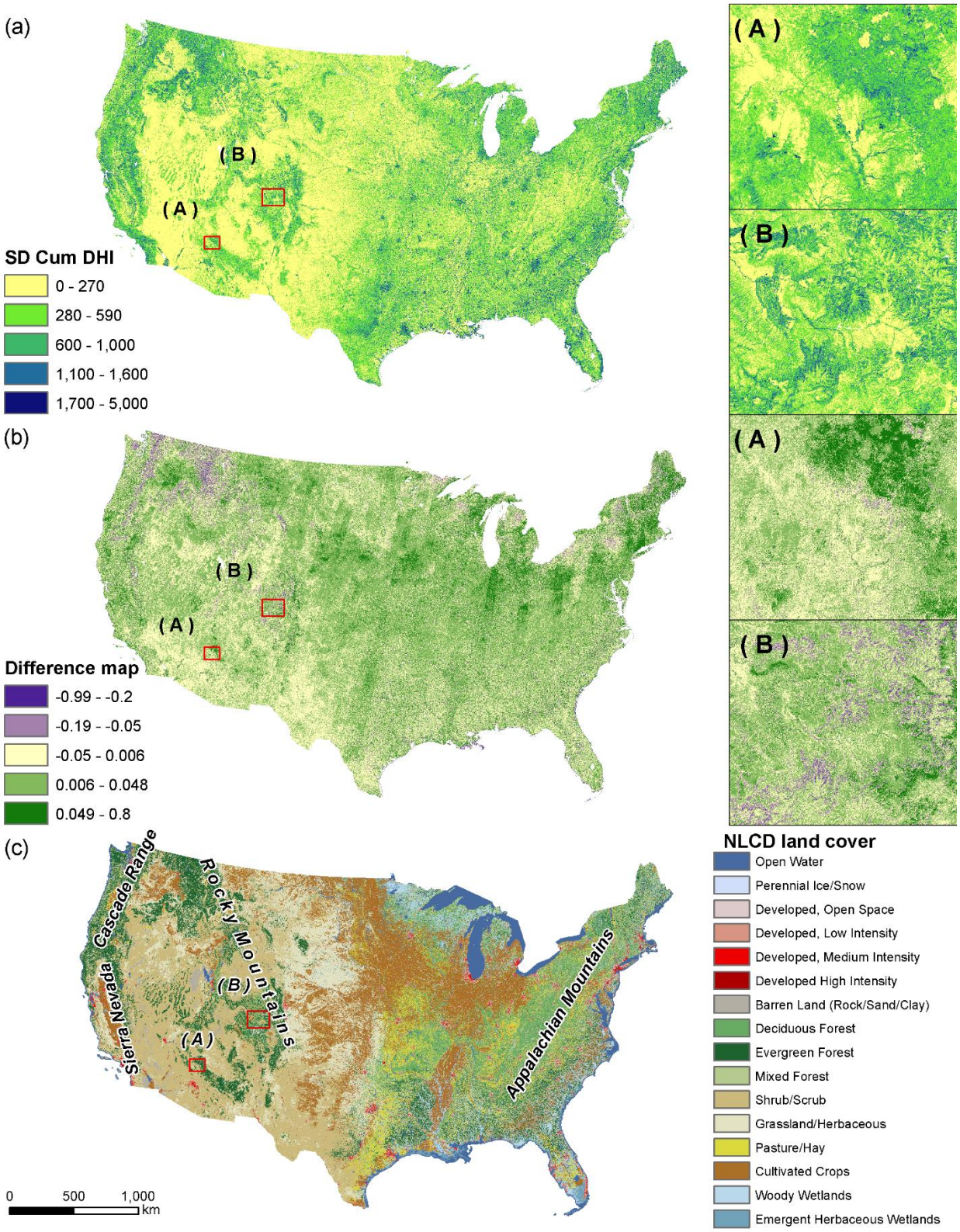
(a)
(B)
(A)
SD Cum DHI
0 - 270
280 - 590
600 - 1,000
1,100 - 1,600
1,700 - 5,000
(b)
(B)
(A)
Difference map
-0.99 - -0.2
-0.19 - -0.05
-0.05 - 0.006
0.006 - 0.048
0.049 - 0.8
(c)
Cascade Range
Rocky Mountains
Sierra Nevada
(B)
(A)
Appalachian Mountains
0
500
1,000
km
(A)
(B)
(A)
(B)
NLCD land cover
Open Water
Perennial Ice/Snow
Developed, Open Space
Developed, Low Intensity
Developed, Medium Intensity
Developed High Intensity
Barren Land (Rock/Sand/Clay)
Deciduous Forest
Evergreen Forest
Mixed Forest
Shrub/Scrub
Grassland/Herbaceous
Pasture/Hay
Cultivated Crops
Woody Wetlands
Emergent Herbaceous Wetlands

Figure 4: (a) The standard deviation of the cumulative DHI based on Landsat within each MODIS pixel; (b) the difference map of the MODIS cumulative DHI and Landsat cumulative DHI for 2011-2020 (MODIS - Landsat); (c) the 2016 version of Landsat-based National Land Cover Database (NLCD). The panel on the right highlight regions with diverse topography and land cover.

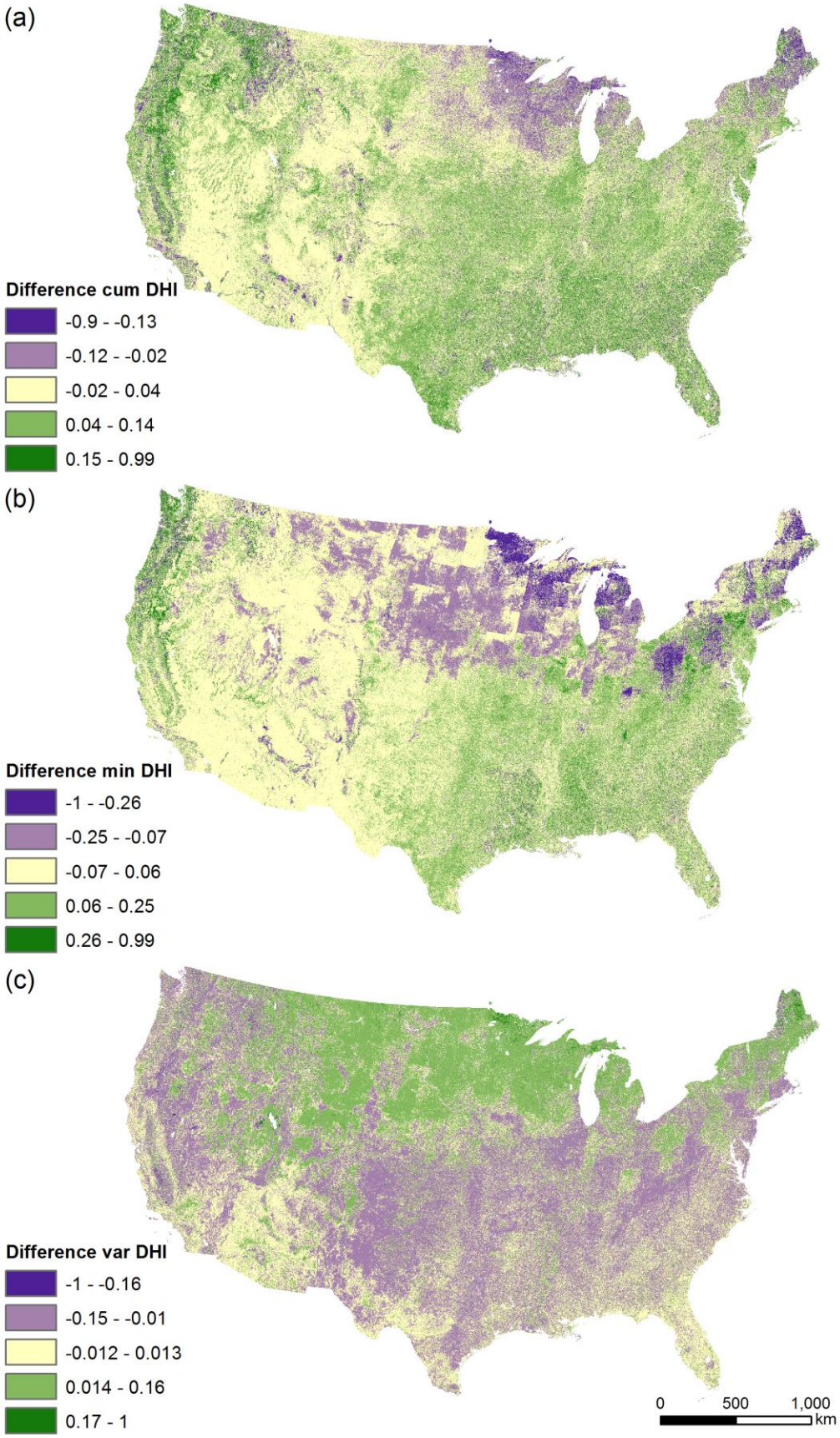
(a)
Difference cum DHI
-0.9 - -0.13
-0.12 - -0.02
-0.02 - 0.04
0.04 - 0.14
0.15 - 0.99
(b)
Difference min DHI
-1 - -0.26
-0.25 - -0.07
-0.07 - 0.06
0.06 - 0.25
0.26 - 0.99
(c)
Difference var DHI
-1 - -0.16
-0.15 - -0.01
-0.012 - 0.013
0.014 - 0.16
0.17 - 1
0
500
1,000
km

Figure 5: The difference map of the Landsat DHIs for 2011-2020 minus those for 1991-2000. Green areas decreased in the respective DHI; purple areas increased.

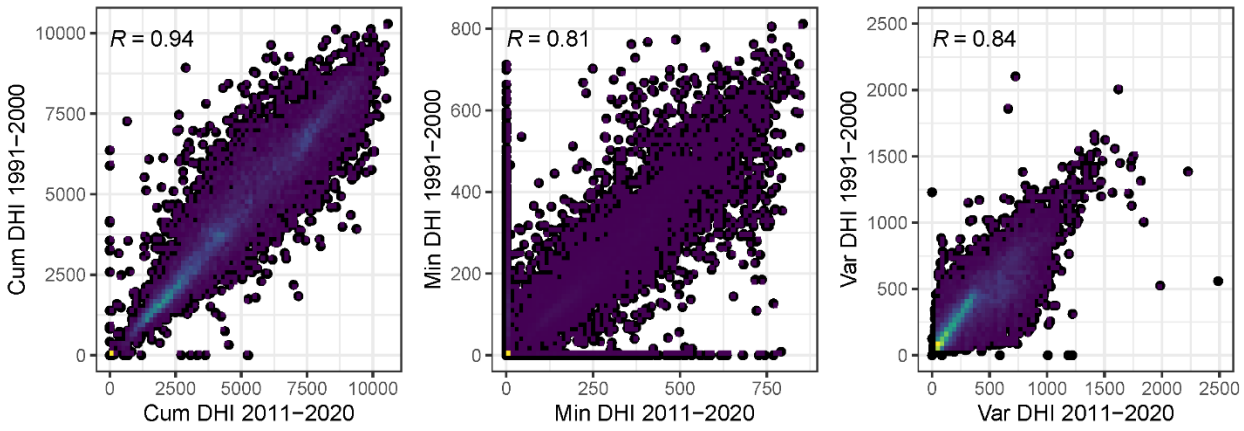

Figure 6: Spearman correlation between the Landsat DHIs calculated over 1991-2000 and 2011-2020.

Appendix 1: Spatial distribution of missing data over conterminous US over five, ten, and twenty years. Missing data over five years (2016-2020) shown in yellow color, over five and ten years (2016-2020 and 2011-2020) in blue color, over five, ten and twenty years (2016-2020, 2011-2020, 2001-2020) are shown in pink color. Gray color indicated that Landsat data are available.

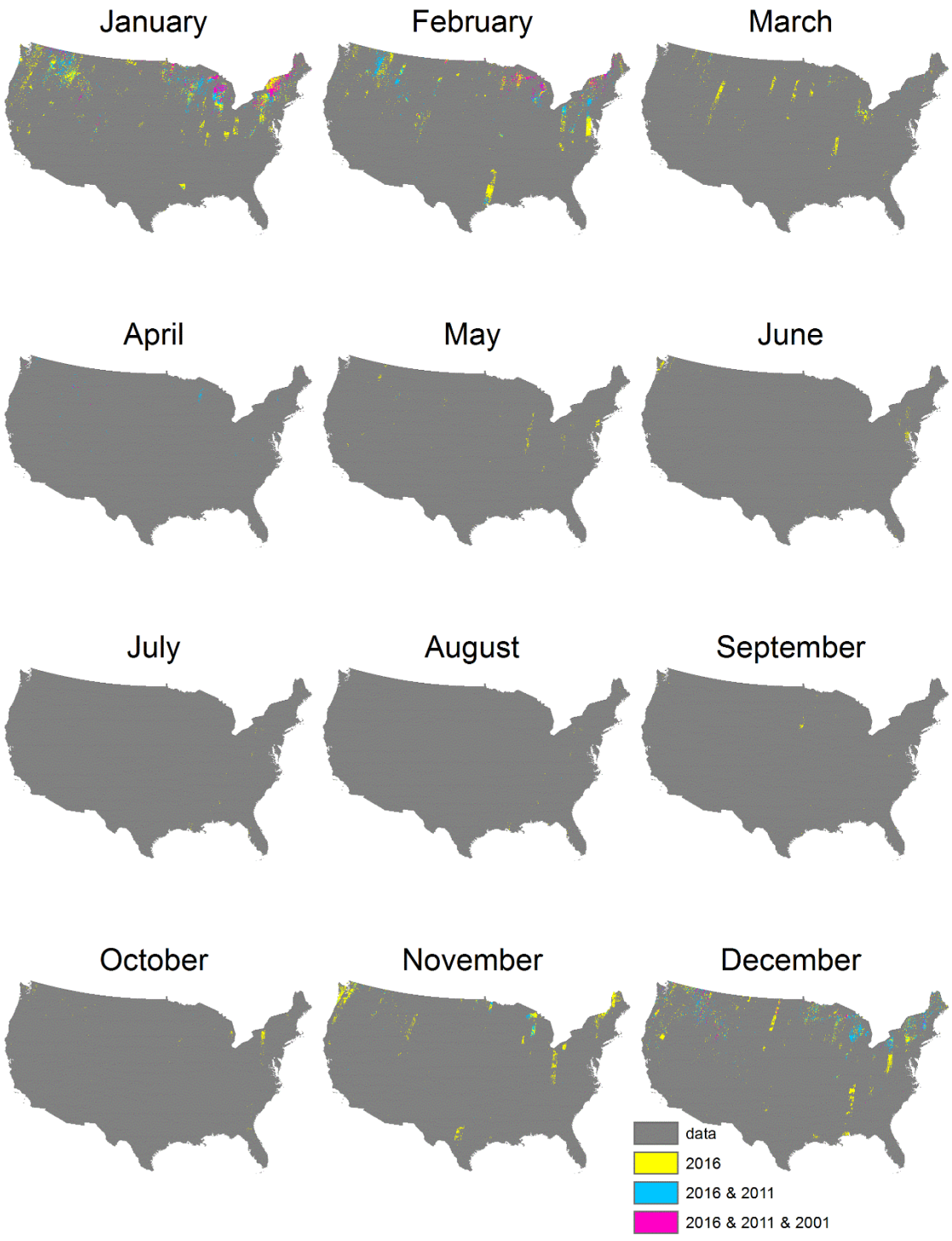
January
February
March
April
May
June
July
August
September
October
November
December
data
2016
2016 & 2011
2016 & 2011 & 2001

Appendix 2: Pearson correlations between explanatory variables in model for second objective. Abbreviations are ElevMean and ElevSD- mean and standard deviation of elevation, TRIMean and TRISD- mean and standard deviation of terrain ruggedness index, pFORCore and pFOREgde- percent of core and percent of edge of forest, pGRCore and pGREgde- percent of core and percent of edge of grassland cover, pSHRCore and pSHREgde- percent of core and percent of edge of shrubland cover.

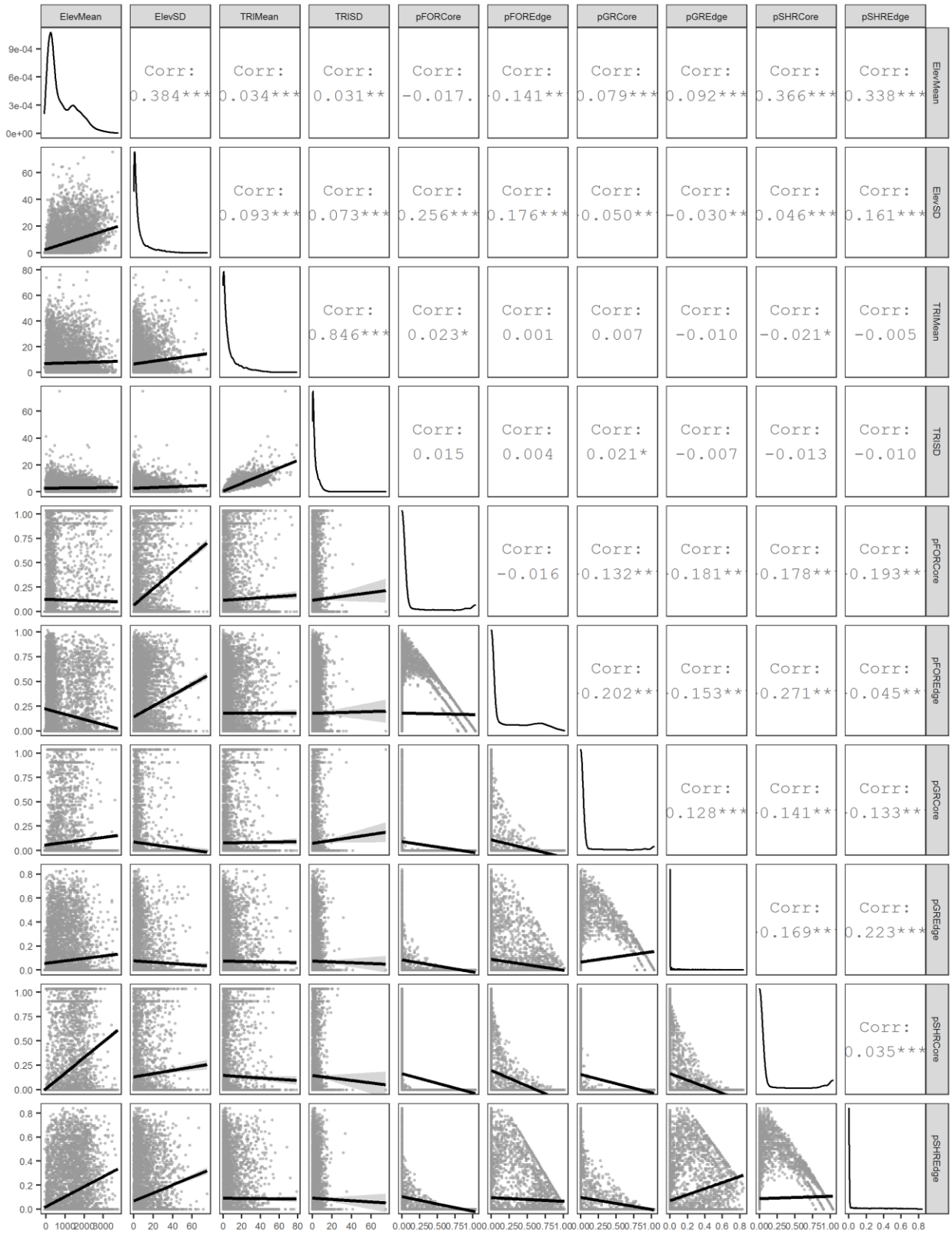
ElevMean
ElevSD
TRIMean
TRISD
pFORCore
pFOREdge
pGRCore
pGREdge
pSHRCore
pSHREdge
Corr: 0.384***
Corr: 0.034***
Corr: 0.031**
Corr: -0.017.
Corr: -0.141**
Corr: 0.079***
Corr: 0.092***
Corr: 0.366***
Corr: 0.338***
Corr: 0.093***
Corr: 0.073***
Corr: 0.256***
Corr: 0.176***
Corr: -0.050**
Corr: -0.030**
Corr: 0.046***
Corr: 0.161***
Corr: 0.846***
Corr: 0.023*
Corr: 0.001
Corr: 0.007
Corr: -0.010
Corr: -0.021*
Corr: -0.005
Corr: 0.015
Corr: 0.004
Corr: 0.021*
Corr: -0.007
Corr: -0.013
Corr: -0.010
Corr: -0.016
Corr: 0.132**
Corr: 0.181**
Corr: 0.178**
Corr: 0.193**
Corr: 0.202**
Corr: 0.153**
Corr: 0.271**
Corr: 0.045**
Corr: 0.128***
Corr: 0.141**
Corr: 0.133**
Corr: 0.169**
Corr: 0.223***
Corr: 0.035***

Chapter 2: Explaining bird richness with the Dynamic Habitat Indices across the conterminous US

Abstract

Biodiversity is declining at an unprecedented rate, and effective conservation necessitates understanding the drivers of species richness patterns. Vegetation productivity derived from satellite data captures available energy in ecosystems, allowing the generation of relevant indices for biodiversity. One such group of indices, the Dynamic Habitat Indices (DHIs) from 1-km MODIS, strongly predict avian species richness. Our goal was to test the ability of the DHIs calculated from higher spatial but lower temporal resolution (30-m, 16-day Landsat) satellites to capture patterns of vegetation productivity and explain bird richness across the conterminous United States and compare their performance with DHIs derived from coarser spatial but higher temporal resolution products (250-m, 1-2 day MODIS). We also assessed the relative importance of Landsat DHIs compared with other commonly used variables to explain bird richness. In addition, we explored the relationship between Landsat DHIs and bird richness from 1991-2000. Using North American Breeding Bird Survey (BBS) data, we calculated richness as four sets of all species and within 21 functional guilds over two periods (1991-2000 and 2011-2019). We calculated the DHIs from Landsat (1991-2000 and 2011-2020) and MODIS data (2011-2020) and summarized both grains at four spatial extents, designed to match the four sets of bird data a) within 85 Level III ecoregions, b) 5-km square buffers around BBS routes, c) 2.5-km square buffers for the first-ten-stops, and d) 0.5-km square buffers for first points. The predictive performance of DHIs based on Landsat and MODIS across the four spatial extents was very similar and explained up to 48% of the variance in bird richness in univariate linear regression models. In multivariate models combining Landsat DHIs with topography and land cover, we found the DHIs complemented other variables and explained up to 64% of the variance in bird

richness. The predictive performance of 1991-2000 Landsat DHIs was similar to that of 2011-2020, suggesting good overall accuracy and consistency. Our results highlight the usefulness of Landsat DHIs for measuring vegetation productivity and explaining species richness at broad scales. We show that Landsat DHIs have great potential for understanding how changes in DHIs over time may influence biodiversity.

Introduction

Biodiversity is declining at an unprecedented rate, and a major cause of this decline is anthropogenic factors (Rockström et al. 2009, Pimm et al. 2014). Humans dramatically change ecosystems through land use and land cover change (Sleeter et al. 2013, Sohl et al. 2014), with profound consequences for biodiversity (Sala et al. 2000, Hansen et al. 2013, Haddad et al. 2015). Effective conservation efforts rely on a broad-scale understanding of the drivers of biodiversity patterns (Pereira et al. 2013). In this capacity, satellite data provide meaningful information about the biophysical characteristics of ecosystems (Turner et al. 2003, Cavender-Bares et al. 2022) and are suitable for monitoring biodiversity patterns across the globe (Wright 1983, Gaston 2000, Mittelbach et al. 2001, Hawkins et al. 2003a, 2003b, Bonn et al. 2004).

Species richness is a key component of biodiversity and is positively correlated with net primary productivity (NPP) (Paruelo et al. 1997). Remotely sensed vegetation indices such as the normalized difference vegetation index (NDVI) characterize NPP at broad scales and consequently are related to species richness (Myneni et al. 1995, Skidmore et al. 2003, Cohen and Goward 2004, Pettorelli et al. 2011). The Dynamic Habitat Indices (DHIs) are integrated measures of vegetation productivity summarized as a) year-round overall productivity; b) available minimum productivity during the winter season; and c) variation in productivity, and are effective predictors of species richness at regional and global scales (Coops et al. 2009, Hobi

et al. 2017, Radeloff et al. 2019). Moreover, the DHIs derived from various MODIS products have been successfully used to explain tropical species richness in Thailand (Suttidate et al. 2019), model distributions of bird species in California (Burns et al. 2020), explain broad patterns of mammal and bird richness in China (Zhu and Guo 2022), and explain abundance and occurrence of mammals (Michaud et al. 2014, Razenkova et al. 2020). The frequency of MODIS observations also allows the calculation of annual DHIs to explain inter annual variability in bird richness (Hobi et al. 2021). However, MODIS DHIs can be too coarse to be useful for relating to some species, as in cases where breeding territories are smaller than a 1-km MODIS pixel. Moreover, higher spatial resolution satellite data can capture spatial heterogeneity at finer scales, which is an important predictor of species distributions and richness. However satellites with higher spatial resolutions capture images less frequently per location than satellites with coarser spatial resolutions, especially prior to the launch of Landsat 7 in 1999. Thus, there are potential tradeoffs between numbers of available images versus spatial resolution, in calculating the DHIs using satellite data for a given period. A key question is: do higher spatial resolution DHIs (Landsat) provide similar explanatory power in models of species richness as the DHIs calculated with coarse resolution (MODIS) data, despite incorporating fewer images?

Another advantage of Landsat is its long-term record, starting in 1972, which allows for long-term monitoring of Earth's surface and advances our understanding of global terrestrial changes (Wulder et al. 2008, 2019, Kennedy et al. 2014). However, Landsat data are not uniformly distributed in space and time, which creates additional challenges in the calculation of DHIs for different time periods. Our next question is: do Landsat DHIs calculated over different time periods provide similar explanatory power in models as those calculated over the most recent decade (2011-2020)? To answer this question, we selected Landsat data from 1991-2000,

when three satellites were in orbit (Landsat 4, 5, and 7). The spatial coverage for some areas was limited, resulting in the DHIs calculated over 1991-2000 requiring more interpolated data (see method for more details).

We modeled bird species richness because birds are effective indicators of biodiversity and respond strongly to vegetation productivity (Hurlbert and Haskell 2003, Bailey et al. 2004, Bonn et al. 2004, Hunt et al. 2022). Moreover, they quickly respond to ecosystem changes, have diverse ecological functions, and are highly mobile (Cody 1981, Sekercioglu 2006). Observed steep declines in bird abundance (Pimm et al. 2014) raise serious concerns about ecosystem health as well as human well-being, because birds provide numerous ecosystem services such as pest control, pollination, fertilizer, and seed dispersal (Sekercioglu 2006). The North American Breeding Bird Survey (BBS, (Sauer et al. 2017)) is a long-term bird abundance and occurrence dataset. It provides an opportunity to explore the relationship between the DHIs and bird richness and test whether higher spatial resolution DHIs provide greater predictive power than coarse DHIs in species richness models. The long record of Landsat and BBS data enables exploration of the relationship between vegetation productivity and bird species richness in the past.

We hypothesized that sites with high vegetation productivity also have high vegetation structural complexity and can therefore support more species than areas with low productivity and structural complexity. Habitat structural complexity is an important determinant of species richness (MacArthur 1964), and vegetation heterogeneity provides more niche space which may, in turn, support greater biodiversity (Tews et al. 2004). Due to their higher spatial resolution, the Landsat DHIs are better suited to capture heterogeneity in vegetation productivity, and thus may provide more explanatory power in modeling birds that depend on heterogeneous landscapes, such as forest and shrubland species (Bar-Massada and Wood 2014, Farwell et al. 2021). We

also expected richness of permanent residents and birds with small body sizes may be better predicted by Landsat DHIs, as these groups must make greater adjustments to maintain suitable body temperature to survive during harsh seasons than migrants and large-bodied species, and heterogeneous landscapes provide a variety of options for escaping unfavorable weather conditions (Scholander et al. 1950, Elsen et al. 2020).

The DHIs contain ecologically relevant and unique information for biodiversity that may complement other environmental variables that drive biodiversity patterns, such as land cover and topography (Suttidate et al. 2019). To evaluate the relative importance of Landsat DHIs against other variables commonly used to model bird richness, we combined the DHIs, topography, and land cover in models. We focused on topography and land cover in particular because both affect bird richness (Turner et al. 2003).

Our primary goal was to evaluate the predictive performance of the DHIs based on 30-m Landsat and compare them with 250-m MODIS in bird richness models. Specifically, we examined the following questions:

- Do the Landsat and MODIS DHIs provide comparable predictive power in models of bird richness across four spatial extents?
- Do the Landsat DHIs provide higher predictive power than MODIS DHIs in models of bird richness within heterogeneous landscapes?
- What is the relative importance of Landsat DHIs in bird richness models compared with topography and land cover?

- What is the predictive power of the Landsat DHIs calculated over 1991-2000 compared with the Landsat DHIs calculated over 2011-2020?

We expected that the Landsat DHIs would have higher predictive power compared to the MODIS DHIs in models of bird guilds for which species richness within a given habitat is typically positively associated with habitat heterogeneity, including forest and shrubland birds, permanent residents, and birds with small body sizes, because Landsat DHIs provide more information about heterogeneous cover than MODIS DHIs, especially in complex terrain. However, we expected no differences in predictive power between the Landsat and MODIS DHIs for grassland birds, because richness in this guild depends on relatively subtle differences in grass species, density, and height, which are probably equally well captured by both satellites. Among our four spatial extents, we expected to see greater differences in predictive power between the Landsat and MODIS DHIs for the first ten-stops (representing one-fifth of BBS data available) and the first stop of BBS routes (representing one-fiftieth of BBS data available) and that the predictive power of models would be highest for ecoregions (the largest extent) and lowest for the first stop along a BBS route (the smallest extent) due to greater species richness dynamic range at the ecoregion scale. For combined models, we expected that the Landsat DHIs would complement the other environmental variables and increase the overall predictive power of the models. Finally, we expected that the Landsat DHIs calculated over 1991-2000 would provide similar predictive power as the Landsat DHIs calculated over 2011-2020, despite a larger percent of interpolated data in the earlier time steps. However, we also expected changes in bird species richness over time associated with land cover and other habitat suitability changes, and in particular we expected a decline in richness of birds of conservation concern (i.e., threatened species).

Methods

The DHIs from Landsat and MODIS data

The Dynamic Habitat Indices (DHIs) summarize vegetation productivity in three ways that are relevant for biodiversity: the overall productivity (cumulative DHI), minimum productivity (minimum DHI), and seasonal variation in vegetation productivity (variation DHI) (Radeloff et al. 2019). We used the DHIs calculated from the normalized difference vegetation index (NDVI) based on 30-m Landsat and 250-m MODIS data. Full details regarding the calculation of the DHIs based on Landsat and MODIS are described previously (Razenkova et al. n.d., Hobi et al. 2017, Radeloff et al. 2019). In short, we calculated the DHIs from a time series of 1991-2000 and 2011-2020 median monthly values of Landsat NDVI for conterminous US. To calculate Landsat NDVI we used bands 3 and 4 of Landsat 4, 5, and 7, and bands 4 and 5 of Landsat 8. To fill gaps in the NDVI composite, we applied linear interpolation. Overall, we interpolated about 29.4% of the data for 1991-2000 and 6.8% for 2011-2020. For the DHIs calculated from MODIS Collection 6, we used the NDVI 16-day composite product at 250-m resolution over 2011-2020. Unlike the monthly NDVI composite for the Landsat DHIs, our MODIS DHIs were based on the median NDVI values for each MODIS time step (16-day composite, 23 total observations) over 2011-2020. Prior to any NDVI calculation, we removed clouds and cloud shadows, replaced pixels with snow and ice with zeros (assuming no photosynthetic activity), and removed water bodies based on a water mask (Hansen et al. 2013). We accessed and processed all remote sensing data in Google Earth Engine (Gorelick et al. 2017). We calculated the three components of the DHIs as follows: 1) cumulative DHI, which is the sum of monthly composite (for Landsat) or 16-day composite (for MODIS) observations; 2)

minimum DHI, which is the lowest NDVI value over the composite; and 3) seasonal DHI, which is the coefficient of variation.

BBS data

BBS data are collected once a year during the breeding season across North America (Sauer et al. 2017). A single BBS route consists of 50 stops spaced evenly along a 39.4-km route along a secondary road. Skilled volunteers observe and record individual birds at each stop, by species, following a standardized protocol. We excluded observations from BBS data when weather conditions during the survey were poor and when surveys were conducted by first-time observers, because these can result in false positive errors (Kendall et al. 1996). We calculated bird species richness by summing the 1991-2000 bird data, and the 2011-2019 data. We organized bird occurrence data into 4 sets that were increasingly site-specific. The most encompassing set included a) all birds detected on BBS routes in each of 85 Level III ecoregions. We also analyzed b) all birds on each BBS route (3,090 routes in 1991-2000 and 3,022 routes in 2011-2019), and subsets of BBS routes. These included c) birds detected on the first 10-stops of each BBS route (2,689 routes in 1991-2000 and 2,979 routes in 2011-2019), and d) birds detected only on the first stop of each route (2,323 routes for 1991-2000 and 2,699 routes for 2011-2019). BBS data were not collected during 2020, so our satellite data extends one year beyond our BBS data.

We separated birds based on habitat association (forest, shrubland, and grassland specialists and affiliates), migratory behavior (residents, short-distance migrants, and long-distance migrants), nest location (ground and mid-story, canopy nesters), IUCN status (threatened species, species with decreasing population trends, and species with stable or increasing population trends), range size (small and large), diet (insectivores, granivores, and

frugivores), and body size (large and small) using BBS classifications and detailed information about bird species from Birds of the World (Billerman et al. 2020). In addition, we separated birds by body size (small and large) by calculating the average body mass of all breeding birds from BBS data, using information about body mass from (Dunning 2008). We assigned species as small-bodied if their average body mass was smaller than the average body mass of all birds; otherwise, we assigned them as large-bodied. In total, we calculated species richness for 21 bird guilds and overall species richness.

Ancillary environmental variables

For elevation, we used the NASA Shuttle Radar Topography Mission (SRTM) digital elevation model (DEM) at 30-m spatial resolution (Farr et al. 2007). From the DEM, we also calculated the terrain ruggedness index (TRI) that characterizes topographic heterogeneity (Riley 1999). We used land cover maps from the 2016 National Land Cover Database (NLCD) at 30-m resolution to characterize land cover composition. We focused on three broad habitat types: forest (including decidious forest, evegreen forest, mixed forest), shrubland (including dwarf scrub, and shrub/scrub), and grassland.

Statistical analysis

For modeling, we calculated the mean and standard deviation of the DHIs based on Landsat (1991-2000 and 2011-2020) and MODIS (2011-2020) at each of four spatial extents, designed to match the four sets of bird data a) within 85 Level III ecoregions, b) 5-km square buffers around the full BBS routes, centered on first-stop locations, c) 2.5-km square buffers for the first-ten-stops, centered on first-stop locations, and d) 0.5-km square buffers for first survey points, centered on first-stop locations (hereafter referred to as four spatial extents: ecoregions, full BBS route, first ten stops, and first stop). We selected buffer sizes based on a previous

assessment of the detection area covered by 1, 10, and 50 BBS survey stops (Carroll et al. 2022). We calculated Spearman correlation coefficients and created scatter plots to explore the relationship between bird richness and the DHIs. For statistical analysis, we fitted a series of linear regressions with our 22 bird richness metrics (overall species richness and richness within 21 guilds) as the response variables and the three components of the Landsat and MODIS DHIs (2011-2020) as the explanatory variables. For each model, we evaluated both linear and quadratic terms of the DHIs to account for potential nonlinear relationships between vegetation productivity and species richness, especially at the finest spatial extent (first stop) (Mittelbach et al. 2001). To compare the performance of the models incorporating Landsat with those using MODIS DHIs (2011-2020) for each functional guild, we considered only one type of regression with either linear or quadratic terms. To assess the predictive power of the Landsat DHIs (1991-2000) in models, we used linear regression, where the response variables were species richness summarized for 1991-2000 for the same bird guilds as above at the four spatial extents (see workflow of the modeling Appendix **3**).

To assess the performance of Landsat and MODIS DHIs in modeling species richness over heterogeneous landscapes, we selected BBS routes only in areas where TRI was >10. TRI provides a quantitative measure of topographic heterogeneity based on the difference between a site's (i.e., pixel’s) elevation and the average deviation of all eight surrounding pixels. Thus, an arbitrarily selected threshold (TRI>10) enabled us to separate homogeneous (i.e., flat) and heterogeneous (i.e., rugged) landscapes and retain a sufficient number of BBS routes for modeling (651 of 3,022 total BBS routes; Appendix **4**). We conducted this analysis only for the full BBS route extent (i.e., 5-km square buffers centered on first-stop locations BBS route) for several functional guilds, including overall species richness, forest affiliates and specialists,

grassland affiliates, shrubland affiliates and specialists, permanent residents, long-distance migrants, short-distance migrants, and small-bodied species. We did not assess grassland specialists due to small sample size. We expected the predictive power would be greater for Landsat than for MODIS DHIs for each of these bird guilds.

To evaluate the relative importance of the DHIs compared with other environmental predictors, we fitted a bird richness model with the Landsat DHIs, elevation, TRI, and proportion of forest, grassland, and shrubland land cover. We ran this analysis only for the full BBS route extent (i.e., 5-km square buffers centered on first-stop locations BBS route). Before fitting models, we first checked the multicollinearity among explanatory variables by calculating Spearman correlation coefficients (Appendix **5**). The highest correlation coefficients were -0.84 between minimum DHI and variation DHI. The remaining variables had a correlation of $|r|<0.8$. We centered and standardized all explanatory variables to make unbiased comparisons of effect sizes. Then, we fitted a linear regression model with all explanatory variables. To identify a set of best performing models, we compared models using the Bayesian Information Criterion (BIC), which penalizes models with larger numbers of explanatory variables. We identified all models with $\Delta BIC<4$, identified the top-ranked model, and then calculated adjusted R2 values for those models to estimate how well each model explained the variation in bird richness. To evaluate the contribution of each explanatory variable in the top-ranked models of species richness (overall species richness and for each of 21 guilds), we plotted standardized regression coefficients with 95% confidence intervals. In addition, we calculated adjusted R2 for top-ranked models without the DHIs. We used variance inflation factors (VIF) to check the top-ranked models for multicollinearity, where a VIF >10 indicates high multicollinearity (O'Brien 2007).

Results

Landsat and MODIS DHIs

We found that Spearman correlation coefficients between the mean of Landsat and MODIS DHIs for 2011-2020 at the four spatial extents were high (0.90 to 1), while the standard deviation varied from 0.51 to 0.93 (Table **4**). As expected, cumulative DHI from the two sensors was most highly correlated among the three components of the DHIs, especially at the broadest spatial scale, ecoregions (r=0.99). The standard deviation of variation DHI had the lowest correlation at the finest spatial scale, the first stop of each BBS route (r=0.51).

BBS routes and bird guilds

The number of BBS observations we analyzed differed across extents and guilds. Across both time periods (1991-2000 and 2011-2019), our BBS data followed expected spatial patterns of species richness with the broadest areas (i.e., ecoregions) having the highest species richness and the smallest areas (i.e., first stops) having the lowest (Figure **7**, Appendix 6). We found that average bird richness was similar between 1991-2000 and 2011-2019, it was slightly lower in the 1991-2000 than in the second period at the scale of the first ten stops and the first stops (Appendix 7). Trends in bird richness varied by guild at the ecoregion scale (Appendix 7). Declines in bird richness ranged from 0.15-1.54 across the two time periods, with forest affiliates experiencing the steepest declines. Some guilds increased in bird richness (ranging from 0.40-1.19), with residents showing the greatest increase.

Landsat and MODIS DHIs as predictors of 2011-2020 species richness

We found that the three components of the Landsat DHIs provide comparable predictive power as the MODIS DHIs, with slightly higher performance for most bird guilds and across all

four spatial extents (Table **5**). However, neither the Landsat nor the MODIS DHIs were uniformly included in the best models across guilds and extents. Cumulative DHI provided the highest predictive power at larger spatial extents (ecoregions and full BBS routes) and explained 10-48% of the variance of the 21 guilds. For example, cumulative DHI was the strongest predictor of shrubland specialists at these extents. At smaller spatial extents (first ten stops and first stop), the cumulative DHI model also best explained variance of the guild composed of species with stable/increasing populations (38%). Overall, the Landsat cumulative DHI was a stronger predictor than the MODIS cumulative DHI for most bird guilds. MODIS DHIs explained more variance than Landsat DHIs only for residents, small-ranged, and large-bodied bird guilds at the ecoregion scale.

Minimum DHI was generally the second strongest predictor of bird species richness. However, it had higher predictive power at the ecoregion scale for grassland specialists, short-distance migrants, and species with decreasing population sizes. (Table **5**). Minimum DHI was a strong predictor of grassland affiliates and specialists, residents, short-distance migrants, ground nesters, granivores, and threatened, decreasing, and large-ranged species, explaining 20-38% of the variation in species richness of these guilds. When comparing the predictive performance of minimum DHI based on Landsat and MODIS, MODIS minimum DHI performed better for more guilds than Landsat overall. However, Landsat minimum DHI performed better for grassland affiliates and specialists across all four spatial extents.

Variation DHI tied with minimum DHI in having high explanatory power for grassland specialists, and also was strongly associated with substantial variation in residents, long-distance and short-distance migrants, decreasing, small-ranged, and large-ranged bird guilds, accounting for 18-47% of the variation in species richness. Landsat variation DHI performed better than

MODIS and was the strongest predictor for large-ranged species. Overall, the Landsat DHIs had higher predictive power than MODIS DHIs for all functional guilds except for residents, short-distance migrants, threatened, small-ranged, and large-bodied species, and had comparable predictive power in models for shrubland specialists and granivores.

In most cases, we observed non-linear relationships between vegetation productivity and species richness across our four spatial extents, as models with quadratic terms performed better than those without (Table **5**). We did not find evidence that the shape or directionality of the relationships between bird richness and the DHIs differed between Landsat and MODIS. However, we noticed directionality differed for some guilds depending on the spatial extent. For example, overall species richness had a negative relationship with cumulative and minimum DHI at the ecoregion scale but a positive relationship at the full route and first ten stops scales (Figure 2). We observed similar patterns for all guilds except grassland affiliates and specialists, and shrubland specialists (Table **5**).

Performance of the Landsat and MODIS DHIs over heterogeneous landscapes

Our second objective was to compare the predictive performance of Landsat and MODIS DHIs in models of bird richness within heterogeneous landscapes. We found that the Landsat DHIs provided greater explanatory power (1-2%) than the MODIS DHIs for overall species richness, forest affiliates and specialists, grassland affiliates, shrubland affiliates and specialists, and species with small body sizes (Table **6**). There was no difference in explanatory power between Landsat and MODIS DHIs in bird richness models for residents (minimum DHI), long-distance migrants (cumulative DHI and minimum DHI), or short-distance migrants (minimum DHI). The predictive power of models for the heterogeneous landscape subset was lower than for the full dataset models except for shrubland affiliates and small-bodied species (Table **5**, Table

6). For example, the Landsat cumulative DHI explained only 21% of the variance in overall species richness in heterogeneous landscapes versus 30% of the same model for the full dataset. In contrast, the Landsat cumulative DHI explained 17 % and 27% of the variance in shrubland affiliates in heterogeneous landscapes compared with 4% of the same models for the full dataset.

Relative importance of the Landsat DHIs in the global model

The top-ranked models explained between 13-64 % of the variance in bird richness and included two topographic (elevation, TRI), three land cover metrics (proportion of forest, grassland, and shrubland cover), and the three Landsat DHIs (cumulative, minimum, and variation DHI; Table 4). The models explaining granivores, ground nesters, and large-bodied species had lower predictive power and explained only 13%, 17%, and 20% of the variance, respectively. Our top-ranked models included different combinations of explanatory variables, but all included at least two components of the Landsat DHIs, one variable related to land cover, and one variable related to topography. Only one top-ranked model (for large-ranged species) did not include any topographic metric. Cumulative DHI had the strongest positive effect on species richness for most bird guilds except grassland specialists and affiliates, shrubland specialists and affiliates, and small-ranged species (Figure **9**). Minimum DHI had the second strongest negative effect on species richness; only a few bird guilds, including shrubland specialists, threatened, and small-ranged species, had positive relationships with minimum DHI. Although variation DHI had the weakest effect among the three DHI components, it strongly negatively affected shrubland affiliates, shrubland specialists, and residents.

Among land cover classes, the proportion of forest cover was the most important predictor, with greater effect than either the proportion of grassland or shrubland cover for forest specialists (as expected), residents, and large- and small-bodied species (Figure **9**). The

proportion of grassland cover had a strong negative effect on overall species richness and forest affiliates, again as expected. Only grassland affiliates and specialists had a positive relationship with the proportion of grassland cover. Yet, although the proportion of grassland cover had a weak effect on other bird guilds, it was included in most top-ranked models and negatively influenced species richness. Based on effect, the proportion of shrub cover had stronger negative effects on granivores than other predictors, and a positive influence on shrub specialists and affiliates, ground nesters, insectivores, small-ranged, and small-bodied species.

Elevation had a strong positive effect on forest affiliates, forest specialists, short-distance migrants, and species with stable/increasing population trends, and a negative effect on shrubland affiliates, shrubland specialists, residents, threatened species, species with decreasing population trends, and granivores, based on top-ranked models (Table **7**). Terrain ruggedness was important and positively influenced overall species richness, forest affiliates, forest specialists, mid-story and canopy nesters, stable/increasing species, small-ranged and small-bodied birds, and insectivores (Figure **9**). Furthermore, terrain ruggedness was selected in top-ranked models (18 of 22) more often than elevation (12 of 22).

Variance inflation factors (VIFs) for all variables in top-ranked models were <10, indicating an acceptable level of collinearity between explanatory variables (Appendix 8) (O'Brien 2007). In summary, we found that the DHIs were important predictors and had a stronger effect on species richness for all bird guilds than topographic and land cover metrics. After removing the DHIs from top-ranked models, adjusted R2 declined from 4-45%, and large-ranged bird had the largest decline in adjusted R2 (last column in Table **7**).

The Landsat DHIs as predictors for species richness for 1991-2000

We found no substantial difference in the performance of Landsat DHIs in bird richness models between 1991-2000 and 2011-2020, at any extents (Table **5**, Table **8**), except granivores. The difference in variance explained by Landsat DHIs for the 1990s compared to the 2010s ranged from 0-0.13. Granivores had the largest decline in variance explained from 40% (cumulative DHI for the 2010s) to 27% (cumulative DHI for the 1990s) at the ecoregion scale.

Discussion

The main goal of this work was to evaluate the performance of the Landsat and MODIS DHIs in modeling species richness for 21 bird guilds and overall species richness at four spatial extents across the conterminous US. We found that the Landsat DHIs provided comparable and, in some cases, slightly higher predictive power than the MODIS DHIs in bird richness models, providing evidence that medium-resolution satellite imagery captures important habitat characteristics at relevant scales for species richness. Individual components of the DHIs can explain up to 48% (Landsat and MODIS cumulative DHI) of the variance in bird richness. However, the predictive power of the DHIs was highly dependent on the bird guilds and spatial extent of analysis. Among the three components of the DHIs, cumulative DHI provided the highest predictive power and performed best in richness models of forest affiliates and specialists (except at the ecoregion scale), grassland affiliates and specialists, and shrubland specialists, across all four spatial extents. Our expectation that Landsat DHIs would perform better than MODIS DHIs was supported for forest specialists and affiliates, shrubland affiliates, and birds with small body sizes, but was not supported for shrubland specialists or permanent residents.

We also found that minimum DHI was important for grassland specialists and affiliates, residents, and short-distance migrants. This result is consistent with previous work that showed

minimum MODIS DHI was a good predictor of grassland birds (Coops et al. 2009, Hobi et al. 2017) and minimum monthly NDVI was important for resident birds (Hurlbert and Haskell 2003). Contrary to our expectation, we observed a notable difference in the performance of Landsat DHIs and MODIS DHIs in richness models of grassland specialists and affiliates. These results highlight the importance of higher spatial resolution satellite data in grassland ecosystems that capture spectral variability of landscapes in more detail than coarse resolution data (Fassnacht et al. 2022). However, our expectation that models would have higher explanatory power at the ecoregion scale was not supported, in most cases. For example, cumulative DHI performed poorly for forest affiliates and specialists, long-distance migrants, threatened species, stable/increasing populations, large-ranged birds, insectivores, and small-bodied birds at the ecoregion scale.

Habitat heterogeneity is an important determinant of species richness (MacArthur and MacArthur 1961), and the Landsat DHIs have great potential to characterize vegetation productivity over heterogeneous landscapes. Indeed, we found that bird richness models based on the Landsat DHIs generally outperformed those based on MODIS DHIs in heterogeneous landscapes, such as grassland affiliates at ecoregion scale. However, we expected to find a larger difference in the performance of models based on Landsat versus MODIS DHIs. The wider swath and coarser spatial resolution of MODIS data introduce geometric and spectral issues in surface reflectance products (e.g., NDVI) that are reduced by MODIS preprocessing but not eliminated completely (Tan et al. 2006, Feng et al. 2012, Peng et al. 2015). Our explanation for finding no substantial differences in the models based on Landsat and MODIS DHIs over heterogeneous areas is a potential bias in BBS route locations, which are not representative of heterogeneous landscapes (Veech et al. 2017, Ankori-Karlinsky et al. 2022). Roughly 80% of

BBS routes are located in areas where the TRI is between 0-10, while only 20% are located in areas with TRI values between 11-54.

When we evaluated the Landsat DHIs in global models, we found that the DHIs complemented other environmental variables in explaining bird richness, including topographic and land cover metrics. Moreover, the DHIs were the strongest predictors and had the largest effects on richness within most guilds. Our results indicate the utility of the DHIs in capturing habitat characteristics is distinct from other commonly used variables, in line with prior studies (Radeloff et al. 2019, Suttidate et al. 2019).

As predicted, the Landsat DHIs calculated over 1991-2000 and 2011-2020 had comparable predictive power in modeling bird richness across the conterminous US. These results show that the Landsat DHIs are suitable for applications spanning multiple decades, back at least until the early 1990s when the number of available satellite images was far lower than it is today. Combining Landsat DHIs over different time periods with BBS data allows for a better understanding of changes in relationship between vegetation productivity and species richness patterns. Indeed, we found a decline in species richness over the past thirty years for all bird guilds except residents, stable/increasing populations, and granivores at the ecoregion and full BBS route scales. These findings are consistent with numerous studies reporting declines of different bird groups across the US (Langham et al. 2015, NABCI 2016, Rosenberg et al. 2019).

This is the first study that compares the performance of the DHIs derived from medium (30-m) and coarse (250-m) spatial resolution satellite data in modeling bird richness across four spatial extents. The relationship between species richness and productivity has been investigated for a long time (Mittelbach et al. 2001, Hawkins et al. 2003a, Bonn et al. 2004), and several

efforts have explored how such relationships are influenced by the spatial scale of analysis (Gross et al. 2000, Hurlbert and Haskell 2003, Bailey et al. 2004). We found that the relationship between species richness and vegetation productivity was unchanged by the spatial resolution of the DHIs (i.e., 30-m Landsat or 250-m MODIS) but was influenced by the spatial extent of analysis (i.e., ecoregion, full BBS route, first ten-stops, or first stop scales). At the ecoregion scale, the relationship between productivity and species richness was linear in most cases but became unimodal or hump-shaped at finer extents (Figure **8**). Our results confirm the findings of earlier work that, for some bird guilds, species richness is linearly related to vegetation productivity, while for others the relationship is better represented by a decelerating curve (Evans et al. 2005, Hobi et al. 2017). We also found that bird guilds had different responses based on the spatial extent of analysis. Some bird guilds had the strongest relationship with vegetation productivity at larger spatial extents (e.g., shrubland specialists at the ecoregion scale), while other guilds showed divergent patterns (e.g., overall species richness at the full BBS route scale or residents at the first ten-stop scale). These findings highlight the importance of analyzing multiple spatial extents to find meaningful relationships for species (Jackson and Fahrig 2012, 2015). However, we were surprised to find that the directionality of the relationship between the DHIs and species richness changed from positive to negative depending on the spatial extent of the analysis. Given this, we speculate that the DHIs are capturing different features or qualities that work to that promote or suppress high species richness at these different scales.

Caveats and limitations

There were some limitations of the remotely sensed data. We applied linear interpolation for the Landsat DHIs to fill in missing data; however, phenology curves are nonlinear, and

therefore we likely overestimated NDVI values for winter and underestimated values for summer. Moreover, there were slight differences in how we calculated the DHIs based on MODIS and Landsat data. The Landsat DHIs were calculated based on monthly NDVI composites, while the MODIS DHIs were based on 16-day NDVI composites. Given the high correlation between Landsat and MODIS DHIs, in all likelihood that difference had minimal effects on our results. The BBS is a great resource for long-term bird data; however, BBS routes are not uniformly distributed across the conterminous US and are especially sparse in remote areas and landscapes with complex terrain (Veech et al. 2017). Moreover, some bird guilds, including frugivorous and threatened species, had a low number of species (especially at the first stop scale). Despite these limitations, our remotely sensed indices provided high predictive power for some bird guilds and our models performed well.

Conclusion

The Dynamic Habitat Indices derived from Landsat data are new remotely sensed indices of vegetation productivity specifically designed to predict biodiversity patterns. The DHIs provide unique information compared with commonly used predictors including land cover and topographic metrics. We showed that Landsat DHIs provide high predictive power in modeling species richness for most bird guilds. The higher spatial resolution of Landsat DHIs characterizes heterogeneous landscapes with greater detail than is possible using MODIS DHIs and provides information at a resolution which better approximates their perception of habitat. Using the Landsat archive we can advance our understanding of how changes in vegetation productivity influence biodiversity patterns. All remotely sensed datasets are freely available at https://silvis.forest.wisc.edu/data/dhis/.

References

Ankori-Karlinsky, R., M. Kalyuzhny, K. F. Barnes, A. M. Wilson, C. Flather, R. Renfrew, J. Walsh, E. Guk, and R. Kadmon. 2022. North American Breeding Bird Survey underestimates regional bird richness compared to Breeding Bird Atlases. Ecosphere 13:1–18.

Bailey, S. A., M. C. Horner-Devine, G. Luck, L. A. Moore, K. M. Carney, S. Anderson, C. Betrus, and E. Fleishman. 2004. Primary productivity and species richness: Relationships among functional guilds, residency groups and vagility classes at multiple spatial scales. Ecography 27:207–217.

Bar-Massada, A., and E. M. Wood. 2014. The richness-heterogeneity relationship differs between heterogeneity measures within and among habitats. Ecography 37:528–535.

Billerman, S. M., B. K. Keeney, P. G. Rodewald, and T. S. Schulenberg. 2020. Birds of the World. Cornell Laboratory of Ornithology, Ithaca, NY, USA.

Bonn, A., D. Storch, and K. J. Gaston. 2004. Structure of the species-energy relationship. Proceedings of the Royal Society B: Biological Sciences 271:1685–1691.

Burns, P., M. Clark, L. Salas, S. Hancock, D. Leland, P. Jantz, R. Dubayah, and S. J. Goetz. 2020. Incorporating canopy structure from simulated GEDI lidar into bird species distribution models. Environmental Research Letters 15.

Carroll, K. A., L. S. Farwell, A. M. Pidgeon, E. Razenkova, D. Gudex-Cross, D. P. Helmers, K. E. Lewińska, P. R. Elsen, and V. C. Radeloff. 2022. Mapping breeding bird species richness at management-relevant resolutions across the United States. Ecological Applications 32.

Cody, M. L. 1981. Habitat Selection in Birds: The Roles of Vegetation Structure, Competitors, and Productivity. BioScience 31:107–113.

Cohen, W. B., and S. N. Goward. 2004. Landsat ’ s Role in Ecological Applications of Remote Sensing. BioScience 54:535–545.

Coops, N. C., R. H. Waring, M. A. Wulder, A. M. Pidgeon, and V. C. Radeloff. 2009. Bird diversity: a predictable function of satellite-derived estimates of seasonal variation in canopy light absorbance across the United States. Journal of Biogeography 36:905–918.

Dunning, J. 2008. CRC Handbook of Avian Body Masses. second ed. CRC Press, Boca Raton.

Elsen, P. R., L. S. Farwell, A. M. Pidgeon, and V. C. Radeloff. 2020. Landsat 8 TIRS-derived relative temperature and thermal heterogeneity predict winter bird species richness patterns across the conterminous United States. Remote Sensing of Environment 236.

Evans, K. L., J. J. D. Greenwood, and K. J. Gaston. 2005. Dissecting the species-energy relationship. Proceedings of the Royal Society B: Biological Sciences 272:2155–2163.

Farr, T. G., P. A. Rosen, E. Caro, R. Crippen, R. Duren, S. Hensley, M. Kobrick, M. Paller, E. Rodriguez, L. Roth, D. Seal, S. Shaffer, J. Shimada, J. Umland, M. Werner, M. Oskin, D. Burbank, and D. E. and Alsdorf. 2007. The shuttle radar topography mission. Reviews of Geophysics 45:1–33.

Farwell, L. S., D. Gudex-Cross, I. E. Anise, M. J. Bosch, A. M. Olah, V. C. Radeloff, E. Razenkova, N. Rogova, E. M. O. Silveira, M. M. Smith, and A. M. Pidgeon. 2021. Satellite image texture captures vegetation heterogeneity and explains patterns of bird richness. Remote Sensing of Environment 253:112175.

Fassnacht, F. E., J. Müllerová, L. Conti, M. Malavasi, and S. Schmidtlein. 2022. About the link between biodiversity and spectral variation. Applied Vegetation Science 25:1–13.

Feng, M., C. Huang, S. Channan, E. F. Vermote, J. G. Masek, and J. R. Townshend. 2012. Quality assessment of Landsat surface reflectance products using MODIS data. Computers and Geosciences 38:9–22.

Gaston, K. J. 2000. Global patterns in biodiversity. Nature 405:220–227.

Gorelick, N., M. Hancher, M. Dixon, S. Ilyushchenko, D. Thau, and R. Moore. 2017. Google Earth Engine: Planetary-scale geospatial analysis for everyone. Remote Sensing of Environment 202:18–27.

Gross, K. L., M. R. Willig, L. Gough, R. Inouye, and S. B. Cox. 2000. Patterns of species density and productivity at different spatial scales in herbaceous plant communities. Oikos 89:417–427.

Haddad, N. M., L. A. Brudvig, J. Clobert, K. F. Davies, A. Gonzalez, R. D. Holt, T. E. Lovejoy, J. O. Sexton, M. P. Austin, C. D. Collins, W. M. Cook, E. I. Damschen, R. M. Ewers, B. L. Foster, C. N. Jenkins, A. J. King, W. F. Laurance, D. J. Levey, C. R. Margules, B. A. Melbourne, A. O. Nicholls, J. L. Orrock, D. X. Song, and J. R. Townshend. 2015. Habitat fragmentation and its lasting impact on Earth's ecosystems. Science Advances 1:1–10.

Hansen, M. C., P. V. Potapov, R. Moore, M. Hancher, S. A. Turubanova, A. Tyukavina, D. Thau, S. V. Stehman, S. J. Goetz, T. R. Loveland, A. Kommareddy, A. Egorov, L. Chini, C. O. Justice, and J. R. G. Townshend. 2013. High-Resolution Global Maps of 21st-Century Forest Cover Change. Science 342:850–853.

Hawkins, B. A., R. Field, H. V. Cornell, D. J. Currie, J. F. Guegan, D. M. Kaufman, J. T. Kerr, G. G. Mittelbach, T. Oberdorff, E. M. O'Brien, E. E. Porter, and J. R. G. Turner. 2003a. Energy, water, and broad-scale geographic patterns of species richness. Ecology 84:3105–3117.

Hawkins, B. A., E. E. Porter, and J. A. F. Diniz-Filho. 2003b. Productivity and history as predictors of the latitudinal diversity gradient of terrestrial birds. Ecology 84:1608–1623.

Hobi, M. L., M. Dubinin, C. H. Graham, N. C. Coops, M. K. Clayton, A. M. Pidgeon, and V. C. Radeloff. 2017. A comparison of Dynamic Habitat Indices derived from different MODIS

products as predictors of avian species richness. Remote Sensing of Environment 195:142–152.

Hobi, M. L., L. S. Farwell, M. Dubinin, D. Kolesov, A. M. Pidgeon, N. C. Coops, and V. C. Radeloff. 2021. Patterns of bird species richness explained by annual variation in remotely sensed Dynamic Habitat Indices. Ecological Indicators 127:107774.

Hurlbert, A. H., and J. P. Haskell. 2003. The effect of energy and seasonality on avian species richness and community composition. American Naturalist 161:83–97.

Jackson, H. B., and L. Fahrig. 2012. What size is a biologically relevant landscape? Landscape Ecology 27:929–941.

Jackson, H. B., and L. Fahrig. 2015. Are ecologists conducting research at the optimal scale? Global Ecology and Biogeography 24:52–63.

Kendall, W. L., B. G. Peterjohn, and J. R. Sauer. 1996. First-time observer effects in the North American Breeding Bird Survey. The Auk 113:823–829.

Langham, G. M., J. G. Schuetz, T. Distler, C. U. Soykan, and C. Wilsey. 2015. Conservation status of North American birds in the face of future climate change. PLoS ONE 10:1–16.

MacArthur, R. H. 1964. Environmental Factors Affecting Bird Species Diversity. The American Naturalist 98:387–397.

MacAthur, R. H., and J. W. MacAthur. 1961. On Bird Species Diversity. Ecology 42:594–598.

Michaud, J. S., N. C. Coops, M. E. Andrew, M. A. Wulder, G. S. Brown, and G. J. M. Rickbeil. 2014. Estimating moose (Alces alces) occurrence and abundance from remotely derived environmental indicators. Remote Sensing of Environment 152:190–201.

Mittelbach, G. G., C. F. Steiner, S. M. Scheiner, K. L. Gross, H. L. Reynolds, R. B. Waide, M. R. Willig, S. I. Dodson, and L. Gough. 2001. What is the observed relationship between species richness and productivity? Ecology 82:2381–2396.

Myneni, R. B., F. G. Hall, P. J. Sellers, and A. L. Marshak. 1995. Interpretation of spectral vegetation indexes. IEEE Transactions on Geoscience and Remote Sensing 33:481–486.

NABCI. 2016. North American Bird Conservation Initiative. 2016. The State of North America's Birds 2016. Environment and Climate Change Canada: Ottawa, Ontario.

O'Brien, R. M. 2007. A caution regarding rules of thumb for variance inflation factors. Quality and Quantity 41:673–690.

Paruelo, J. M., H. E. Epstein, W. K. Lauenroth, and I. C. Burke. 1997. ANPP estimates from NDVI for the central grassland region of the United States. Ecology 78:953–958.

Peng, J., Q. Liu, L. Wang, Q. Liu, W. Fan, M. Lu, and J. Wen. 2015. Characterizing the pixel footprint of satellite albedo products derived from MODIS reflectance in the Heihe River Basin, China. Remote Sensing 7:6886–6907.

Pereira, H. M., S. Ferrier, M. Walters, G. N. Geller, R. H. G. Jongman, R. J. Scholes, M. W. Bruford, N. Brummitt, S. H. M. Butchart, A. C. Cardoso, N. C. Coops, E. Dulloo, D. P. Faith, J. Freyhof, R. D. Gregory, C. Heip, R. Höft, G. Hurtt, W. Jetz, D. S. Karp, M. A. McGeoch, D. Obura, Y. Onoda, N. Pettorelli, B. Reyers, R. Sayre, J. P. W. Scharlemann, S. N. Stuart, E. Turak, M. Walpole, and M. Wegmann. 2013. Essential Biodiversity Variables. Science 339:277–278.

Pettorelli, N., S. Ryan, T. Mueller, N. Bunnefeld, B. Jedrzejewska, M. Lima, and K. Kausrud. 2011. The Normalized Difference Vegetation Index (NDVI): Unforeseen successes in animal ecology. Climate Research 46:15–27.

Pimm, S. L., C. N. Jenkins, R. Abell, T. M. Brooks, J. L. Gittleman, L. N. Joppa, P. H. Raven, C. M. Roberts, and J. O. Sexton. 2014. The biodiversity of species and their rates of extinction, distribution, and protection. Science 344.

Radeloff, V. C., M. Dubinin, N. C. Coops, A. M. Allen, T. M. Brooks, M. K. Clayton, G. C. Costa, C. H. Graham, D. P. Helmers, A. R. Ives, D. Kolesov, A. M. Pidgeon, G. Rapacciuolo, E. Razenkova, N. Suttidate, B. E. Young, L. Zhu, and M. L. Hobi. 2019. The Dynamic Habitat Indices (DHIs) from MODIS and global biodiversity. Remote Sensing of Environment 222:204–214.

Razenkova, E., K. E. Lewińska, H. Yin, L. S. Farwell, A. M. Pidgeon, P. Hostert, N. C. Coops, V. Radeloff, and O. C. (n.d.). Medium-resolution Dynamic Habitat Indices from Landsat satellite imagery. in review.

Razenkova, E., V. C. Radeloff, M. Dubinin, E. V Bragina, M. Allen, M. K. Clayton, A. M. Pidgeon, L. M. Baskin, C. Nicholas, and M. L. Hobi. 2020. Vegetation productivity summarized by the Dynamic Habitat Indices explains patterns of moose abundance across Russia. Scientific Reports 10:1–12.

Riley, S. 1999. Index that quantifies topographic heterogeneity.

Rockström, J., W. Steffen, K. Noone, Å. Persson, F. S. Chapin, E. Lambin, T. M. Lenton, M. Scheffer, C. Folke, H. J. Schellnhuber, B. Nykvist, C. A. de Wit, T. Hughes, S. van der Leeuw, H. Rodhe, S. Sörlin, P. K. Snyder, R. Costanza, U. Svedin, M. Falkenmark, L. Karlberg, R. W. Corell, V. J. Fabry, J. Hansen, B. Walker, D. Liverman, K. Richardson, P. Crutzen, and J. Foley. 2009. A safe operating space for humanity. Nature 461:472–475.

Rosenberg, K. V., A. M. Dokter, P. J. Blancher, J. R. Sauer, A. C. Smith, P. A. Smith, J. C. Stanton, A. Panjabi, L. Helft, M. Parr, and P. P. Marra. 2019. Decline of the North American avifauna. Science 366:120–124.

Sala, O. E., F. S. Chapin, J. J. Armesto, E. Berlow, J. Bloomfield, R. Dirzo, E. Huber-Sanwald, L. F. Huenneke, R. B. Jackson, A. Kinzig, R. Leemans, D. M. Lodge, H. A. Mooney, M. Oesterheld, N. L. R. Poff, M. T. Sykes, B. H. Walker, M. Walker, and D. H. Wall. 2000. Global biodiversity scenarios for the year 2100. Science 287:1770–1774.

Sauer, J. R., D. K. Niven, J. E. Hines, D. J. Ziolkowski, K. L. Pardieck, J. E. Fallon, and W. A. Link. 2017. The North American Breeding Bird Survey, Results and Analysis 1966–2013. USGS Patuxent Wildlife Research Center, Laurel, MD.

Scholander, P. F., R. Hock, V. Walters, F. Johnson, and L. Irving. 1950. HEAT REGULATION IN SOME ARCTIC AND TROPICAL MAMMALS AND BIRDS. The Biological Bulletin 99.

Sekercioglu, C. H. 2006. Increasing awareness of avian ecological function. Trends in Ecology and Evolution 21:464–471.

Skidmore, A. K., B. O. Oindo, and M. Y. Said. 2003. Biodiversity Assessment by Remote Sensing. Proceedings of the 30th International symposium on remote sensing of the environment: information for risk management and sustainable development:1–4.

Suttidate, N., M. L. Hobi, A. M. Pidgeon, P. D. Round, N. C. Coops, D. P. Helmers, N. S. Keuler, M. Dubinin, B. L. Bateman, and V. C. Radeloff. 2019. Tropical bird species richness is strongly associated with patterns of primary productivity captured by the Dynamic Habitat Indices. Remote Sensing of Environment 232:1–10.

Tan, B., C. E. Woodcock, J. Hu, P. Zhang, M. Ozdogan, D. Huang, W. Yang, Y. Knyazikhin, and R. B. Myneni. 2006. The impact of gridding artifacts on the local spatial properties of MODIS data: Implications for validation, compositing, and band-to-band registration across resolutions. Remote Sensing of Environment 105:98–114.

Tews, J., U. Brose, V. Grimm, K. Tielbörger, M. C. Wichmann, M. Schwager, and F. Jeltsch. 2004. Animal species diversity driven by habitat heterogeneity/diversity: The importance of keystone structures. Journal of Biogeography 31:79–92.

Turner, W., S. Spector, N. Gardiner, M. Fladeland, E. Sterling, and M. Steininger. 2003. Remote sensing for biodiversity science and conservation. Trends in Ecology and Evolution 18:306–314.

Veech, J. A., K. L. Pardieck, and D. J. Ziolkowski. 2017. How well do route survey areas represent landscapes at larger spatial extents? An analysis of land cover composition along breeding bird survey routes. Condor 119:607–615.

Wright, D. H. 1983. Species-energy theory: an extension of species–area theory. Oikos 41:496–506.

Zhu, L., and Y. Guo. 2022. Remotely Sensed Winter Habitat Indices Improve the Explanation of Broad-Scale Patterns of Mammal and Bird Species Richness in China. Remote Sensing 14.

Table 4: Spearman correlation coefficients between mean and standard deviation MODIS and Landsat DHIs calculated for 2011-2020 at four spatial extents: within 85 ecoregions, a 5-km square buffer around centered on first-stop locations of BBS routes, a 2.5-km square buffer for the first ten stops of BBS routes, and a 0.5-km square buffer around the first stop of BBS routes. Abbreviations: Cum DHI = cumulative DHI, Min DHI = minimum DHI, Var DHI = variation DHI.

Variable/Scale	Ecoregions	Full route	10-stops	1-stop
Mean				
Cum DHI	0.99	0.97	0.97	0.96
Min DHI	0.98	0.94	0.93	0.90
Var DHI	0.99	0.94	0.93	0.93
Standard deviation				
Cum DHI	0.93	0.88	0.88	0.69
Min DHI	0.86	0.76	0.73	0.59
Var DHI	0.61	0.78	0.74	0.51

Table 5: Results of linear regressions between the individual Landsat and MODIS DHIs and species richness for overall species richness and 21 functional bird guilds at four spatial extents: ecoregions, full BBS route, first ten stops, and first stop. The adjusted R^2 values are shown for each model; the highest values of adjusted R^2 within a functional guild are highlighted in bold. Abbreviations: (–) = negative relationship, (+) = positive relationship, and (0) = no relationship; "l" = linear and "q" = quadratic indicate the type of regression; Cum DHI = cumulative DHI, Min DHI = minimum DHI, Var DHI = variation DHI.

Species richness	Extents		Landsat Cum DHI		MODIS Cum DHI		Landsat Min DHI		MODIS Min DHI		Landsat Var DHI		MODIS Var DHI
Overall Species Richness	Ecoregion	q	(–) 0.25	q	(–) 0.26	l	(–) 0.17	l	(–) 0.18	q	(+) 0.02	l	(+) 0.01
	Full route	q	(+) 0.30	q	(+) 0.28	q	(+) 0.01		-	q	(+) 0.05	q	(+) 0.03
	10-Stops	q	(+) **0.31**	q	(+) 0.29	q	(+) 0.02	q	(+) 0.02	q	(+) 0.04	q	(+) 0.01
	1-Stop	q	(+) 0.06	q	(+) 0.06	q	(–) 0.01		-	q	(+) 0.02	q	(+) 0.02
Forest Affiliates	Ecoregion	q	(–) -0.01		-	l	(–) 0.05	l	(–) 0.06	q	(+) 0.09	q	(+) 0.08
	Full route	q	(+) **0.42**	q	(+) 0.39	q	(+) 0.04	q	(+) 0.05	q	(+) 0.01	q	(+) 0.01
	10-Stops	q	(+) **0.42**	q	(+) 0.39	q	(+) 0.07	q	(+) 0.07	q	(+) 0.01		-
	1-Stop	q	(+) 0.21	q	(+) 0.20	q	(+) 0.04	q	(+) 0.04		-		-
Grassland Affiliates	Ecoregion	q	(–) 0.27	q	(–) 0.25	l	(–) 0.26	l	(–) 0.21	l	(+) 0.15	l	(+) 0.11
	Full route	q	(–) **0.41**	q	(–) 0.36	q	(–) 0.25	q	(–) 0.23	q	(+) 0.11	q	(+) 0.08
	10-Stops	q	(–) 0.35	q	(–) 0.31	l	(–) 0.18	q	(–) 0.15	q	(+) 0.08	q	(+) 0.06
	1-Stop	l	(–) 0.27	l	(–) 0.23	q	(–) 0.11	q	(–) 0.09	q	(+) 0.05	q	(+) 0.06
Shrubland Affiliates	Ecoregion	q	(–) **0.43**	q	(–) 0.42	q	(–) 0.11	q	(–) 0.14	l	(–) 0.10	q	(–) 0.11
	Full route	q	(–) 0.04	q	(–) 0.04	q	(+) 0.08	q	(+) 0.07	q	(–) 0.08	q	(–) 0.09
	10-Stops	q	(–) 0.01	q	(–) 0.01	q	(+) 0.10	q	(+) 0.10	l	(–) 0.06	q	(–) 0.07
	1-Stop	q	(–) 0.01	q	(–) 0.01	q	(+) 0.08	q	(+) 0.09	l	(–) 0.05	q	(–) 0.04
Forest Specialists	Ecoregion		-		-	q	(–) 0.05	q	(–) 0.11	q	(+) 0.14	q	(+) 0.14
	Full route	q	(+) **0.31**	q	(+) 0.28	q	(+) 0.03	q	(+) 0.05	l	(+) 0.01	l	(+) 0.02
	10-Stops	q	(+) 0.30	q	(+) 0.27	q	(+) 0.03	q	(+) 0.05	l	-	l	(+) 0.01
	1-Stop	q	(+) 0.09		(+) 0.08	q	(–) 0.02	q	(–) 0.06	l	(+) 0.03	l	(+) 0.03
Grassland Specialists	Ecoregion	q	(–) 0.20	q	(–) 0.18	l	(–) **0.31**	l	(–) 0.26	l	(+) **0.31**	l	(+) 0.24
	Full route	q	(–) **0.30**	q	(–) 0.27	q	(–) 0.24	q	(–) 0.21	q	(+) 0.22	q	(+) 0.17
	10-Stops	q	(–) 0.26	q	(–) 0.23	l	(–) 0.18	l	(–) 0.14	q	(+) 0.15	q	(+) 0.12

	1-Stop	q	(–) 0.19	q	(–) 0.17	l	(–) 0.10	l	(–) 0.08	q	(+) 0.07	q	(+) 0.08
Shrubland Specialists	Ecoregion	q	(–) **0.48**	q	(–) **0.48**	q	(–) 0.07	q	(–) 0.10	q	(–) 0.15	q	(–) 0.17
	Full route	q	(–) 0.29	q	(–) 0.28	q	(–) 0.03	q	(–) 0.03	q	(–) 0.12	q	(–) 0.10
	10-Stops	q	(–) 0.20	q	(–) 0.19	q	(–) 0.03	q	(–) 0.03	q	(–) 0.11	q	(–) 0.09
	1-Stop	q	(–) 0.14	q	(–) 0.14	q	(0) 0.02	q	(–) 0.02	q	(–) 0.05	q	(–) 0.07
Residents	Ecoregion	q	(–) 0.29	q	(–) **0.30**	q	(–) 0.03	q	(–) 0.05	q	(–) 0.11	q	(–) 0.12
	Full route	q	(+) 0.15	q	(+) 0.14	q	(+) 0.24	q	(+) 0.23	q	(–) 0.19	q	(–) 0.18
	10-Stops	q	(+) 0.19	q	(+) 0.18	q	(+) **0.30**	q	(+) **0.30**	q	(–) 0.20	q	(–) 0.20
	1-Stop	q	(+) 0.06	q	(+) 0.06	q	(+) 0.19	q	(+) 0.22	l	(–) 0.17	l	(–) 0.17
Long-Distance Migrants	Ecoregion	l	(–) -0.01	l	(–) -0.01	l	(–) 0.12	l	(–) 0.11	q	(+) 0.22	q	(+) 0.18
	Full route	q	(+) **0.33**	q	(+) 0.32	l	(+) 0.01	l	(+) 0.01	q	(+) 0.06	q	(+) 0.03
	10-Stops	q	(+) 0.31	q	(+) 0.30	q	(+) 0.02	q	(+) 0.02	q	(+) 0.04	q	(+) 0.02
	1-Stop	q	(+) 0.07	q	(+) 0.07		-		-	q	(+) 0.02	q	(+) 0.02
Short-Distance Migrants	Ecoregion	l	(–) 0.28	l	(–) 0.29	q	(–) 0.36	q	(–) **0.38**	q	(+) 0.18	q	(+) 0.18
	Full route	q	(+) 0.14	q	(+) 0.13	q	(–) 0.12	q	(–) 0.13	q	(+) 0.27	q	(+) 0.24
	10-Stops	q	(+) 0.16	q	(+) 0.15	l	(–) 0.06	l	(–) 0.05	q	(+) 0.20	q	(+) 0.17
	1-Stop	q	(–) 0.06	q	(–) 0.06	l	(–) 0.10	l	(–) 0.08	q	(+) 0.10	q	(+) 0.12
Ground Nesters	Ecoregion	q	(–) **0.37**	q	(–) 0.36	l	(–) 0.32	l	(–) 0.31	q	(+) 0.08	q	(+) 0.06
	Full route	q	(+) 0.11	q	(+) 0.11	q	(–) 0.01	q	(–) 0.01	q	(+) 0.06	q	(+) 0.04
	10-Stops	q	(+) 0.12	q	(+) 0.12	q	(+) 0.01	q	(+) 0.01	q	(+) 0.03	q	(+) 0.02
	1-Stop	q	(0) 0.02	q	(+) 0.02	q	(–) 0.01	q	(–) 0.01	q	(+) 0.02	q	(+) 0.01
Mid-Story/Canopy Nesters	Ecoregion	q	(–) 0.13	q	(–) 0.14	l	(–) 0.07	l	(–) 0.08		-	l	(+) -0.01
	Full route	q	(+) **0.36**	q	(+) 0.34	q	(+) 0.01	q	(+) 0.01	q	(+) 0.05	q	(+) 0.02
	10-Stops	q	(+) **0.36**	q	(+) 0.33	l	(+) 0.02	l	(+) 0.02	q	(+) 0.04	q	(+) 0.01
	1-Stop	q	(+) 0.09	q	(+) 0.08		-		-	q	(+) 0.01	q	(+) 0.02
Threatened	Ecoregion	l	(–) -0.01	l	(+) -0.01	l	(+) -0.01	l	(+) -0.01		-	q	(–) 0.02
	Full route	q	(+) 0.14	q	(+) 0.15	q	(+) 0.18	q	(+) **0.21**	l	(–) 0.06	l	(–) 0.07
	10-Stops	q	(+) 0.15	q	(+) 0.14	q	(+) 0.18	q	(+) **0.21**	l	(–) 0.07	l	(–) 0.08
	1-Stop	l	(+) 0.06	l	(+) 0.06	q	(+) 0.07	q	(+) 0.08	l	(–) 0.04	l	(–) 0.04
Decreasing	Ecoregion	l	(–) 0.27	l	(–) 0.26	l	(–) **0.35**	l	(–) 0.33	q	(+) 0.18	q	(+) 0.16
	Full route	q	(+) 0.15	q	(+) 0.15	q	(–) 0.05	q	(–) 0.05	q	(+) 0.18	q	(+) 0.13
	10-Stops	q	(+) 0.12	q	(+) 0.12	q	(–) 0.03	q	(–) 0.03	q	(+) 0.09	q	(+) 0.07
	1-Stop	q	(–) 0.07	q	(–) 0.07	q	(–) 0.07	q	(–) 0.06	q	(+) 0.07	q	(+) 0.08

Stable/ Increasing	Ecoregion	q	(–) 0.20	q	(–) 0.22	q	(–) 0.08	q	(–) 0.08	l	(–) -0.01	l	(0) -0.01
	Full route	q	(+) 0.34	q	(+) 0.31	l	(+) 0.03	l	(+) 0.03	q	(+) 0.01		-
	10-Stops	q	(+) **0.38**	q	(+) 0.34	l	(+) 0.06	l	(+) 0.06	q	(–) 0.02		-
	1-Stop	q	(+) 0.14	q	(+) 0.13	q	(+) 0.01	q	(+) 0.01		-		-
Small-Ranged	Ecoregion	q	(–) 0.35	q	(–) **0.37**	q	(–) 0.02	q	(–) 0.03	q	(–) 0.15	q	(–) 0.16
	Full route	q	(–) 0.07	q	(–) 0.07	l	(+) 0.01	l	(+) 0.01	q	(–) 0.18	q	(–) 0.14
	10-Stops	q	(–) 0.04	q	(–) 0.05	q	(+) 0.02	q	(+) 0.01	q	(–) 0.16	q	(–) 0.12
	1-Stop	q	(–) 0.05	q	(–) 0.06	q	(+) 0.01	q	(+) 0.01	q	(–) 0.07	q	(–) 0.10
Large-Ranged	Ecoregion		-		-	l	(–) 0.25	l	(–) 0.24	q	(+) **0.47**	q	(+) 0.43
	Full route	q	(+) 0.36	q	(+) 0.35		-		-	q	(+) 0.13	q	(+) 0.08
	10-Stops	q	(+) 0.34	q	(+) 0.32	q	(+) 0.01	q	(+) 0.01	q	(+) 0.08	q	(+) 0.04
	1-Stop	q	(+) 0.09	q	(+) 0.09	q	(–) 0.01		-	q	(+) 0.04	q	(+) 0.05
Insectivores	Ecoregion	l	(–) 0.04	l	(–) 0.03	q	(–) 0.10	q	(–) 0.09	q	(+) 0.06	q	(+) 0.03
	Full route	q	(+) **0.36**	q	(+) 0.34	q	(+) 0.03	q	(+) 0.03	q	(+) 0.02	q	(+) 0.01
	10-Stops	q	(+) 0.35	q	(+) 0.33	q	(+) 0.05	q	(+) 0.05	q	(–) 0.02		-
	1-Stop	q	(+) 0.09	q	(+) 0.09	l	(+) 0.01		-		-		-
Granivores	Ecoregion	q	(–) **0.40**	q	(–) **0.40**	q	(–) 0.20	q	(–) 0.20	l	(+) 0.04	l	(+) 0.05
	Full route	q	(+)0.20	q	(+) 0.20	q	(–) 0.03	q	(–) 0.03	q	(+) 0.04	q	(+) 0.02
	10-Stops	q	(+) 0.22	q	(+) 0.21	q	(–) 0.06	q	(+) 0.07	q	(+) 0.05	q	(+) 0.02
	1-Stop	q	(+) 0.11	q	(+) 0.11	q	(–) 0.05	q	(+) 0.08	q	(–) 0.02	q	(+) 0.03
Frugivores	Ecoregion	q	(–) 0.09	q	(–) 0.10	l	(–) -0.01		-		-	l	(–) -0.01
	Full route	q	(+) 0.09	q	(+) 0.08		-		-	q	(+) 0.01	q	(+) 0.01
	10-Stops	q	(+) 0.06	q	(+) 0.05		-		-	q	(+) 0.01	q	(+) 0.01
	1-Stop	q	(+) 0.01		-		-	q	(–) 0.01		-		-
Large body	Ecoregion	q	(–) 0.43	q	(–) **0.44**	l	(–) 0.15	q	(–) 0.16	l	(+) -0.01		-
	Full route	q	(+) 0.25	q	(+) 0.24	q	(+) 0.03	q	(+) 0.03	q	(+) 0.05	q	(+) 0.02
	10-Stops	q	(+) 0.22	q	(+) 0.21	q	(+) 0.06	q	(+) 0.07	q	(–) 0.04	q	(–) 0.02
	1-Stop	q	(+) 0.03	q	(+) 0.03	q	(+) 0.03	q	(+) 0.04	q	(–) 0.01	q	(–) 0.01
Small body	Ecoregion	l	(–) 0.03	l	(–) 0.03	l	(–) 0.12	l	(–) 0.13	q	(+) 0.08	q	(+) 0.05
	Full route	q	(+) **0.26**	q	(+) 0.25		-	q	(+) 0.01	q	(+) 0.04	q	(+) 0.03
	10-Stops	q	(+) **0.26**	q	(+) 0.24		-	q	(+) 0.01	q	(+) 0.03	q	(+) 0.02
	1-Stop	q	(+) 0.07	q	(+) 0.06	q	(–) 0.01	q	(–) 0.02	q	(+) 0.04	q	(+) 0.04

Table 6: Results of linear regressions between the individual DHIs based on Landsat and MODIS for overall species richness and richness of several functional bird guilds over heterogeneous landscapes (for which terrain ruggedness index was >10) for a 5-km square buffer around centered on first-stop locations of BBS routes. The adjusted R^2 values are shown for each model; the highest values of adjusted R^2 within a functional guild are highlighted in bold. Abbreviations: "l" = linear and "q" = quadratic indicate the type of regression; Cum DHI = cumulative DHI, Min DHI = minimum DHI, Var DHI = variation DHI.

Species group		Landsat Cum DHI		MODIS Cum DHI		Landsat Min DHI		MODIS Min DHI		Landsat Var DHI		MODIS Var DHI
Overall species richness	q	**0.21**	q	0.20	q	**0.07**	q	0.06	q	**0.06**	q	0.04
Forest affiliates	q	**0.34**	q	0.33	q	**0.04**	q	0.02	q	**0.03**	q	0.01
Grass affiliates	l	**0.38**	l	0.35	l	**0.26**	q	0.24	q	**0.12**	q	0.10
Shrubland affiliates	l	**0.17**	q	0.14	q	0.06	q	**0.08**	q	**0.04**	**q**	**0.04**
Forest specialists	q	**0.30**	q	0.28	q	**0.02**	q	0.01	q	0.01	q	-
Shrubland specialists	q	**0.29**	q	0.28	q	0.01	q	**0.02**	q	**0.11**	q	0.08
Residents	q	0.05	q	**0.06**	q	**0.20**	**q**	**0.20**	q	**0.26**	q	0.25
Long-Distance Migrants	q	**0.26**	**q**	**0.26**	q	**0.11**	**q**	**0.11**	q	**0.13**	q	0.09
Short-Distance Migrants	q	**0.08**	q	0.07	q	**0.10**	**q**	**0.10**	q	**0.16**	q	0.14
Small body	q	**0.27**	q	0.26	q	0.07	q	0.05	q	**0.05**	q	0.03

Table 7: Results of BIC model selection for multivariate models including the LAndat DHIs (2011-2020, topographic and land cover metrics for overall species richness and 21 functional bird guilds for a 5-km square buffer around centered on first-stop locations of BBS routes, summarized for top-ranked models (ΔBIC<4). Standardized coefficients are shown for each predictor, with model degrees of freedom (df), fit statistics (logLik, BIC, ΔBIC), weights (Wt), and adjusted R^2 values. Explanatory variables are intercept (Int), elevation (Elev), terrain ruggedness index (TRI), the proportion of forest cover (Forest), the proportion of grassland cover (Grass), the proportion of shrubland cover (Shrub), cumulative DHI (Cum DHI), minimum DHI (Min DHI), and variation DHI (Var DHI). The last column show the adjusted R^2 values for the top-ranked model that excluded any components of the DHIs.

Species group	Rank	Int.	Elev	TRI	Forest	Grass	Shrub	Cum DHI	Min DHI	Var DHI	df	logLik	BIC	ΔBIC	Wt.	R^2_{adj}	Model without DHIs R^2_{adj}
Overall species	1	59.29	-	1.85	-	-1.50	-	13.61	-10.07	-	6	-11871	23789	0	0.91	0.39	0.11
Forest affiliates	1	26.86	2.28	1.58	1.36	-1.49	-	13.40	-7.22	-	8	-10469	21001	0	0.95	0.64	0.45
Grass affiliates	1	3.08	-	-0.40	-0.25	0.41	-	-0.96	-	0.32	7	-5728	11512	0	0.55	0.49	0.30
	2	3.08	-	-0.39	-0.24	0.37	-0.12	-1.06	-	0.27	8	-5724	11513	0.80	0.37	0.49	-
Shrub affiliates	1	10.50	-0.50	0.28	-	-0.54	0.75	-1.23	-0.72	-1.96	9	-8054	16181	0	0.68	0.27	0.17
	2	10.50	-0.43	0.30	-0.21	-0.55	0.76	-1.00	-0.82	-1.97	10	-8052	16184	2.61	0.19	0.27	-
Forest specialists	1	13.04	1.83	1.14	2.36	-0.83	-	8.03	-4.85	-	8	-9287	18639	0	0.88	0.65	0.51
Grass specialists	1	2.48	-	-0.31	-0.40	0.33	-0.21	-0.41	-	0.64	8	-5386	10836	0	0.55	0.45	0.25
	2	2.48	-0.12	-0.27	-0.38	0.33	-0.19	-0.50	-	0.65	9	-5382	10836	0.61	0.40	0.45	-
Shrub specialists	1	2.22	-0.22	0.41	0.18	-0.29	0.68	-1.95	-	-1.44	9	-6236	12544	0	0.65	0.57	0.41
	2	2.22	-0.25	0.42	0.21	-0.29	0.68	-2.13	0.25	-1.30	10	-6233	12544	1.56	0.30	0.57	-
Residents	1	12.18	-0.68	0.94	-0.76	-0.62	-	0.64	-	-1.35	8	-8118	16301	0	0.73	0.29	0.16
	2	12.18	-0.62	0.91	-0.81	-0.62	-	0.94	-0.43	-1.59	9	-8115	16303	2.48	0.21	0.30	-

Long-distance migrants	1	26.08	-	0.77	-	-0.61	-	9.37	-6.56	-	6	-10155	20359	0	0.56	0.46	0.10
	2	26.08	-	0.64	0.44	-0.60	-	9.03	-6.39	-	7	-10152	20360	1.29	0.29	0.46	-
Short-distance migrants	1	21.03	1.27	-	-	-0.31	-	4.66	-3.98	1.14	7	-8620	17297	0	0.81	0.43	0.03
Ground Nesters	1	21.12	-	-	-	-	0.66	4.08	-3.49	-	5	-9268	18576	0	0.42	0.17	0.02
	2	21.12	-0.50	0.43	-	-	0.66	3.65	-3.43	-	7	-9268	18576	0.10	0.40	0.18	-
	3	21.12	-	0.21	-	-	0.62	3.99	-3.45	-	6	-9268	18580	3.36	0.08	0.17	-
Mid-story/ Canopy nesters	1	34.62	0.71	1.56	-	-1.26	-	10.99	-7.37	-	7	-10486	21027	0	0.41	0.5	0.24
	2	34.62	0.78	1.61	-	-1.44	-0.55	10.46	-7.08	-	8	-10482	21027	0.27	0.36	0.5	-
	3	34.62	-	1.88	-	-1.25	-	10.46	-7.32	-	6	-10490	21029	2.04	0.15	0.5	-
Threatened	1	2.86	-0.14	-0.38	-0.20	-	-	0.42	0.33	-	7	-5260	10576	0	0.45	0.28	0.19
	2	2.86	-0.15	-0.37	-0.19	-	-	0.34	0.48	0.13	8	-5256	10577	1.02	0.27	0.28	-
	3	2.86	-	-0.43	-0.23	-	-	0.55	0.30	-	6	-5265	10578	2.63	0.12	0.27	-
Decreasing	1	22.01	-1.16	-0.34	-	-	-	2.69	-3.13	1.00	7	-9178	18413	0	0.32	0.28	0.05
	2	22.01	-1.17	-0.34	-	0.27	-	2.79	-3.16	1.02	8	-9175	18414	0.5	0.24	0.28	-
	3	22.01	-1.41	-	-	-	-	2.41	-3.01	1.07	6	-9183	18414	1.08	0.19	0.27	-
	4	22.01	-1.42	-	-	0.28	-	2.53	-3.05	1.08	7	-9179	18414	1.18	0.18	0.28	-
Stable increasing	1	37.28	1.08	2.23	-	-1.76	-	10.75	-6.93	-1.04	8	-10800	21663	0	0.76	0.46	0.27
	2	37.28	0.97	2.31	-	-1.75	-	10.17	-5.72	-	7	-10805	21666	3.59	0.13	0.46	-
Small range	1	4.90	-	1.87	-	-0.37	0.51	-2.99	1.26	-2.01	8	-8984	18032	0	0.73	0.36	0.22
	2	4.90	-	1.80	0.24	-0.37	0.49	-3.19	1.35	-2.02	9	-8981	18035	3.75	0.11	0.36	-
Large range	1	54.39	-	-	-	-0.96	-	17.03	-11.40	2.19	6	-11678	23404	0	0.60	0.52	0.07
	2	54.39	-	-	-0.62	-0.98	-	17.56	-11.67	2.16	7	-11675	23406	2.38	0.18	0.52	-
	3	54.39	-	-	-	-1.19	-0.69	16.46	-11.36	1.90	7	-11675	23407	2.78	0.15	0.52	-

Insectivores	1	32.06	-	1.22	1.01	-1.17	-	10.04	-7.04	-0.92	8	-10539	21142	0	0.64	0.49	0.29
	2	32.06	-	1.25	1.02	-1.16	-	9.59	-5.97	-	7	-10545	21145	2.96	0.15	0.49	-
	3	32.06	-	1.18	0.97	-0.98	0.55	10.20	-6.28	-	8	-10541	21146	3.55	0.11	0.49	-
Granivores	1	11.62	-0.44	0.33	-0.18	-	-2.44	0.91	-1.01	-	8	-7489	15043	0	0.92	0.13	0.09
Frugivores	1	1.29	-0.17	0.32	-	-0.15	-	0.38	-0.54	-0.18	8	-3550	7164	0	0.96	0.29	0.21
Large body	1	34.46	-	-	-1.83	-0.58	-0.65	5.02	-3.33	-	7	-9931	19918	0	0.79	0.20	0.12
	2	34.46	-0.35	-	-1.69	-0.55	-0.60	4.72	-3.29	-	8	-9929	19922	3.85	0.12	0.20	-
Small body	1	24.77	-	2.18	1.41	-1.14	-	8.20	-6.54	-	7	-10198	20453	0	0.42	0.52	0.33
	2	24.77	-	2.12	1.38	-0.98	0.49	8.74	-6.81	-	8	-10195	20453	0.75	0.29	0.52	-
	3	24.77	0.53	1.98	1.28	-1.15	-	8.70	-6.63	-	8	-10195	20454	1.78	0.17	0.52	-
	4	24.77	0.48	1.95	1.26	-1.01	0.45	9.15	-6.87	-	9	-10192	20456	3.72	0.06	0.52	-

Table 8: Results of linear regressions between the individual DHIs based on Landsat for overall species richness and richness of 21 functional bird guilds at four spatial extents: ecoregions, full BBS route, first ten stops, and first stop over 1991-2000. The adjusted R^2 values are shown for each model; the highest values of adjusted R^2 within a functional guild are highlighted in bold. Abbreviations: "l" = linear and "q" = quadratic indicate the type of regression; Cum DHI = cumulative DHI, Min DHI = minimum DHI, Var DHI = variation DHI.

Species richness	Extents		Landsat Cum DHI		Landsat Min DHI		Landsat Var DHI
Overall Species Richness	Ecoregion	q	0.19	l	0.18	q	0.01
	Full route	q	0.34	q	0.03	q	0.08
	10-Stops	q	0.35	q	0.08	q	0.06
	1-Stop	l	0.02		-		-
Forest Affiliates	Ecoregion	q	0.01	l	0.03	q	0.06
	Full route	q	0.45	l	0.06	q	0.02
	10-Stops	q	0.45	l	0.11	q	0.01
	1-Stop	l	0.19	l	0.05		-
Grassland Affiliates	Ecoregion	q	0.26	q	0.29	q	0.14
	Full route	q	0.36	q	0.27	q	0.12
	10-Stops	q	0.29	q	0.16	q	0.07
	1-Stop	l	0.18	l	0.09	l	0.05
Shrubland Affiliates	Ecoregion	q	0.45	l	0.06	q	0.10
	Full route	l	0.04	q	0.04	q	0.05
	10-Stops	q	0.01	q	0.08	q	0.06
	1-Stop	q	0.04	q	0.04	l	0.04
Forest Specialists	Ecoregion	q	0.03		-	q	0.08
	Full route	q	0.35	q	0.04	q	0.02
	10-Stops	l	0.32	q	0.05		-
	1-Stop	l	0.08	q	0.02	l	0.02
Grassland Specialists	Ecoregion	q	0.17	l	0.23	q	0.21
	Full route	q	0.25	q	0.20	q	0.20
	10-Stops	q	0.22	q	0.15	q	0.14

	1-Stop	l	0.13	l	0.07	l	0.05
Shrubland Specialists	Ecoregion	q	0.49	l	0.04	q	0.18
	Full route	q	0.30	l	0.03	q	0.14
	10-Stops	q	0.19	q	0.01	q	0.10
	1-Stop	l	0.10	q	0.02	l	0.02
Residents	Ecoregion	q	0.26		-	q	0.14
	Full route	q	0.15	q	0.20	q	0.11
	10-Stops	q	0.16	q	0.29	q	0.17
	1-Stop	q	0.14	q	0.14	l	0.14
Long-Distance Migrants	Ecoregion	l	-0.01	q	0.11	q	0.22
	Full route	q	0.39	q	0.05	q	0.10
	10-Stops	q	0.36	q	0.06	q	0.05
	1-Stop	l	0.06		-		-
Short-Distance Migrants	Ecoregion	l	0.20	q	0.33	q	0.13
	Full route	q	0.12	q	0.06	q	0.25
	10-Stops	q	0.18	q	0.03	q	0.18
	1-Stop	q	0.08	q	0.08	l	0.08
Ground Nesters	Ecoregion	q	0.27	l	0.29	q	0.05
	Full route	q	0.16	q	0.03	q	0.09
	10-Stops	q	0.16	q	0.06	q	0.05
	1-Stop		-		-		-
Mid-Story/Canopy Nesters	Ecoregion	q	0.10	l	0.08	q	-0.01
	Full route	q	0.39	q	0.03	q	0.06
	10-Stops	q	0.39	q	0.07	q	0.04
	1-Stop	l	0.04		-		-
Threatened	Ecoregion		-	q	0.05	q	0.16
	Full route	q	0.19	q	0.19	q	0.03
	10-Stops	q	0.17	q	0.22	l	0.06
	1-Stop	l	0.07	l	0.05	l	0.02
Decreasing	Ecoregion	l	0.19	q	0.29	q	0.15
	Full route	q	0.19	q	0.05	q	0.21
	10-Stops	q	0.14	q	0.06	q	0.15
	1-Stop	q	0.03	l	0.03	l	0.03

Stable/ Increasing	Ecoregion	q	0.17	l	0.08	l	-0.01
	Full route	q	0.36	q	0.04	q	0.02
	10-Stops	q	0.42	q	0.11	q	0.02
	1-Stop	l	0.10	l	0.01		-
Small-Ranged	Ecoregion	q	0.35	l	0.02	q	0.17
	Full route	q	0.06	q	0.02	q	0.16
	10-Stops	q	0.04	q	0.01	q	0.13
	1-Stop	q	0.03	q	0.03	l	0.03
Large-Ranged	Ecoregion	l	-0.01	l	0.14	q	0.43
	Full route	q	0.41	q	0.03	q	0.17
	10-Stops	q	0.38	q	0.07	q	0.09
	1-Stop	l	0.03	q	0.01	l	0.01
Insectivores	Ecoregion	q	0.01	q	0.08	q	0.06
	Full route	q	0.41	q	0.06	q	0.05
	10-Stops	q	0.39	q	0.10	q	0.03
	1-Stop	l	0.09	l	0.01		-
Granivores	Ecoregion	q	0.27	q	0.21	l	0.03
	Full route	q	0.22	q	0.04	q	0.10
	10-Stops	q	0.24	q	0.12	q	0.08
	1-Stop	l	0.01		-		-
Frugivores	Ecoregion	q	0.15	q	0.05	q	-0.01
	Full route	q	0.10	q	0.01		-
	10-Stops	q	0.06		-	q	0.01
	1-Stop		-		-		-
Large body	Ecoregion	q	0.42	l	0.22	l	-0.01
	Full route	q	0.30	q	0.05	q	0.09
	10-Stops	q	0.24	q	0.13	q	0.06
	1-Stop		-		-		-
Small body	Ecoregion		-	l	0.07	q	0.07
	Full route	q	0.30	q	0.01	q	0.06
	10-Stops	q	0.30	q	0.02	q	0.04
	1-Stop	l	0.04	q	0.02	l	0.02

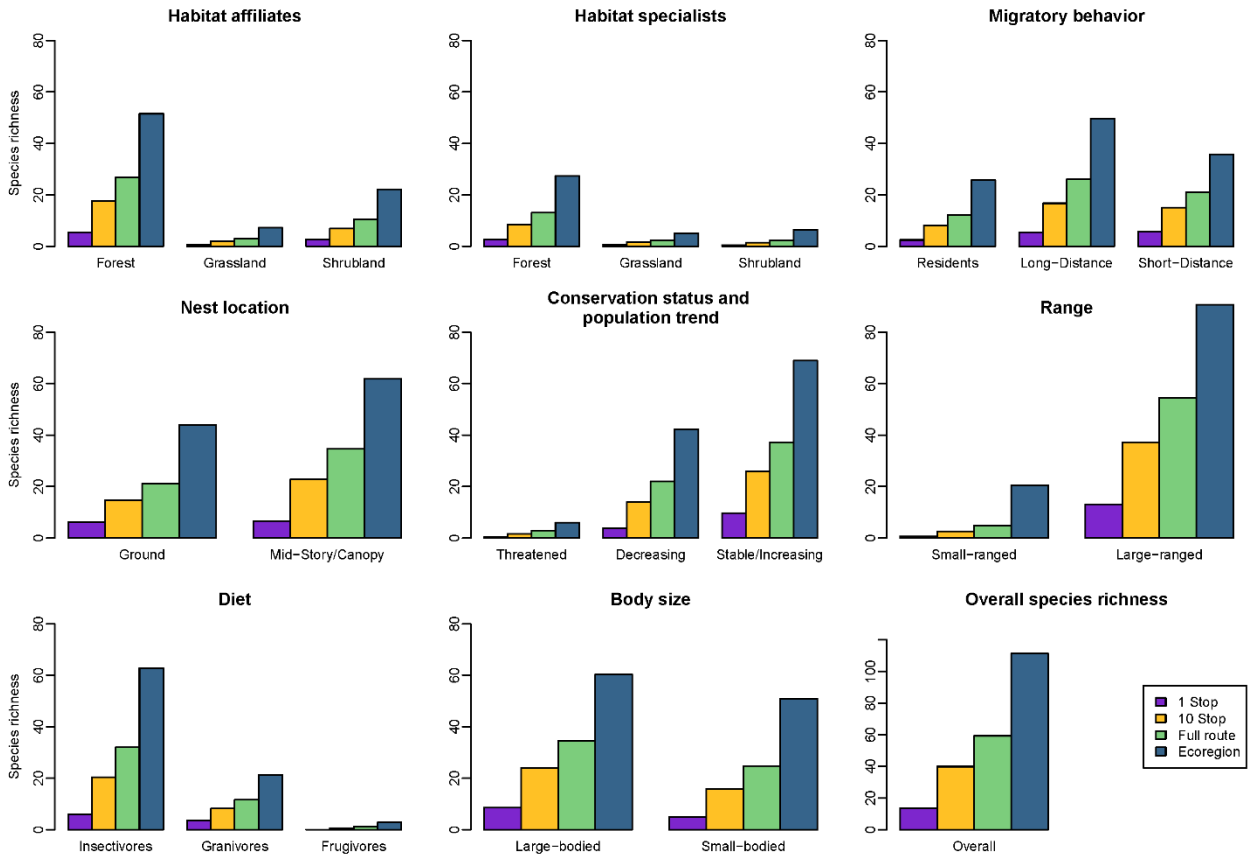

Figure 7. Average species richness for 21 bird guilds and overall species richness modeled at four sets of all species over 2011-2019. Note: the y-axis scale changes for overall species richness.

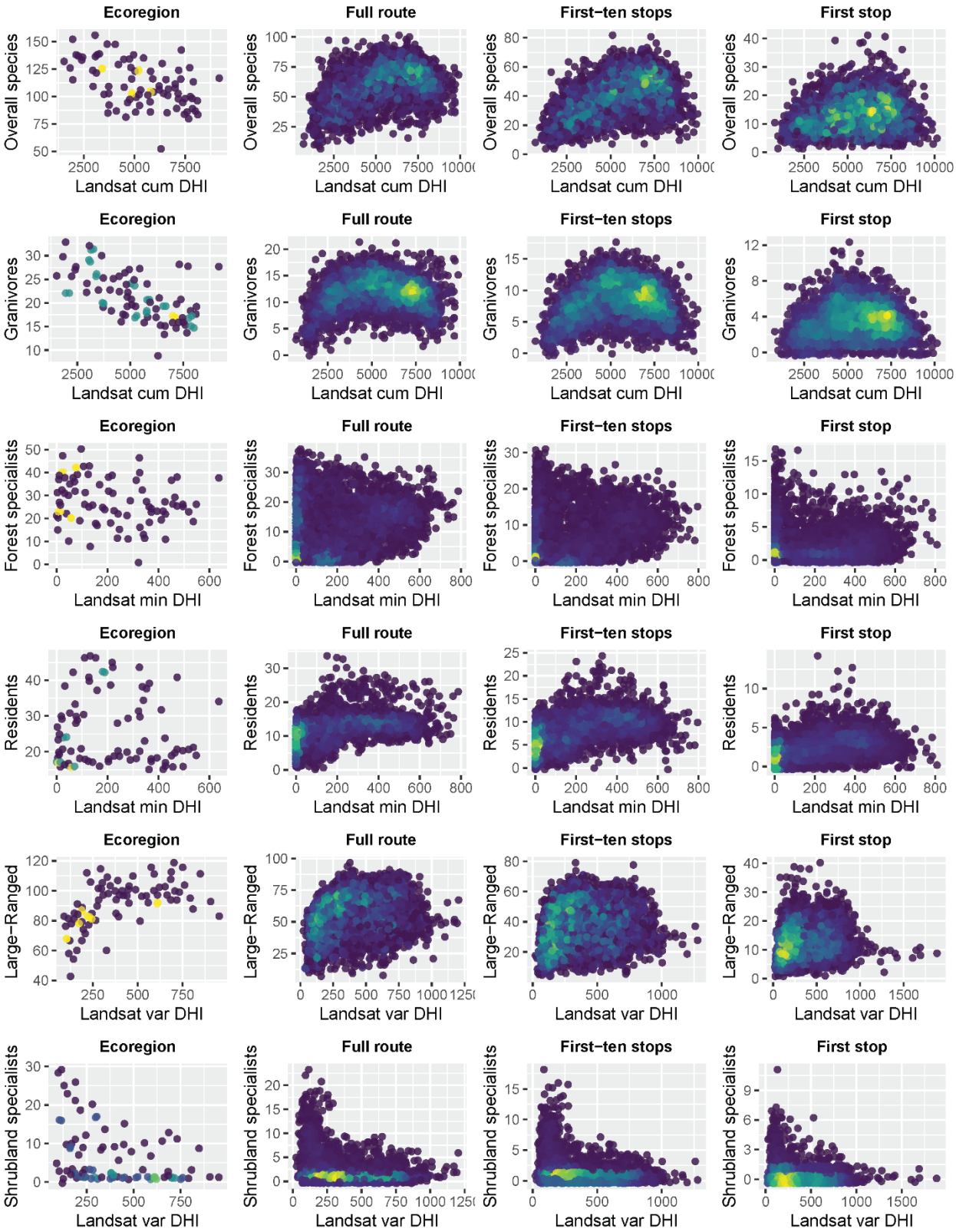
Ecoregion
Full route
First−ten stops
First stop
Overall species
Landsat cum DHI
Granivores
Landsat cum DHI
Forest specialists
Landsat min DHI
Residents
Landsat min DHI
Large−Ranged
Landsat var DHI
Shrubland specialists
Landsat var DHI

Figure 8: Subset of plots illustrating different type of relationship between species richness and the individual DHIs based on Landsat calculated for 2011-2020 at four spatial extents: (first column) ecoregion, (second column) full BBS route, (third column) first ten stops, and (fourth column) first stop.

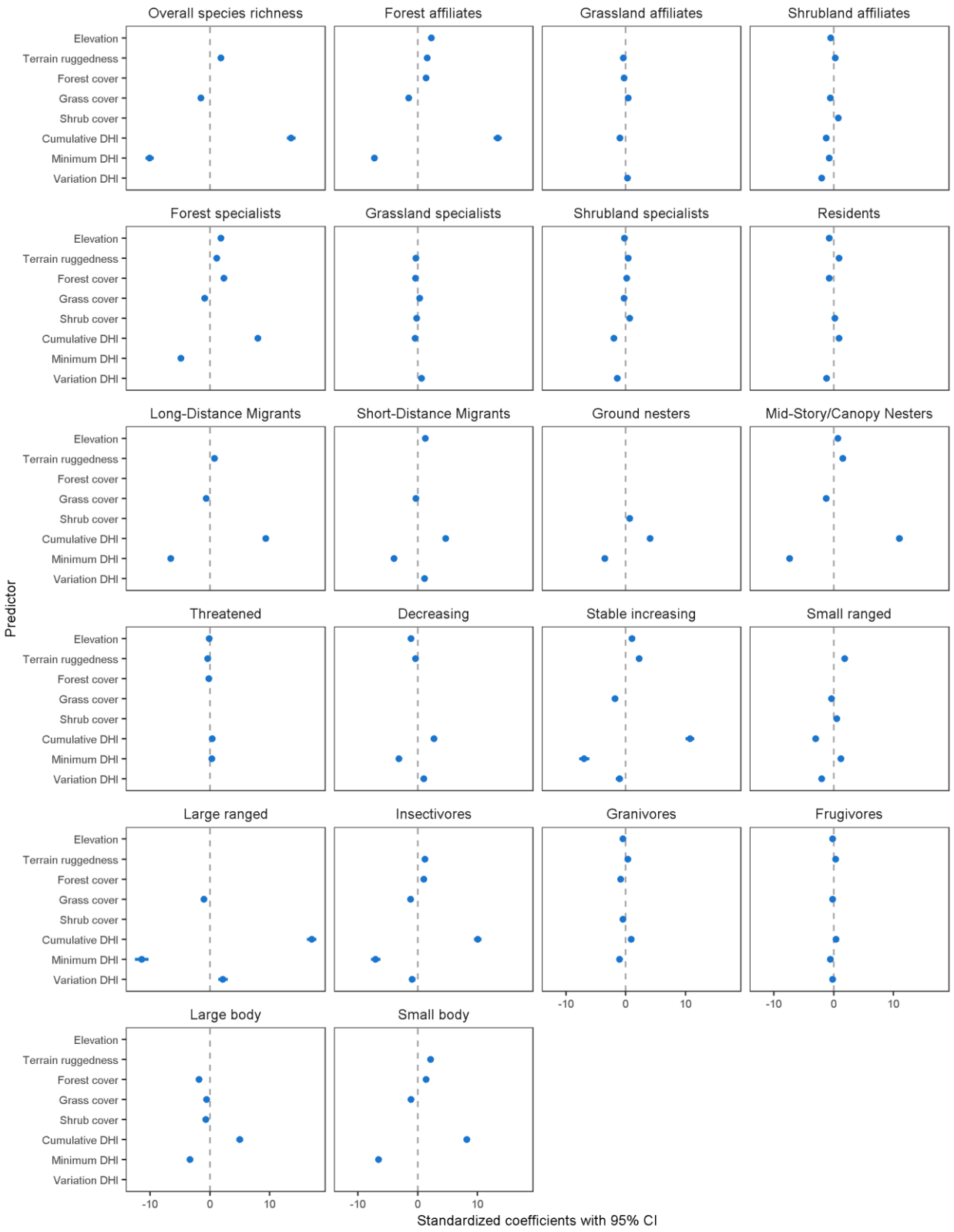
Overall species richness
Forest affiliates
Grassland affiliates
Shrubland affiliates
Forest specialists
Grassland specialists
Shrubland specialists
Residents
Long-Distance Migrants
Short-Distance Migrants
Ground nesters
Mid-Story/Canopy Nesters
Threatened
Decreasing
Stable increasing
Small ranged
Large ranged
Insectivores
Granivores
Frugivores
Large body
Small body
Elevation
Terrain ruggedness
Forest cover
Grass cover
Shrub cover
Cumulative DHI
Minimum DHI
Variation DHI
Predictor
-10
0
10
Standardized coefficients with 95% CI

Figure 9: Standardized coefficients with 95% confidence interval for explanatory variables in top-ranked models for overall species richness and 21 functional bird guilds. Variables with no values were not included in top-ranked models.

Appendix 3: Workflow of the modeling our four objectives.

Appendix 4: a) A histogram showing the distribution of terrain ruggedness index (TRI) within a 5-km square buffer around centered on first-stop locations of BBS routes, b) Number of BBS routes depending on terrain ruggedness.

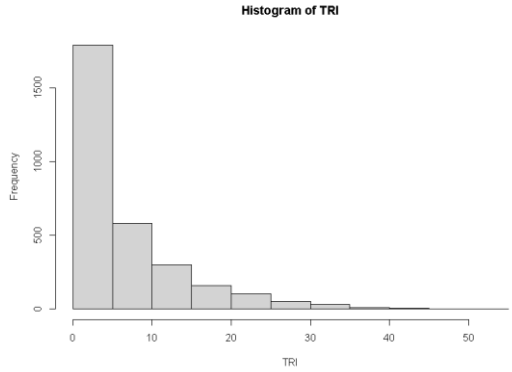

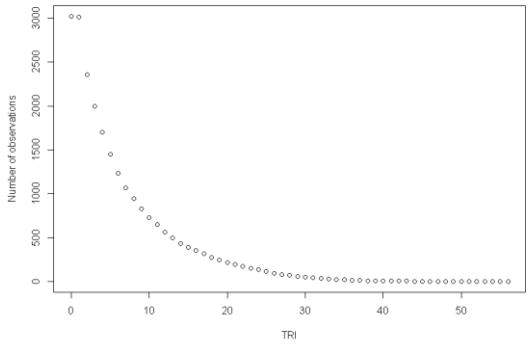

Appendix 5: Spearman correlation between explanatory variables in the combined model. Variables are elevation, terrain ruggedness index (TRI), the proportion of forest, grassland, and shrubland land cover, cumulative DHI, minimum DHI, and variation DHI.

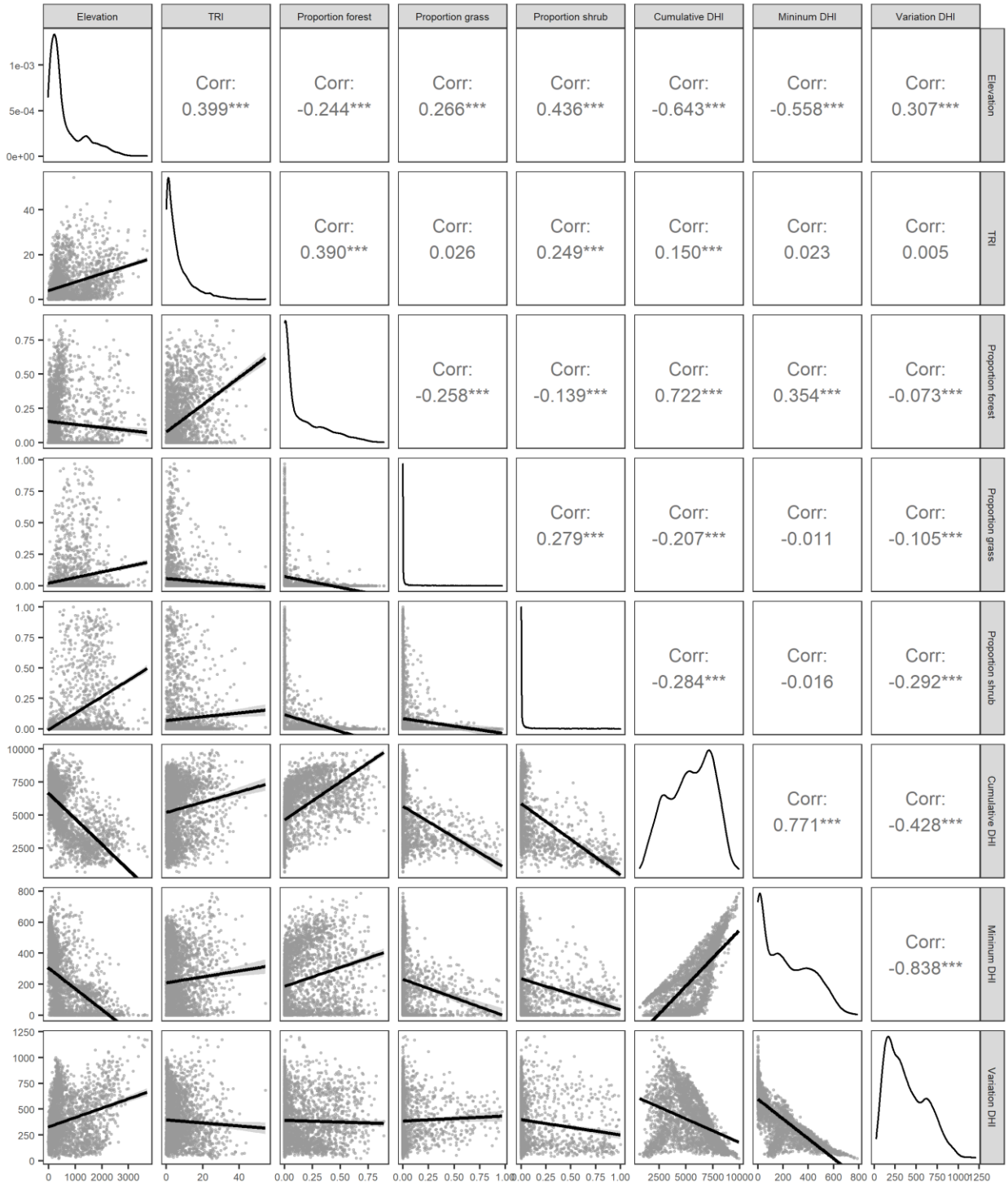

Appendix 6: Spatial patterns of overall species richness and 21 functional bird guilds across four spatial extents.

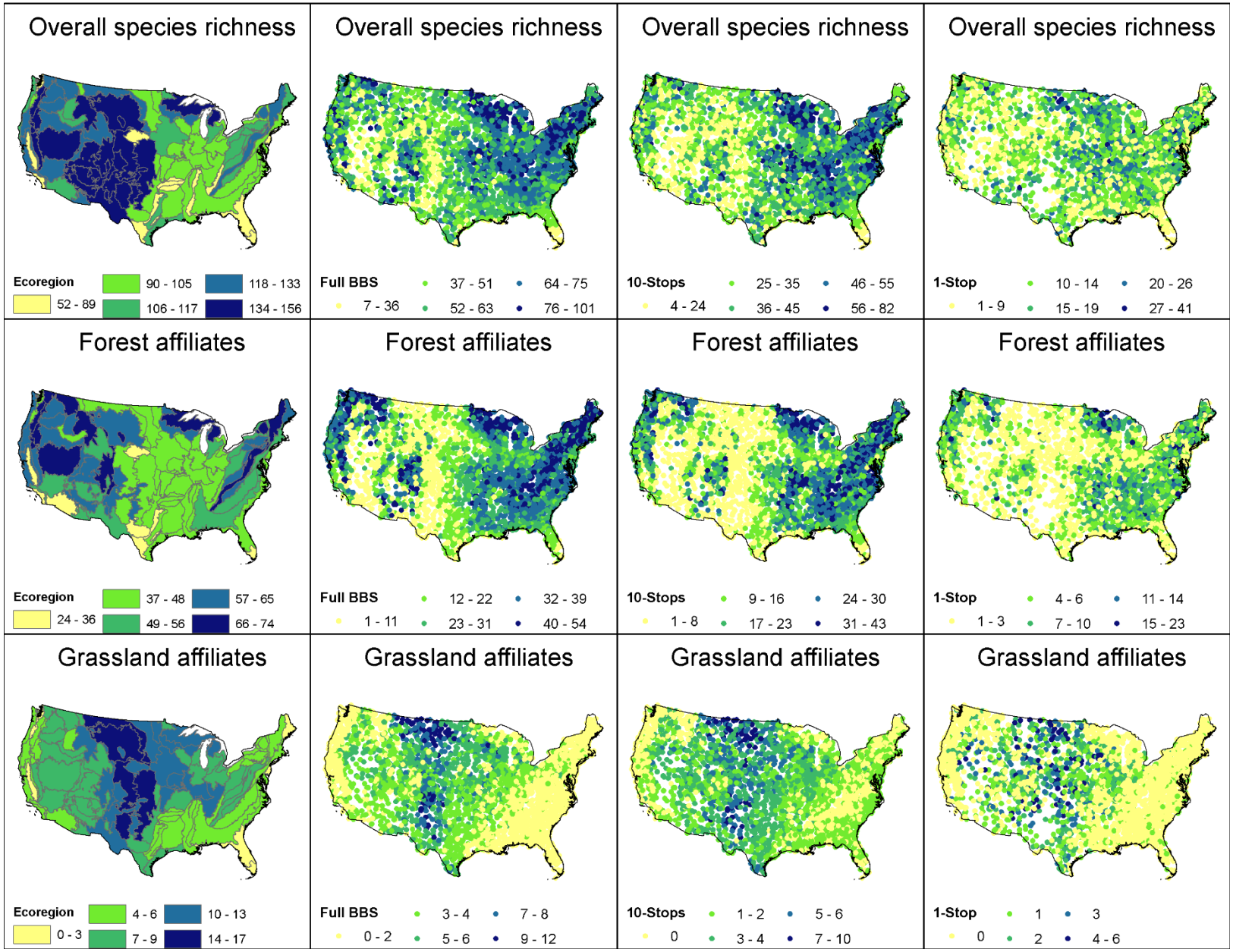
Overall species richness
Ecoregion
52 - 89
90 - 105
106 - 117
118 - 133
134 - 156
Overall species richness
Full BBS
7 - 36
37 - 51
52 - 63
64 - 75
76 - 101
Overall species richness
10-Stops
4 - 24
25 - 35
36 - 45
46 - 55
56 - 82
Overall species richness
1-Stop
1 - 9
10 - 14
15 - 19
20 - 26
27 - 41
Forest affiliates
Ecoregion
24 - 36
37 - 48
49 - 56
57 - 65
66 - 74
Forest affiliates
Full BBS
1 - 11
12 - 22
23 - 31
32 - 39
40 - 54
Forest affiliates
10-Stops
1 - 8
9 - 16
17 - 23
24 - 30
31 - 43
Forest affiliates
1-Stop
1 - 3
4 - 6
7 - 10
11 - 14
15 - 23
Grassland affiliates
Ecoregion
0 - 3
4 - 6
7 - 9
10 - 13
14 - 17
Grassland affiliates
Full BBS
0 - 2
3 - 4
5 - 6
7 - 8
9 - 12
Grassland affiliates
10-Stops
0
1 - 2
3 - 4
5 - 6
7 - 10
Grassland affiliates
1-Stop
0
1
2
3
4 - 6

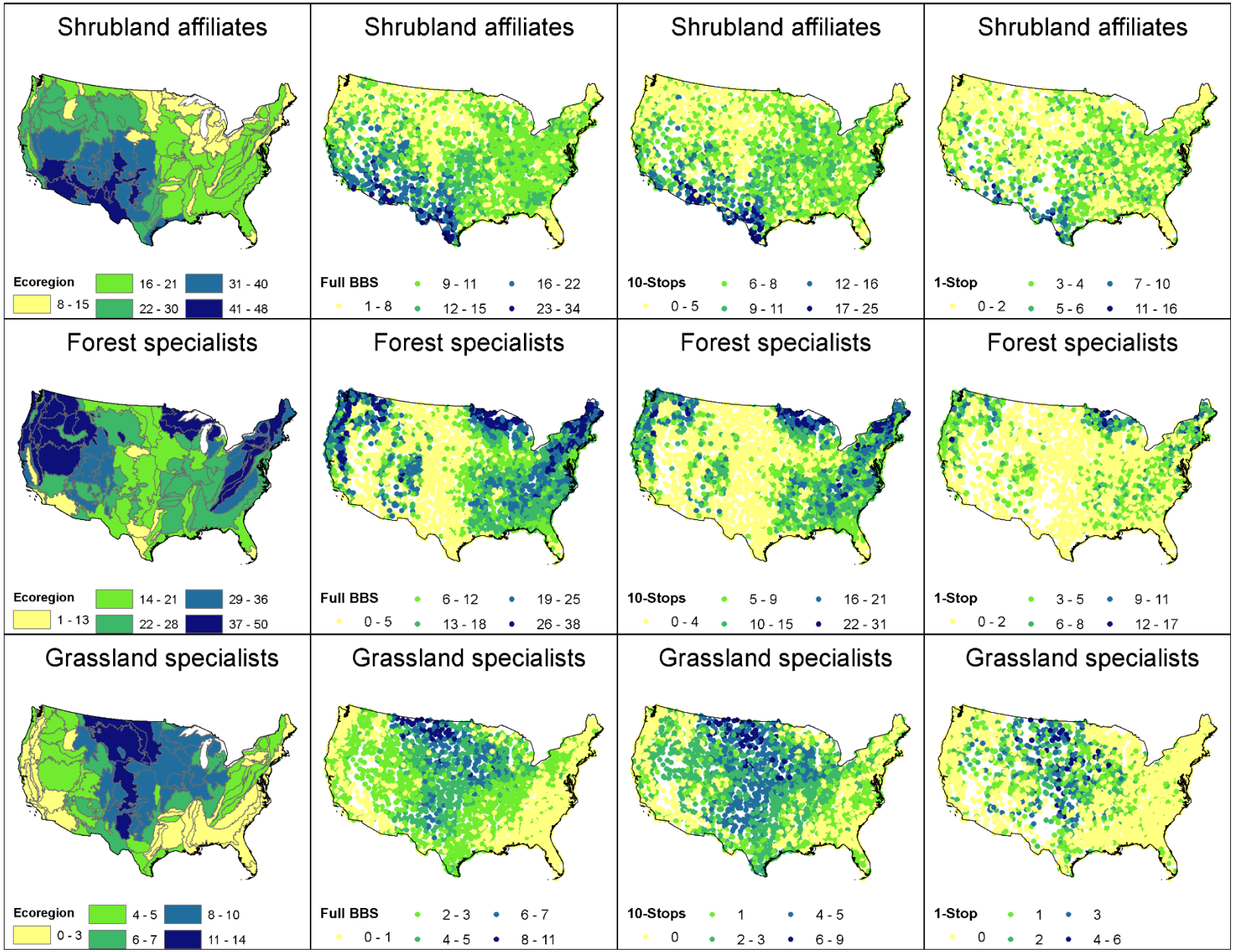
Shrubland affiliates
Ecoregion
8 - 15
16 - 21
22 - 30
31 - 40
41 - 48
Shrubland affiliates
Full BBS
1 - 8
9 - 11
12 - 15
16 - 22
23 - 34
Shrubland affiliates
10-Stops
0 - 5
6 - 8
9 - 11
12 - 16
17 - 25
Shrubland affiliates
1-Stop
0 - 2
3 - 4
5 - 6
7 - 10
11 - 16
Forest specialists
Ecoregion
1 - 13
14 - 21
22 - 28
29 - 36
37 - 50
Forest specialists
Full BBS
0 - 5
6 - 12
13 - 18
19 - 25
26 - 38
Forest specialists
10-Stops
0 - 4
5 - 9
10 - 15
16 - 21
22 - 31
Forest specialists
1-Stop
0 - 2
3 - 5
6 - 8
9 - 11
12 - 17
Grassland specialists
Ecoregion
0 - 3
4 - 5
6 - 7
8 - 10
11 - 14
Grassland specialists
Full BBS
0 - 1
2 - 3
4 - 5
6 - 7
8 - 11
Grassland specialists
10-Stops
0
1
2 - 3
4 - 5
6 - 9
Grassland specialists
1-Stop
0
1
2
3
4 - 6

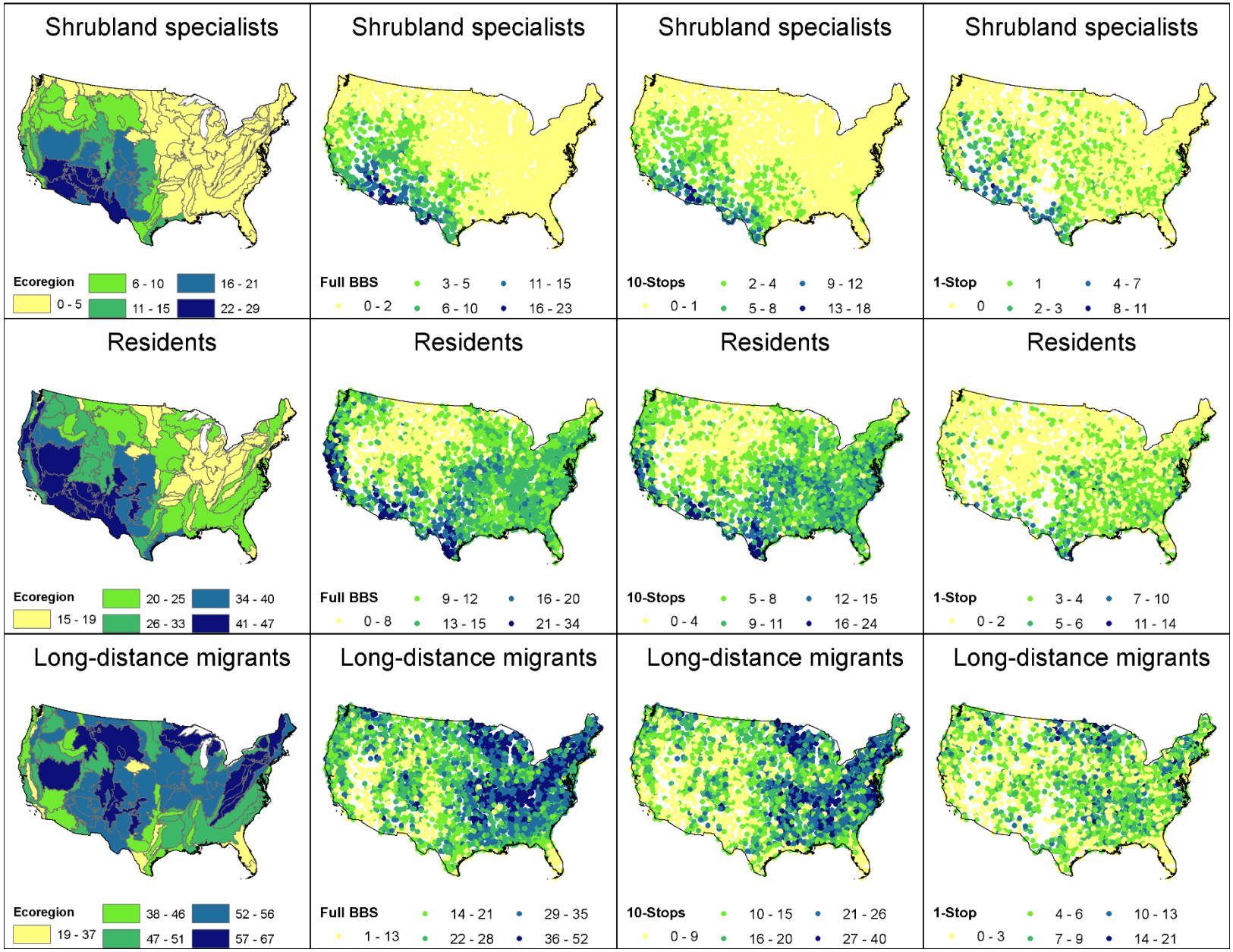
Shrubland specialists
Ecoregion
0 - 5
6 - 10
11 - 15
16 - 21
22 - 29
Shrubland specialists
Full BBS
0 - 2
3 - 5
6 - 10
11 - 15
16 - 23
Shrubland specialists
10-Stops
0 - 1
2 - 4
5 - 8
9 - 12
13 - 18
Shrubland specialists
1-Stop
0
1
2 - 3
4 - 7
8 - 11
Residents
Ecoregion
15 - 19
20 - 25
26 - 33
34 - 40
41 - 47
Residents
Full BBS
0 - 8
9 - 12
13 - 15
16 - 20
21 - 34
Residents
10-Stops
0 - 4
5 - 8
9 - 11
12 - 15
16 - 24
Residents
1-Stop
0 - 2
3 - 4
5 - 6
7 - 10
11 - 14
Long-distance migrants
Ecoregion
19 - 37
38 - 46
47 - 51
52 - 56
57 - 67
Long-distance migrants
Full BBS
1 - 13
14 - 21
22 - 28
29 - 35
36 - 52
Long-distance migrants
10-Stops
0 - 9
10 - 15
16 - 20
21 - 26
27 - 40
Long-distance migrants
1-Stop
0 - 3
4 - 6
7 - 9
10 - 13
14 - 21

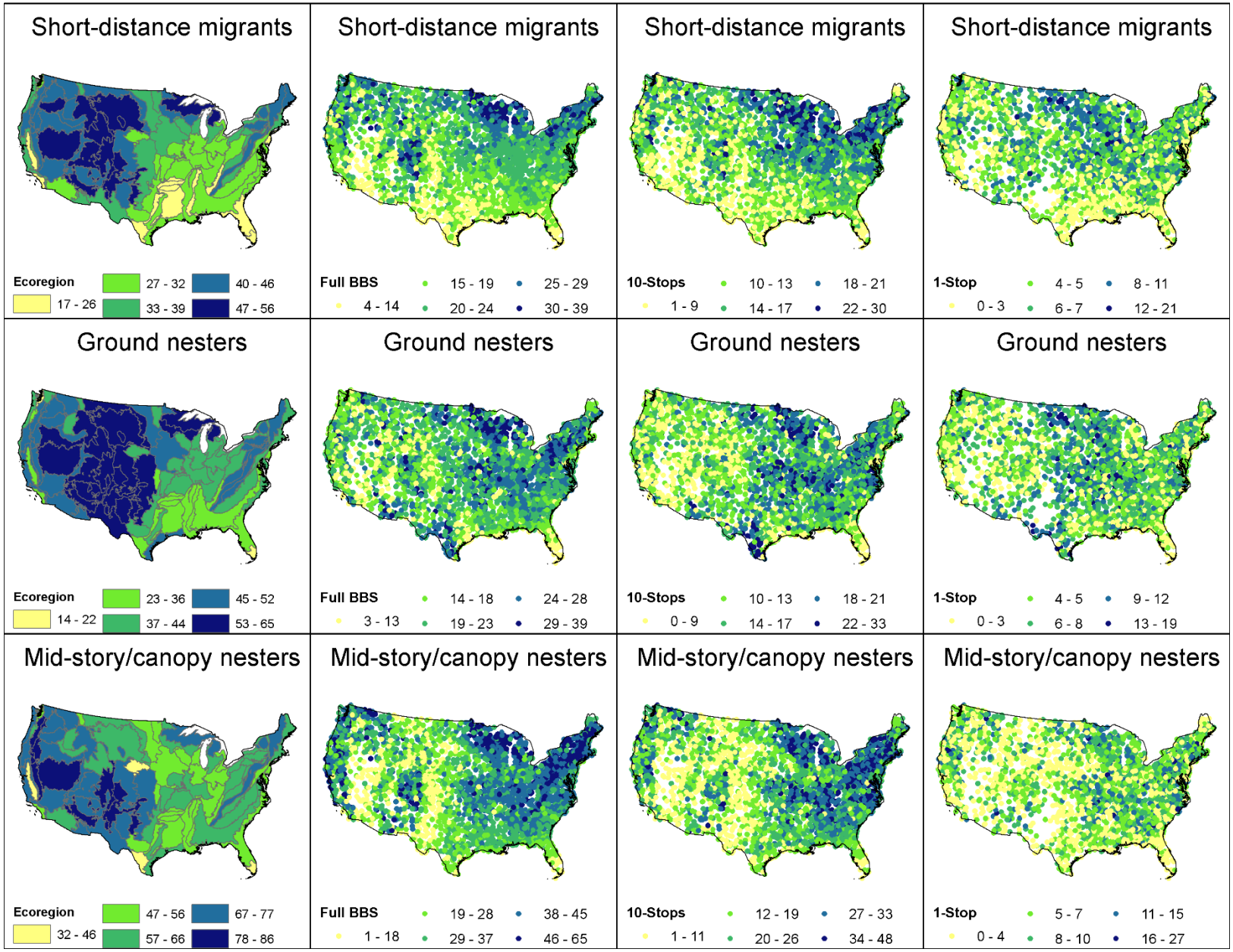
Short-distance migrants
Ecoregion
17 - 26
27 - 32
33 - 39
40 - 46
47 - 56
Short-distance migrants
Full BBS
4 - 14
15 - 19
20 - 24
25 - 29
30 - 39
Short-distance migrants
10-Stops
1 - 9
10 - 13
14 - 17
18 - 21
22 - 30
Short-distance migrants
1-Stop
0 - 3
4 - 5
6 - 7
8 - 11
12 - 21
Ground nesters
Ecoregion
14 - 22
23 - 36
37 - 44
45 - 52
53 - 65
Ground nesters
Full BBS
3 - 13
14 - 18
19 - 23
24 - 28
29 - 39
Ground nesters
10-Stops
0 - 9
10 - 13
14 - 17
18 - 21
22 - 33
Ground nesters
1-Stop
0 - 3
4 - 5
6 - 8
9 - 12
13 - 19
Mid-story/canopy nesters
Ecoregion
32 - 46
47 - 56
57 - 66
67 - 77
78 - 86
Mid-story/canopy nesters
Full BBS
1 - 18
19 - 28
29 - 37
38 - 45
46 - 65
Mid-story/canopy nesters
10-Stops
1 - 11
12 - 19
20 - 26
27 - 33
34 - 48
Mid-story/canopy nesters
1-Stop
0 - 4
5 - 7
8 - 10
11 - 15
16 - 27

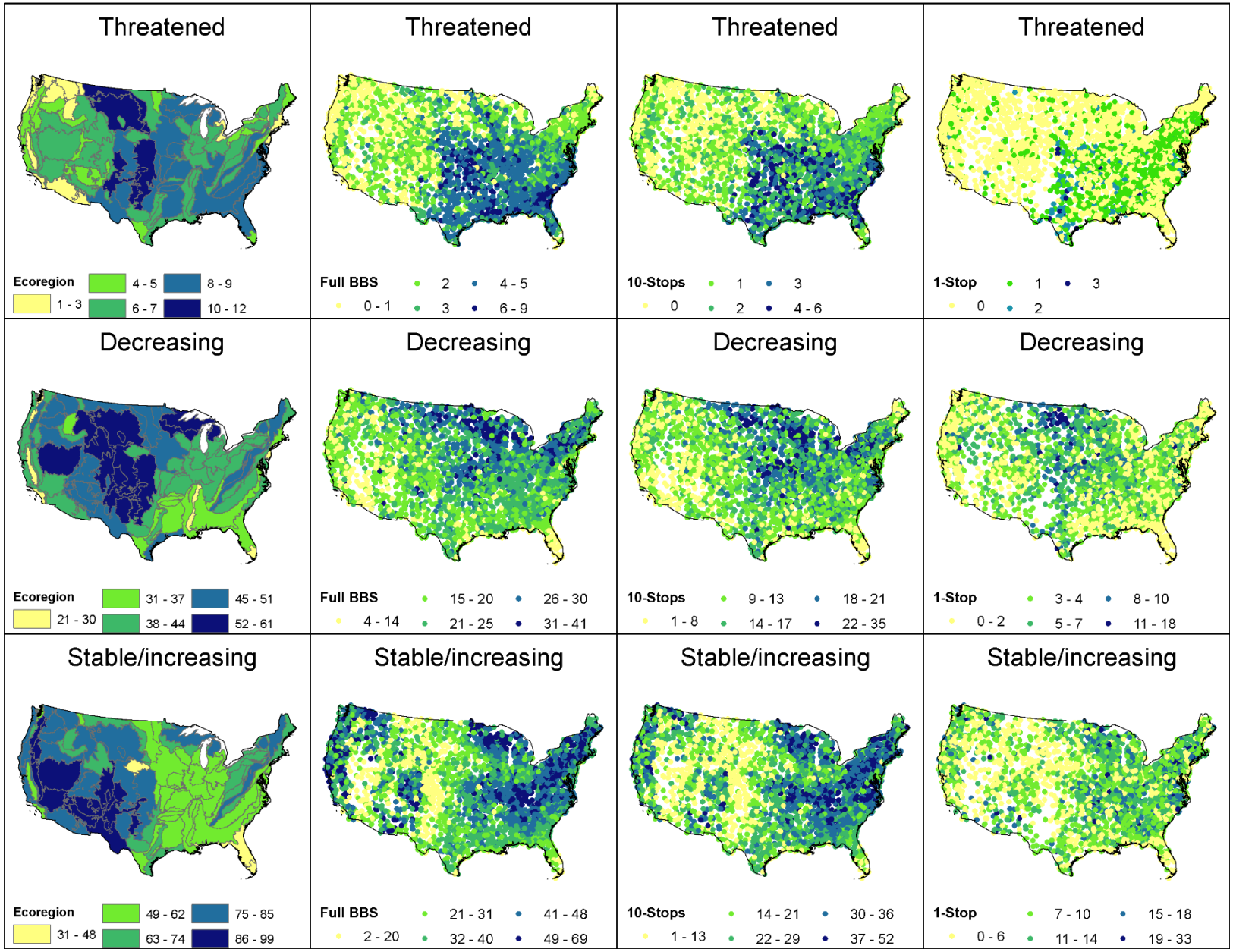
Threatened
Ecoregion
1 - 3
4 - 5
6 - 7
8 - 9
10 - 12
Threatened
Full BBS
0 - 1
2
3
4 - 5
6 - 9
Threatened
10-Stops
0
1
2
3
4 - 6
Threatened
1-Stop
0
1
2
3
Decreasing
Ecoregion
21 - 30
31 - 37
38 - 44
45 - 51
52 - 61
Decreasing
Full BBS
4 - 14
15 - 20
21 - 25
26 - 30
31 - 41
Decreasing
10-Stops
1 - 8
9 - 13
14 - 17
18 - 21
22 - 35
Decreasing
1-Stop
0 - 2
3 - 4
5 - 7
8 - 10
11 - 18
Stable/increasing
Ecoregion
31 - 48
49 - 62
63 - 74
75 - 85
86 - 99
Stable/increasing
Full BBS
2 - 20
21 - 31
32 - 40
41 - 48
49 - 69
Stable/increasing
10-Stops
1 - 13
14 - 21
22 - 29
30 - 36
37 - 52
Stable/increasing
1-Stop
0 - 6
7 - 10
11 - 14
15 - 18
19 - 33

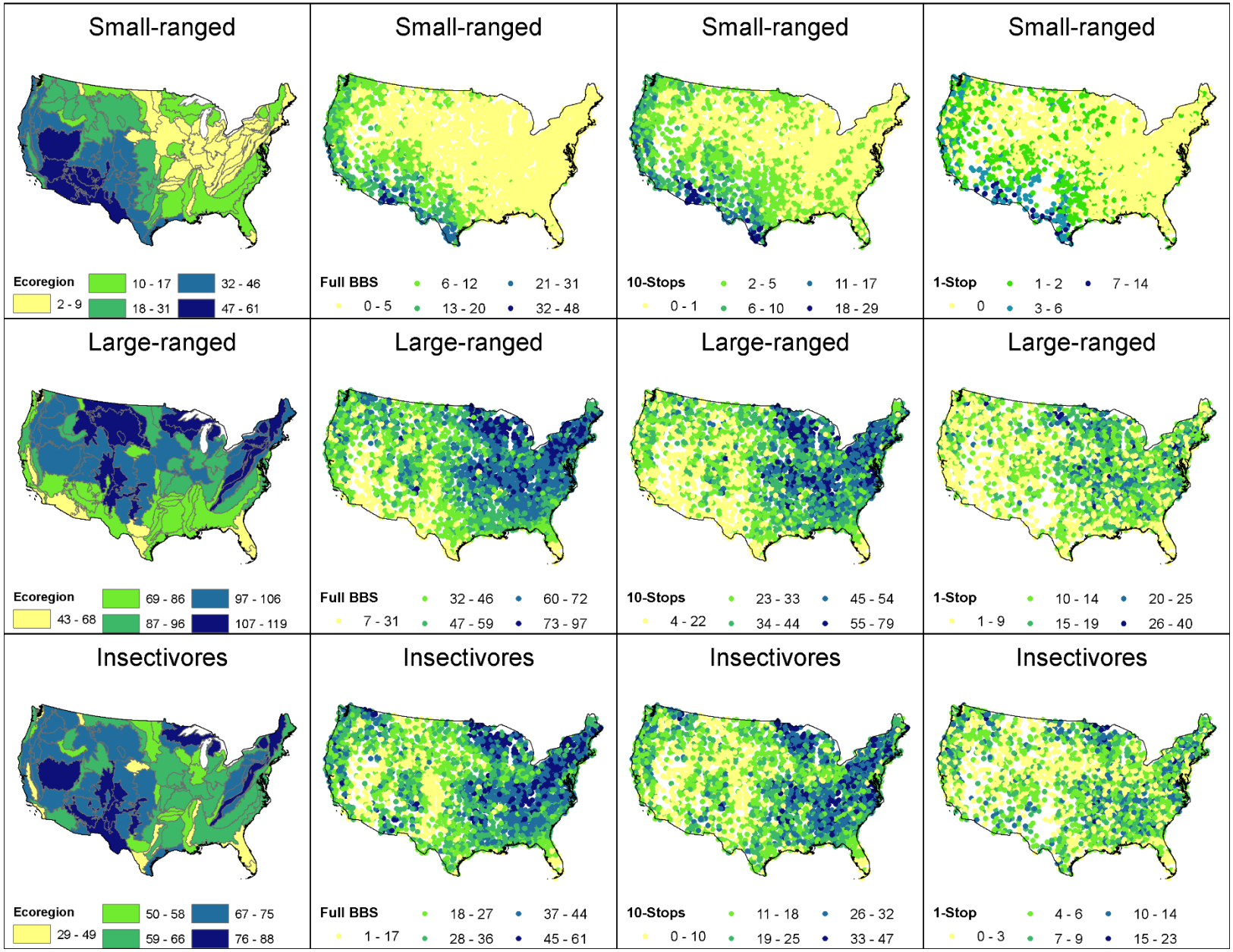
Small-ranged
Ecoregion
2 - 9
10 - 17
18 - 31
32 - 46
47 - 61
Small-ranged
Full BBS
0 - 5
6 - 12
13 - 20
21 - 31
32 - 48
Small-ranged
10-Stops
0 - 1
2 - 5
6 - 10
11 - 17
18 - 29
Small-ranged
1-Stop
0
1 - 2
3 - 6
7 - 14
Large-ranged
Ecoregion
43 - 68
69 - 86
87 - 96
97 - 106
107 - 119
Large-ranged
Full BBS
7 - 31
32 - 46
47 - 59
60 - 72
73 - 97
Large-ranged
10-Stops
4 - 22
23 - 33
34 - 44
45 - 54
55 - 79
Large-ranged
1-Stop
1 - 9
10 - 14
15 - 19
20 - 25
26 - 40
Insectivores
Ecoregion
29 - 49
50 - 58
59 - 66
67 - 75
76 - 88
Insectivores
Full BBS
1 - 17
18 - 27
28 - 36
37 - 44
45 - 61
Insectivores
10-Stops
0 - 10
11 - 18
19 - 25
26 - 32
33 - 47
Insectivores
1-Stop
0 - 3
4 - 6
7 - 9
10 - 14
15 - 23

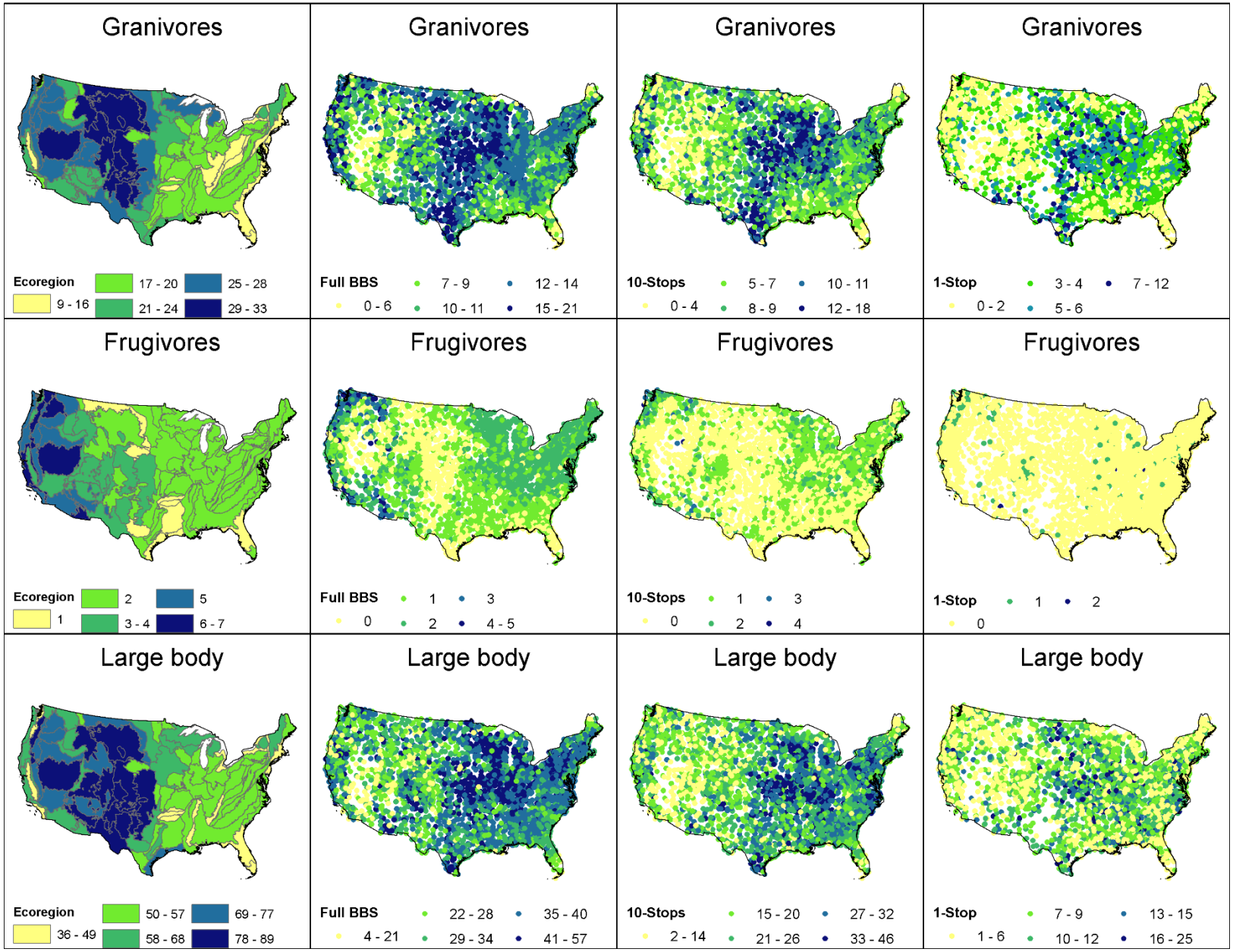
Granivores
Ecoregion
9 - 16
17 - 20
21 - 24
25 - 28
29 - 33
Granivores
Full BBS
0 - 6
7 - 9
10 - 11
12 - 14
15 - 21
Granivores
10-Stops
0 - 4
5 - 7
8 - 9
10 - 11
12 - 18
Granivores
1-Stop
0 - 2
3 - 4
5 - 6
7 - 12
Frugivores
Ecoregion
1
2
3 - 4
5
6 - 7
Frugivores
Full BBS
0
1
2
3
4 - 5
Frugivores
10-Stops
0
1
2
3
4
Frugivores
1-Stop
0
1
2
Large body
Ecoregion
36 - 49
50 - 57
58 - 68
69 - 77
78 - 89
Large body
Full BBS
4 - 21
22 - 28
29 - 34
35 - 40
41 - 57
Large body
10-Stops
2 - 14
15 - 20
21 - 26
27 - 32
33 - 46
Large body
1-Stop
1 - 6
7 - 9
10 - 12
13 - 15
16 - 25

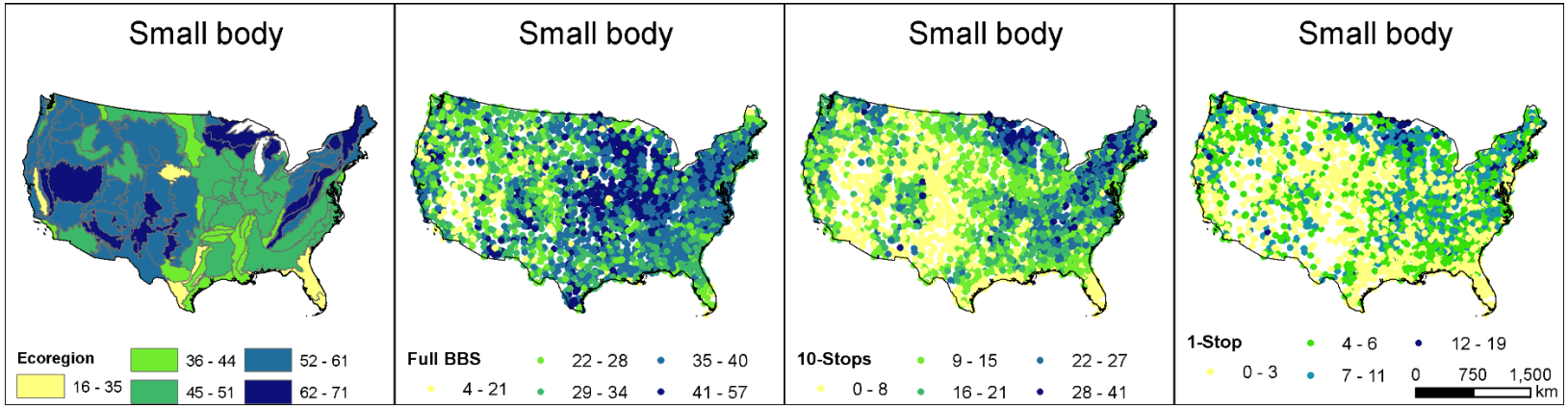
Small body
Ecoregion
16 - 35
36 - 44
45 - 51
52 - 61
62 - 71
Small body
Full BBS
4 - 21
22 - 28
29 - 34
35 - 40
41 - 57
Small body
10-Stops
0 - 8
9 - 15
16 - 21
22 - 27
28 - 41
Small body
1-Stop
0 - 3
4 - 6
7 - 11
12 - 19
0
750
1,500
km

Appendix 7: Average species richness for 21 bird guilds and overall species richness over 2011-2019 and 1991-2000 and the difference between the two periods.

Species group	Years	Ecoregion	Full route	10-Stops	1-Stop
Overall Species Richness	2011-2019	111.19	59.29	39.83	13.64
	1991-2000	112.45	60.54	34.30	10.76
	difference	-1.26	-1.25	5.53	2.87
Forest Affiliates	2011-2019	51.55	26.86	17.63	5.55
	1991-2000	53.09	27.38	14.69	4.40
	difference	-1.54	-0.52	2.94	1.15
Grassland Affiliates	2011-2019	7.20	3.08	1.96	0.67
	1991-2000	7.36	3.15	1.60	0.44
	difference	-0.16	-0.07	0.36	0.23
Shrubland Affiliates	2011-2019	22.14	10.50	7.01	2.77
	1991-2000	22.56	10.90	6.11	2.17
	difference	-0.42	-0.40	0.91	0.60
Forest Specialist	2011-2019	27.34	13.04	8.39	2.67
	1991-2000	28.39	13.48	6.99	2.24
	difference	-1.05	-0.44	1.39	0.43
Grassland Specialists	2011-2019	5.02	2.48	1.64	0.61
	1991-2000	5.19	2.64	1.50	0.47
	difference	-0.16	-0.16	0.13	0.13
Shrubland Specialists	2011-2019	6.52	2.22	1.45	0.46
	1991-2000	6.65	2.32	1.19	0.29
	difference	-0.13	-0.11	0.26	0.17
Residents	2011-2019	25.74	12.18	8.09	2.48
	1991-2000	24.55	11.74	6.41	1.83
	difference	1.19	0.43	1.68	0.65
Long-Distance Migrants	2011-2019	49.64	26.08	16.73	5.48
	1991-2000	51.11	26.85	14.21	4.21
	difference	-1.47	-0.77	2.52	1.27
Short-Distance Migrants	2011-2019	35.81	21.03	15.01	5.68
	1991-2000	36.79	21.94	13.68	4.73
	difference	-0.98	-0.91	1.33	0.95
Ground Nesters	2011-2019	43.84	21.12	14.73	6.10
	1991-2000	45.18	22.07	13.13	5.00
	difference	-1.34	-0.94	1.60	1.11
Mid-Story/Canopy Nesters	2011-2019	61.85	34.62	22.75	6.67
	1991-2000	62.44	35.23	19.24	5.11
	difference	-0.59	-0.61	3.51	1.56
Threatened	2011-2019	6.04	2.86	1.65	0.42
	1991-2000	6.54	3.17	1.57	0.42
	difference	-0.51	-0.31	0.08	0
Decreasing	2011-2019	42.27	22.01	13.99	3.92

	1991-2000	44.07	23.83	12.73	3.23
	difference	-1.80	-1.82	1.25	0.68
Stable/ Increasing	2011-2019	68.92	37.28	25.84	9.72
	1991-2000	68.38	36.71	21.57	7.53
	difference	0.54	0.57	4.28	2.19
Small-Ranged	2011-2019	20.53	4.90	2.60	0.59
	1991-2000	20.88	5.09	2.00	0.41
	difference	-0.35	-0.19	0.61	0.18
Large-Ranged	2011-2019	90.66	54.39	7.23	13.04
	1991-2000	91.56	55.44	32.30	10.36
	difference	-0.91	-1.05	4.93	2.69
Insectivores	2011-2019	62.84	32.05	20.37	5.98
	1991-2000	63.95	33.27	17.25	4.50
	difference	-1.12	-1.21	3.12	1.48
Granivores	2011-2019	21.24	11.62	8.19	3.55
	1991-2000	20.84	11.46	7.09	2.84
	difference	0.40	0.16	1.11	0.71
Frugivores	2011-2019	2.85	1.29	0.61	0.05
	1991-2000	3.00	1.27	0.44	0.03
	difference	-0.15	0.02	0.16	0.01
Large body	2011-2019	60.31	34.46	23.92	8.62
	1991-2000	60.66	34.93	20.83	6.99
	difference	-0.35	-0.48	3.08	1.63
Small body	2011-2019	50.88	24.76	15.91	5.02
	1991-2000	51.79	25.60	13.47	3.77
	difference	-0.91	-0.84	2.45	1.25

Appendix 8: Summary statistics of top-ranked models for overall species richness and 21 bird guilds.

Species group	Term	Estimate	Std. error	Statistic	*p*	Lower CI	Upper CI	VIF
Overall species	Intercept	59.29	0.22	264.86	0.00	58.85	59.73	-
	Terrain ruggedness	1.85	0.23	8.19	0.00	1.41	2.30	1.02
	Proportion grassland	-1.50	0.24	-6.27	0.00	-1.96	-1.03	1.13
	Cumulative DHI	13.61	0.37	37.21	0.00	12.89	14.32	2.67
	Minimum DHI	-10.07	0.35	-28.85	0.00	-10.76	-9.39	2.43
Forest affiliates	Intercept	26.86	0.14	190.78	0.00	26.59	27.14	-
	Elevation	2.28	0.23	9.79	0.00	1.83	2.74	2.75
	Terrain ruggedness	1.58	0.18	8.98	0.00	1.24	1.93	1.56
	Proportion forest	1.36	0.20	6.93	0.00	0.98	1.75	1.96
	Proportion grassland	-1.49	0.15	-9.92	0.00	-1.78	-1.19	1.14
	Cumulative DHI	13.40	0.35	38.29	0.00	12.71	14.09	6.18
	Minimum DHI	-7.22	0.23	-30.85	0.00	-7.68	-6.76	2.77
Grass affiliates	Intercept	3.08	0.03	105.04	0.00	3.02	3.14	-
	Terrain ruggedness	-0.40	0.03	-12.45	0.00	-0.46	-0.33	1.18
	Proportion forest	-0.25	0.04	-6.49	0.00	-0.33	-0.17	1.73
	Proportion grassland	0.41	0.03	13.15	0.00	0.35	0.47	1.14
	Cumulative DHI	-0.96	0.04	-23.76	0.00	-1.04	-0.88	1.91
	Variation DHI	0.32	0.03	9.60	0.00	0.25	0.38	1.29
Shrub affiliates	Intercept	10.50	0.06	165.69	0.00	10.37	10.62	-
	Elevation	-0.50	0.10	-4.88	0.00	-0.70	-0.30	2.62
	Terrain ruggedness	0.28	0.08	3.49	0.00	0.12	0.43	1.55
	Proportion grassland	-0.54	0.07	-7.25	0.00	-0.69	-0.39	1.38
	Proportion shrubland	0.75	0.09	8.06	0.00	0.57	0.94	2.18
	Cumulative DHI	-1.23	0.16	-7.64	0.00	-1.54	-0.91	6.45
	Minimum DHI	-0.72	0.18	-4.11	0.00	-1.06	-0.38	7.65
	Variation DHI	-1.96	0.13	-15.17	0.00	-2.21	-1.71	4.16
Forest specialists	Intercept	13.04	0.10	136.94	0.00	12.86	13.23	-
	Elevation	1.83	0.16	11.58	0.00	1.52	2.14	2.75
	Terrain ruggedness	1.14	0.12	9.58	0.00	0.91	1.37	1.56

	Proportion forest	2.36	0.13	17.71	0.00	2.10	2.62	1.96
	Proportion grassland	-0.83	0.10	-8.18	0.00	-1.03	-0.63	1.14
	Cumulative DHI	8.03	0.24	33.91	0.00	7.56	8.49	6.18
	Minimum DHI	-4.85	0.16	-30.64	0.00	-5.16	-4.54	2.77
Grass specialists	Intercept	2.48	0.03	94.63	0.00	2.43	2.53	-
	Terrain ruggedness	-0.31	0.03	-10.77	0.00	-0.37	-0.25	1.21
	Proportion forest	-0.40	0.03	-11.64	0.00	-0.47	-0.33	1.74
	Proportion grassland	0.33	0.03	10.61	0.00	0.27	0.39	1.37
	Proportion shrubland	-0.21	0.04	-5.38	0.00	-0.28	-0.13	2.13
	Cumulative DHI	-0.41	0.05	-8.43	0.00	-0.51	-0.32	3.52
	Variation DHI	0.64	0.03	18.68	0.00	0.58	0.71	1.73
Shrub specialists	Intercept	2.22	0.03	63.91	0.00	2.15	2.29	-
	Elevation	-0.22	0.06	-3.87	0.00	-0.33	-0.11	2.74
	Terrain ruggedness	0.40	0.04	9.31	0.00	0.32	0.49	1.57
	Proportion forest	0.18	0.05	3.83	0.00	0.09	0.27	1.86
	Proportion grassland	-0.29	0.04	-7.02	0.00	-0.37	-0.21	1.38
	Proportion shrubland	0.68	0.05	13.23	0.00	0.58	0.78	2.18
	Cumulative DHI	-1.95	0.08	-25.53	0.00	-2.10	-1.80	4.84
	Variation DHI	-1.44	0.05	-31.45	0.00	-1.53	-1.35	1.73
Residents	Intercept	12.18	0.07	185.92	0.00	12.05	12.31	-
	Elevation	-0.75	0.11	-6.93	0.00	-0.96	-0.54	2.71
	Terrain ruggedness	0.94	0.08	11.46	0.00	0.78	1.10	1.57
	Proportion forest	-0.73	0.09	-8.20	0.00	-0.91	-0.56	1.85
	Proportion shrubland	0.20	0.09	2.33	0.02	0.03	0.38	1.79
	Cumulative DHI	0.94	0.14	6.93	0.00	0.68	1.21	4.31
	Variation DHI	-1.20	0.08	-14.57	0.00	-1.36	-1.04	1.59
Long-distance migrants	Intercept	26.08	0.13	205.56	0.00	25.83	26.33	-
	Terrain ruggedness	0.77	0.13	6.00	0.00	0.52	1.02	1.02
	Proportion grassland	-0.61	0.14	-4.51	0.00	-0.87	-0.34	1.13
	Cumulative DHI	9.37	0.21	45.20	0.00	8.96	9.77	2.67
	Minimum DHI	-6.56	0.20	-33.13	0.00	-6.95	-6.17	2.43
Short-distance migrants	Intercept	21.03	0.08	275.42	0.00	20.88	21.18	-
	Elevation	1.27	0.10	12.74	0.00	1.07	1.46	1.69

	Proportion grassland	-0.31	0.08	-3.82	0.00	-0.47	-0.15	1.13
	Cumulative DHI	4.65	0.16	29.16	0.00	4.34	4.97	4.37
	Minimum DHI	-3.98	0.21	-19.05	0.00	-4.39	-3.57	7.47
	Variation DHI	1.14	0.15	7.73	0.00	0.85	1.43	3.71
Ground Nesters	Intercept	21.12	0.09	223.32	0.00	20.94	21.31	-
	Proportion shrubland	0.66	0.12	5.58	0.00	0.43	0.90	1.59
	Cumulative DHI	4.08	0.18	22.61	0.00	3.72	4.43	3.63
	Minimum DHI	-3.49	0.16	-22.28	0.00	-3.80	-3.18	2.74
Mid-story/ Canopy nesters	Intercept	34.62	0.14	244.59	0.00	34.34	34.90	-
	Elevation	0.71	0.22	3.17	0.00	0.27	1.15	2.51
	Terrain ruggedness	1.56	0.17	8.92	0.00	1.22	1.90	1.53
	Proportion grassland	-1.26	0.15	-8.35	0.00	-1.55	-0.96	1.13
	Cumulative DHI	10.99	0.29	38.35	0.00	10.43	11.56	4.10
	Minimum DHI	-7.37	0.22	-33.27	0.00	-7.81	-6.94	2.45
Threatened	Intercept	2.86	0.03	113.97	0.00	2.81	2.91	-
	Elevation	-0.14	0.04	-3.26	0.00	-0.22	-0.05	2.74
	Terrain ruggedness	-0.38	0.03	-12.04	0.00	-0.44	-0.32	1.56
	Proportion forest	-0.20	0.04	-5.59	0.00	-0.27	-0.13	1.95
	Cumulative DHI	0.42	0.06	6.75	0.00	0.30	0.54	6.02
	Minimum DHI	0.32	0.04	7.82	0.00	0.24	0.41	2.74
Decreasing	Intercept	22.01	0.09	239.65	0.00	21.83	22.19	-
	Elevation	-1.16	0.15	-7.89	0.00	-1.44	-0.87	2.55
	Terrain ruggedness	-0.34	0.11	-3.01	0.00	-0.57	-0.12	1.55
	Cumulative DHI	2.69	0.21	12.91	0.00	2.28	3.09	5.13
	Minimum DHI	-3.13	0.25	-12.33	0.00	-3.63	-2.63	7.63
	Variation DHI	1.00	0.18	5.63	0.00	0.65	1.35	3.76
Stable increasing	Intercept	37.28	0.16	237.32	0.00	36.97	37.59	-
	Elevation	1.08	0.25	4.29	0.00	0.58	1.57	2.55
	Terrain ruggedness	2.23	0.20	11.41	0.00	1.85	2.61	1.55
	Proportion grassland	-1.76	0.17	-10.53	0.00	-2.09	-1.43	1.14
	Cumulative DHI	10.75	0.36	29.70	0.00	10.04	11.46	5.31
	Minimum DHI	-6.93	0.43	-15.97	0.00	-7.79	-6.08	7.64
	Variation DHI	-1.04	0.30	-3.41	0.00	-1.64	-0.44	3.77
Small range	Intercept	4.90	0.09	56.87	0.00	4.73	5.07	-
	Terrain ruggedness	1.87	0.09	21.03	0.00	1.69	2.04	1.06
	Proportion grassland	-0.37	0.10	-3.62	0.00	-0.56	-0.17	1.37

	Proportion shrubland	0.51	0.13	4.06	0.00	0.26	0.76	2.12
	Cumulative DHI	-2.99	0.20	-15.27	0.00	-3.37	-2.60	5.15
	Minimum DHI	1.26	0.24	5.34	0.00	0.80	1.72	7.48
	Variation DHI	-2.01	0.17	-11.61	0.00	-2.35	-1.67	4.04
Large range	Intercept	54.39	0.21	259.00	0.00	53.98	54.80	-
	Proportion grassland	-0.96	0.22	-4.29	0.00	-1.40	-0.52	1.13
	Cumulative DHI	17.03	0.39	43.43	1.63	16.26	17.80	3.49
	Minimum DHI	-11.39	0.57	-19.91	0.00	-12.52	-10.27	7.42
	Variation DHI	2.19	0.40	5.42	0.00	1.40	2.98	3.69
Insectivores	Intercept	32.05	0.14	222.42	0.00	31.77	32.34	-
	Terrain ruggedness	1.22	0.16	7.77	0.00	0.91	1.53	1.18
	Proportion forest	1.01	0.19	5.26	0.00	0.64	1.39	1.79
	Proportion grassland	-1.17	0.15	-7.61	0.00	-1.47	-0.87	1.14
	Cumulative DHI	10.04	0.31	32.44	0.00	9.43	10.64	4.61
	Minimum DHI	-7.04	0.40	-17.58	0.00	-7.83	-6.26	7.72
	Variation DHI	-0.92	0.28	-3.31	0.00	-1.46	-0.37	3.70
Granivores	Intercept	11.62	0.05	221.25	0.00	11.52	11.73	-
	Elevation	-0.44	0.09	-5.08	0.00	-0.61	-0.27	2.76
	Terrain ruggedness	0.33	0.07	5.07	0.00	0.20	0.46	1.58
	Proportion forest	-0.81	0.07	-11.04	0.00	-0.96	-0.67	1.96
	Proportion shrubland	-0.48	0.07	-7.06	0.00	-0.61	-0.35	1.67
	Cumulative DHI	0.91	0.14	6.42	0.00	0.63	1.19	7.35
	Minimum DHI	-1.01	0.09	-10.79	0.00	-1.19	-0.82	3.16
Frugivores	Intercept	1.29	0.01	90.18	0.00	1.26	1.31	-
	Elevation	-0.17	0.02	-7.36	0.00	-0.21	-0.12	2.55
	Terrain ruggedness	0.32	0.02	18.20	0.00	0.29	0.36	1.55
	Proportion grassland	-0.15	0.02	-9.82	0.00	-0.18	-0.12	1.14
	Cumulative DHI	0.38	0.03	11.61	0.00	0.32	0.45	5.31
	Minimum DHI	-0.54	0.04	-13.78	0.00	-0.62	-0.47	7.64
	Variation DHI	-0.17	0.03	-6.31	0.00	-0.23	-0.12	3.77
Large body	Intercept	34.46	0.12	292.44	0.00	34.23	34.69	-
	Proportion forest	-1.83	0.15	-12.37	0.00	-2.12	-1.54	1.58
	Proportion grassland	-0.58	0.14	-4.22	0.00	-0.84	-0.31	1.34
	Proportion shrubland	-0.65	0.16	-3.99	0.00	-0.97	-0.33	1.91
	Cumulative DHI	5.02	0.29	17.11	0.00	4.44	5.59	6.19
	Minimum DHI	-3.33	0.21	-15.54	0.00	-3.76	-2.91	3.32
Small body	Intercept	24.76	0.13	192.39	0.00	24.51	25.02	-
	Terrain ruggedness	2.18	0.14	15.58	0.00	1.91	2.45	1.18

Proportion forest	1.41	0.17	8.22	0.00	1.08	1.75	1.79
Proportion grassland	-1.14	0.14	-8.32	0.00	-1.41	-0.87	1.14
Cumulative DHI	8.20	0.25	33.03	0.00	7.71	8.68	3.72
Minimum DHI	-6.54	0.21	-31.01	0.00	-6.95	-6.12	2.68

Chapter 3: Explaining bird abundance with the Dynamic Habitat Indices across the Western United States

Abstract

Biodiversity is declining and for effective management it is crucial to understand the underlying mechanisms influencing spatial patterns of species abundance over broad scales. The Dynamic Habitat Indices (DHIs) are three measures of vegetation productivity – cumulative, minimum, and variation DHI – that provide information about habitat quality and foraging conditions. Our goal was to test the usefulness of the DHIs to predict bird abundance. We analyzed point count data obtained from the Integrated Monitoring in Bird Conservation Regions (IMBCR) Program for twenty bird species across the Western United States. To estimate detection-corrected avian abundance, we used hierarchical distance-sampling models with the three DHIs as abundance covariates, and primary habitat, start time, and year as detection covariates. The DHIs were calculated from the Normalized Difference Vegetation Index (NDVI), based on 30-m Landsat data from 2011-2020. We predicted that higher cumulative DHI and minimum DHI and lower variation DHI would be associated with higher abundances, and we tested the More Individuals Hypothesis (MIH), postulates that areas with greater food resources support higher total numbers of individuals in a community. We also assessed whether different components of the DHIs are associated with different migratory habits of birds. We found that the DHIs were significant for predicting abundance of 17 of the 20 species tested, however higher bird abundance of only 5 species associated with higher productivity. Among the three DHIs, minimum DHI and variation DHI were more often included in top-ranked bird abundance models. We observed stronger relationships between the DHIs and abundance of rare species than common species. Residents and long-distance migrants showed stronger associations with minimum DHI and variation DHI, while short distance migrants showed

stronger relationships with cumulative DHI. Our results highlight the usefulness of the Landsat DHIs for modeling avian abundance at broad scales, especially for rare bird species, and that the DHIs can be used to inform conservation planning.

Introduction

According to the North American Bird Conservation Initiative (NABCI), 37% of all birds in North America are at risk of extinction, with many species in coastal, grassland, and arid habitats declining steeply (NABCI 2016, Rosenberg et al. 2019). With limited resources, conservationists want to maximize conservation return (Wilson et al. 2011), and consequently often focus on identifying and protecting areas with higher biodiversity. To do so, there are different biodiversity indices focusing on species richness, or the functional diversity of species in given area. However, none of these metrics provide information about how many individuals of a given species live in an area. Monitoring abundance highlights when a species starts to decline, which may trigger changes in the abundance of other species (Rosenberg et al. 2019). Moreover, there are many uncertainties about species responses to climate change (Langham et al. 2015). Thus, it is also important to monitor species abundances.

Obtaining accurate estimates of abundance data is difficult and time consuming (Buckland et al. 2008, Callaghan et al. 2021), especially in remote and hard-to-reach areas. Moreover, abundance can fluctuate from year to year because there many factors influence species abundance, including weather, low primary productivity, predation, disturbance (fire, wind fall, clear cuts, etc.), competition, and disease (Currie et al. 1993). Even if it is possible to obtain all these data for one species or over a small spatial extent, it is infeasible to obtain it for all species or across large extents. Another approach is to assess the underlying mechanisms influencing spatial patterns of species abundance over broad scales. Remote sensing provides a

great opportunity for monitoring species abundance because it provides information about environmental characteristics of habitat, and captures dynamic changes on the ground. Moreover, data are collected systematically and provide wall-to-wall global coverage (Nagendra 2013).

We explore the effectiveness of the Dynamic Habitat Indices (DHIs) derived from remotely sensed vegetation indices to explain bird abundance patterns. Birds can easily move over long distances to find suitable habitat. Hence, declines in bird abundance in some areas are not always driven by mortality, but can also be caused by outmigration (Pavlacky et al. 2017). The DHIs integrate three measures of vegetation productivity that provide information about habitat and forage conditions (Coops et al. 2008). Birds are a good taxon for understanding the utility of the DHIs because they exhibit a wide range of behaviors and strategies to find food and suitable habitat. The More Individuals Hypothesis (MIH) postulates that areas with greater food resources support higher total numbers of individuals in a community (Srivastava and Lawton 1998, Storch et al. 2018). While the MIH was developed to explain spatial patterns of species richness, it can be applied to explain patterns of species abundance as well. The underlying mechanism of MIH is closely connected to extinction rates, with the assumption that the number of species increases with the number of individuals, whereas low population sizes have a higher probability of extinction and cannot support high species richness (Srivastava and Lawton 1998, Storch et al. 2018).

The mechanism of the MIH reflects abundance-dependent extinction rates. However the relationship between species richness, abundance and available energy might be different for common versus rare species (Storch et al. 2018). Because an increase of available energy should decrease extinction risk, especially in rare species due to low number of individuals, rare species should show stronger species-energy relationships (Evans et al. 2005, 2006). In this regard the

DHIs are very promising for testing the MIH for individual species, because these indices provide information about available energy over the entire year (cumulative DHI) and during winter months (minimum DHI), and show the stability of available energy in the system (variation DHI) through photosynthetic activity (Connell and Orias 1964, Wright 1983, Hurlbert and Haskell 2003, Radeloff et al. 2019).

The three different measures of available energy may help explain the abundance of different bird species. For example, resident birds stay close to their breeding areas all year round, but one limiting factor for this guild is available food resources during winter. Therefore, resident birds may have a stronger response to minimum vegetation productivity. Conversely, long-distance migrants travel great distances to take advantages of seasonal abundance of insect food, so for this guild seasonal variation in productivity may be more important. Prior studies show the effectiveness of the DHIs for explaining the abundance of mammals (Michaud et al. 2014, Razenkova et al. 2020, 2023), but not for the abundance of birds nor different bird guilds.

Our primary goal was to evaluate the utility of the DHIs to explain bird abundance across the Western United States (U.S.). Specifically, we examined the following questions:

- Does bird abundance vary between productive and less productive areas as the MIH predicts?
- Is available energy more relevant for rare species than for common bird species?
- Does abundance of resident birds have a stronger relationship with higher minimum productivity during winter?

- Does abundance of long-distance migrants have a stronger relationship with cumulative productivity or seasonal variation in productivity?

We expected to find support for the MIH and to see higher numbers of individuals in more productive areas. Common species would show strong relationships with the DHIs. We expected to find that residents have a stronger relationship with minimum DHI, while long-distance migrants have a stronger response to variation DHI. Whereas Evans et al. (2005) assumed a stronger species-energy relationship in rare birds, we expected to find weak or no relationship between the DHIs and abundance for rare species, because vegetation productivity is not the limiting factor for these species.

Methods

Study Area

Our study area encompassed 8 of the 67 North American Bird Conservation Regions (BCRs), including: Great Basin (BCR 9), Northern Rockies (BCR 10), Prairie Potholes (BCR 11), Southern Rockies/Colorado Plateau (BCR 16), Badlands And Prairies (BCR 17), Shortgrass Prairie (BCR 18), Central Mixed Grass Prairie (BCR 19), and Sierra Madre Occidental (BCR 34; Figure **10**). We excluded BCR 15 and 33, because we had less than 100 detection points for our species in those regions (see bird data preprocessing).

The Dynamic Habitat Indices

We used the Dynamic Habitat Indices (DHIs) calculated from the Normalized Difference Vegetation Index (NDVI) based on 30-m Landsat data from 2011-2020 (Razenkova et al. n.d.). The DHIs are three measure of vegetation productivity: overall productivity (cumulative DHI), minimum productivity (minimum DHI), and seasonal variation in vegetation productivity

(variation DHI). To calculate NDVI, we used bands 4 and 5 based on Landsat 8. We removed clouds, cloud shadows, and water bodies (Hansen et al. 2013). Pixels with snow and ice we replaced by zero. We extracted median NDVI values for each month from a time series of 2011-2020. In total, we had twelve NDVI values that represent a phenology curve. For some areas, we had pixels with fewer NDVI values, and for these areas, we applied linear interpolation to fill up to four months of missing data. In total, we interpolated 6.8% of missing data for conterminous U.S. From the resulting monthly NDVI composites we calculated the DHIs as follows: 1) cumulative DHI is the sum of monthly NDVI composites; 2) minimum DHI is the lowest value among monthly NDVI composites; and 3) variation DHI is the coefficient of variation of monthly NDVI composites (for additional details about the calculation of DHIs see (Razenkova et al. n.d., Hobi et al. 2017, Radeloff et al. 2019). The DHIs data are available at https://silvis.forest.wisc.edu/data/dhis/.

Bird data

We obtained data from the Integrated Monitoring in Bird Conservation Regions (IMBCR) Program (Pavlacky et al. 2017). The main advantages of IMBCR data are that they are collected using a rigorous sampling design that allows to monitor bird abundance at broad scales. Data are publicly available for the Western US since 2005. The IMBCR design defines sampling units as 1-km² cells, each containing 16 evenly-spaced sample points, 250 m apart (Figure 1) (Woiderski et al. 2018). Trained field observers conducted six-minute point counts during which they recorded all non-independent detections of birds, and provided a variety of data for estimating incomplete detection. We analyzed data collected from 2010 to 2020 to match our remotely sensed data. We selected twenty bird species with different migration strategies and IUCN statuses for which a sufficient number of observations were available (Table 9, Table **10**).

Prior to any analyses, we cleaned the data by removing observations that did not meet the following criteria: the observer had conducted at least 100 surveys, the data had a valid survey start time, the habitat type was specified, the survey occurred in June or July. Additionally, we selected only one randomly chosen survey for each location. To avoid double counting the same species at two adjacent locations, we limited our buffer zone to 125 m and truncated any observations beyond this distance. We considered each point count as an independent single survey.

Statistical analysis

To estimate detection-corrected avian abundance, we used hierarchical distance-sampling abundance models (Buckland et al. 2001) implemented in the "unmarked" R package (Royle et al. 2004, Chandler et al. 2011). To model the relationship between detection probability and distance we used a 'half-normal' detection function, which is commonly used for birds that are increasingly hard to detect at greater distances (Buckland et al. 2001, Royle et al. 2004). We considered several possible abundance models for each species, first testing Poisson regression, but switching to negative binomial in the case of overdispersion. To select the appropriate distribution, we fitted a model with only one explanatory variable and checked the goodness-of-fit using parametric bootstrapping, in which 100 simulated data sets generated from our model were refit to the same model and the values of the reference and observed distributions were compared using the Freeman-Tukey fit statistic (Sillett et al. 2012). Model fit is indicated by the observed value not being beyond the 0.05 percentile of the reference distribution (Sillett et al. 2012). We also tested for overdispersion using the Chi-squared statistic (Reidy et al. 2014, Kéry and Royle 2016). After selecting the distribution, we built a null model for each species that did not contain any detection or abundance covariates and calculated the Akaike Information

Criterion (AIC) score for this model. Next, we ran models with one of the three DHIs (cumulative, minimum, or variation DHI) as abundance covariates and did not include any detection covariates. Because the three DHIs are correlated, we did not run any combinations of the DHIs. Instead, in our multivariate models we used one of the components of the DHIs as an abundance covariate and a unique combination of three detection covariates including type of primary habitat, year of the survey, and start time of the survey. In total we ran 25 candidate models for each species (the null model plus three abundance covariates times eight detection covariates). We used the AIC score to identify the top models for which $\Delta AIC < 4$. From the five top models, we selected the most parsimonious model (i.e., the model with the fewest variables) and double-checked goodness-of-fit and overdispersion, again using parametric bootstrapping with 1,000 iterations and the Chi-squared statistic.

Results

Bird species

We analyzed a set of bird species with different IUCN statuses and population trends, migratory strategies, and habitat preferences (Table 9). Most of our species were common species because we requested data for species which had a high number of point count detections and were widely distributed across BCR regions (in order to have a wide range of DHIs values). A few species had least concern statuses with increasing population trends based on IUCN, including American Crow, Black-capped Chickadee, Gray Vireo, and House Wren (Table 9). However, there were also a few species that are rare based on small range for Western US: Baird's Sparrow, Field Sparrow, Gray Vireo, Lark Bunting, Northern Bobwhite, Pinyon Jay, and Virginia Warbler. The IUCN trends for these species are decreasing except for Baird's Sparrow and Gray Vireo. Even though Baird's Sparrow has a least concern status and stable trend based

on IUCN, we considered this species to be rare, because of the small range in general, the dependence on grasslands and their migration to the Neotropics. Both grassland obligates and Neotropical migrant bird species are experiencing declines (Knopf 1994, Thompson et al. 1999, Carter et al. 2000, Rosenberg et al. 2019). Similarly, Gray Vireo has a least concern status and an increasing population trend, but this species has a restricted range and is a Neotropical migrant (Schlossberg 2006, Hargrove and Unitt 2017). We had the highest number of detections for Brewer's Sparrow (37,305 detections) and Chipping Sparrow (26,884) and the lowest number for Loggerhead Shrike (509), Gray Vireo (645), and Bullock's Oriole (983) (Table 2).

Avian abundance

We found that for all species except American Crow our top models (selected by ΔAIC <4 than other candidate models) included the DHIs rather than a null model (Appendix 9). If multiple models were within 4 AIC of the top, we selected the most parsimonious model (Appendix 9, Table **11**, Appendix 10, Appendix 11). The top model and the most parsimonious model were the same for most species except Black-headed Grosbeak, Gray Vireo, Virginia's Warbler, and Yellow Warbler. Even if the most parsimonious model provided the lowest AIC score, there were cases where the null model and the most parsimonious model had similar performance. For example, Black-billed Magpie, Bullock's Oriole, Gray Vireo, Loggerhead Shrike, Northern Bobwhite, and Pinyon Jay all had null models ranking within 5 AIC of the top model (Table **11**). We observed that the negative binomial distribution fit better than Poisson regression for most of our models and resulted in lower AIC scores (Table **10**). Among detection covariates, primary habitat appeared in the most models (eight), followed by survey year (seven), and finally survey time (two). None of the three detection covariates ever appeared in a top model simultaneously. For the most parsimonious model for each species, we checked goodness-

of-fit and overdispersion, using parametric bootstrapping with 1,000 iterations and the Chi-squared statistic (Appendix 12).

Rare versus common species

For rare species we found the DHIs were significantly important ($p < 0.01$) for all except Northern Bobwhite ($p = 0.06$) (Table **11**). The most parsimonious top models included detection covariates only for Baird's Sparrow (year) and Field Sparrow (year and time). Minimum DHI was selected more often than other components of the DHIs and appeared in four of seven models. The relationship between minimum DHI and bird abundance varied from positive for Lark Bunting and Pinyon Jay to negative for Field Sparrow and Gray Vireo. Variation DHI appeared in two models for rare species with strong negative influence on Northern Bobwhite abundance and weak positive effect on Virginia's Warbler abundance. Cumulative DHI had strong negative effect on Baird's Sparrow abundance. Overall, we found that all three DHIs had a strong influence on bird abundance of rare species (except Virginia's Warbler) and that minimum DHI had the strongest effect for rare species (Figure **11**). Predicted abundance was low for rare species, except Virginia's Warbler (Figure 12).

We found that common species were also strongly related to the DHIs, except for American Crow ($p = 0.42$), Bullock's Oriole ($p = 0.15$). However, among the top-selected models of some species there was a switch from one component of the DHIs to another. For example, the top-ranked model for Yellow Warbler included cumulative DHI the second top model included variation DHI (Appendix 9). Similarly, we found that competitive models used different components of the DHIs for Chipping Sparrow, Loggerhead Shrike, and Yellow Warbler; four species that live in open woodland. Based on the most parsimonious models we found that variation DHI was selected more often than the other components of the DHIs and

appeared in six out of 13 models for common species. Variation DHI had a strong positive effect on Grasshopper Sparrow and Black-capped Chickadee and a strong negative influence on House Wren (Figure **11**). Minimum DHI had negative influence on Black-billed Magpie, Common Nighthawk, and Chipping Sparrow, and a weak positive effect on Black-headed Grosbeak. Cumulative DHI had a strong positive effect on Loggerhead Shrike, a weak positive influence on Northern Flicker, and a negative influence on Bullock's Oriole. Predicted abundance was high for Brewer's Sparrow, Chipping Sparrow, Grasshopper Sparrow, and House Wren (Figure 12).

Primary habitat was a detection covariate in the top models of only common species, and some of the habitats were significant detection covariates ($p < 0.05$) (Appendix 10, Appendix 11). For two common species, Chipping Sparrow and Northern Flicker, none of the primary habitats were significant. The primary habitat type varied in importance by bird species (habitat descriptions can be found in Appendix 11).

Productive versus less productive areas

We hypothesized that sites with higher vegetation productivity, characterized by higher values for cumulative and minimum DHI and lower values for variation DHI, would have higher bird abundances. By comparing the sign of estimates of our models for each component of the DHIs for each species, we found that the relationship between vegetation productivity and bird abundance varied substantially (Appendix 13). As expected, we found higher bird abundance associated with higher productivity for Black-headed Grosbeak, House Wren, Lark Bunting, Loggerhead Shrike, and Pinyon Jay. However, abundances of Baird's Sparrow, Chipping Sparrow, Field Sparrow, Virginia's Warbler were associated with lower productivity (i.e., negative relationship with cumulative DHI and minimum DHI and positive with variation DHI). The remaining eleven bird species had divergent patterns. For example, American Crow, Black-

billed Magpie, and Bullock's Oriole had a negative relationship with all three DHIs. The most common relationship between the DHIs and bird abundance was a positive relationship with cumulative DHI and variation DHI, and a negative relationship with minimum DHI. For example, Black-capped Chickadee, Brewer's Sparrow, Common Nighthawk, Grasshopper Sparrow, Gray Vireo, Northern Flicker, and Yellow Warbler followed this pattern. Northern Bobwhite had a unique relationship with the DHIs, showing a negative relationship with cumulative and variation DHI and positive with minimum DHI.

The DHIs for residents and migrant bird species

The relationships of the DHIs with bird abundance of residents and migrant bird species was highly dependent on the bird species. Overall, we found that minimum DHI and variation DHI were the strongest predictors for resident species. The directionality of the relationship between minimum DHI and resident woodland species varied in that there was a positive relationship for Pinyon Jay, but a negative relationship for Black-billed Magpie. Similarly, resident forest species such as Black-capped Chickadee had a positive relationship with variation DHI, while resident grassland species such as Northern Bobwhite had a negative relationship with variation DHI. For long distance migrants, we observed strong associations with variation DHI (5 species) and minimum DHI (5 species), but not for cumulative DHI (only 2 species). In contrast, short distance migrants showed stronger associations with cumulative DHI (2 species), and in lesser degree with minimum DHI (1 species) and variation DHI (1 species).

Discussion

Our main goal was to test the Dynamic Habitat Indices derived from 30-m Landsat data from 2011-2020 as predictors of bird abundance, using a diverse set of 20 species across the Western U.S. as focal species. We found that the DHIs were important predictors in modeling

detection-corrected avian abundance for all species, with the exception of American Crow, Bullock's Oriole, and Northern Bobwhite. Models with DHIs as abundance covariates provided lower AIC scores than null models that did not contain any abundance or detection covariates. Our results demonstrate the usefulness of medium-resolution DHIs for capturing important habitat characteristics for individual bird species. This work expands on prior studies that show the effectiveness of remote sensing data for mapping suitable habitat (Hunt et al. 2022), for explaining species richness (Hurlbert and Haskell 2003, Skidmore et al. 2003, Coops et al. 2009, Hobi et al. 2017, Radeloff et al. 2019), as well as explaining mammal abundance (Michaud et al. 2014, Razenkova et al. 2020, 2023).

We were skeptical about finding stronger relationship with vegetation productivity for rare species because of the limited number of available detections. However, our results show that vegetation productivity has a strong influence on rare species. Even for Northern Bobwhite, we observed a strong negative influence of variation DHI, although this was not significant ($p = 0.06$). For common species, the relationship between bird abundance and vegetation productivity was significant, with the exception of American Crow and Bullock's Oriole. This could indicate that many generalist species are sensitive to environmental patterns, and that future changes to these patterns could result in population declines. The American Crow is a generalist and far-ranging species, thus the DHIs probably do not constrict their ability to find food, nest sites, shelter from predators, or places for roosts during winter. Moreover, this species is well-adapted to human-modified landscapes and can benefit from close proximity to settlements (Shoemaker and Phillips 2011), therefore other factors could play a larger role than the DHIs in shaping distributions of American Crow. Bullock's Orioles are also a widespread and common species in the Western U.S. As a Neotropical migrant this species is facing many conservation threats,

including habitat loss, but at least Bullock's Oriole can minimize negative effects from nest parasitism by recognizing and destroying parasitic eggs (Peer and Sealy 2004).

We observed that relationships between the three components of the DHIs and bird abundance varied among species, indicating complex responses likely driven by habitat selection. For example, we found that five species increased in abundance at sites with higher vegetation productivity, while in contrast, four species were less abundant at productive sites. Responses to the DHIs could also be driven by migration strategy. For example, the majority of species that showed the most common relationship to the DHIs (i.e., a positive relationship with cumulative DHI and variation DHI, and a negative relationship with minimum DHI) were Neotropical migrants. The two exceptions in this group were Northern Flicker (short-distance migrant) and Black-capped Chickadee (permanent resident). Both of these species are cavity nesters and so this specific habitat requirement may force them to select habitat with high overall productivity and high seasonality, which could result in higher tree mortality and thus cavity availability. In general, we speculate that the three components of the DHIs are capturing different features or qualities that species respond to differently, depending on their life history and habitat preferences.

Our results show that minimum DHI and variation DHI were the strongest predictors for both resident and Neotropical bird abundance in our study area. Previous work has shown that the richness of the resident bird guild in Thailand is strongly associated with cumulative DHI and minimum DHI, but weakly associated with variation DHI (Suttidate et al. 2019). However, our resident species persist in a temperate zone or mountain areas with strictly defined seasons, which is why variation DHI may be more important in our study area than in the tropics. As we expected, long-distance migrants were associated with highly seasonal habitats, showing that the

life history strategy of these birds allows them to increase reproductive success by taking advantage of habitats that are harsh in the winter but productive in the breeding season (Salewski and Bruderer 2007). On the other hand, short-distance migrants respond more strongly to cumulative DHI than minimum and variation DHI, potentially because they have more flexibility in migration timing and can thus respond to good habitat opportunities.

Caveats and Limitations

There were some limitations of our analysis due to both the remote sensing data and the bird count data. Some uncertainties come from Landsat DHIs, which required interpolating data for some months (6.8 % interpolated data for the conterminous U.S.). Regarding our bird abundance estimates, we chose to include all point count locations with at least one survey rather than restricting to the subset of point locations with multiple surveys. Having multiple observations provides more precise estimates of the bird community, but analyzing only those locations would have spatially limited our study area and hence our assessment of the DHIs. However, to avoid double counting the same individuals at adjacent point count locations, we restricted our analysis to observations within 125-m. Previous work shows significant variation in detection distance among bird species, and by using the buffer zone we may have underestimated actual abundance of some species (Wolf et al. 1995). To minimize bias associated with sampling, we randomly selected the survey year to include for each point count location that had been surveyed in multiple years (Thompson 2002). Because point count data were collected by many individual observers, we were unable to include ‘observer’ as a detection covariate and thus account for observer differences. However, to minimize observer error associated with misidentification of bird species, we excluded observations from less experienced observers (i.e., observers who had conducted less than 100 surveys for this dataset).

Another potential limitation of our study is that point count data were collected during the morning, which may have reduced detections of nocturnal species such as Common Nighthawk. Point count data are also not ideal for flocking and wide-ranging species such as American Crow. However, these two species were frequently detected (>4000 detections) despite these limitations.

Conclusion

In summary, we showed that all three components of the DHIs captured important habitat characteristics for individual bird species and were important in modeling their abundance. Our results highlight the complexity of relationships between the DHIs and bird abundance, which depend on life history and habitat preferences of our modeled species. The DHIs show promise for modeling abundance of rare species as well as common species, which is important because common species can mask the trends of rare species. The Landsat DHIs are freely available at https://silvis.forest.wisc.edu/data/dhis/.

References

Blakesley, J. A., and J. M. Timmer. 2019. Bird Conservancy of the Rockies available support for USFWS wildlife refuges participating in the Integrated Monitoring in Bird Conservation Regions (IMBCR) landbird monitoring program.

Buckland, S. T., D. R. Anderson, K. P. Burnham, J. L. Laake, D. L. Borchers, and L. Thomas. 2001. Introduction to Distance Sampling – Estimating Abundance of Biological Populations. Oxford University Press, Oxford.

Buckland, S. T., S. J. Marsden, and R. E. Green. 2008. Estimating bird abundance: Making methods work. Bird Conservation International 18:S91–S108.

Callaghan, C. T., S. Nakagawa, and W. K. Cornwell. 2021. Global abundance estimates for 9,700 bird species. Proceedings of the National Academy of Sciences of the United States of America 118:1–10.

Carter, M. F., W. C. Hunter, D. N. Pashley, and K. V. Rosenberg. 2000. Conservation Report: Setting Conservation Priorities for Landbirds in the United States: The Partners in Flight Approach. The Auk 117:541–548.

Chandler, R. B., J. A. Royle, and D. I. King. 2011. Inference about density and temporary emigration in unmarked populations. Ecology 92:1429–1435.

Connell, J. H., and E. Orias. 1964. The Ecological Regulation of Species Diversity. The American Naturalist 98:399–414.

Coops, N. C., R. H. Waring, M. A. Wulder, A. M. Pidgeon, and V. C. Radeloff. 2009. Bird diversity: a predictable function of satellite-derived estimates of seasonal variation in canopy light absorbance across the United States. Journal of Biogeography 36:905–918.

Coops, N. C., M. A. Wulder, D. C. Duro, T. Han, and S. Berry. 2008. The development of a Canadian dynamic habitat index using multi-temporal satellite estimates of canopy light absorbance. Ecological Indicators 8:754–766.

Currie, D. J., J. T. Fritz, D. J. Currie, J. T. Fritz, and J. T. Global. 1993. Global Patterns of Animal Abundance and Species Energy Use. Nordic Society Oikos 67:56–68.

Evans, K. L., J. J. D. Greenwood, and K. J. Gaston. 2005. The roles of extinction and colonization in generating species-energy relationships. Journal of Animal Ecology 74:498–507.

Evans, K. L., N. A. James, and K. J. Gaston. 2006. Abundance, species richness and energy availability in the North American avifauna. Global Ecology and Biogeography 15:372–385.

Hansen, M. C., P. V. Potapov, R. Moore, M. Hancher, S. A. Turubanova, A. Tyukavina, D. Thau, S. V. Stehman, S. J. Goetz, T. R. Loveland, A. Kommareddy, A. Egorov, L. Chini, C. O. Justice, and J. R. G. Townshend. 2013. High-Resolution Global Maps of 21st-Century Forest Cover Change. Science 342:850–853.

Hargrove, L., and P. Unitt. 2017. Poor reproductive success of Gray Vireos in a declining California population. Journal of Field Ornithology 88:16–29.

Hobi, M. L., M. Dubinin, C. H. Graham, N. C. Coops, M. K. Clayton, A. M. Pidgeon, and V. C. Radeloff. 2017. A comparison of Dynamic Habitat Indices derived from different MODIS products as predictors of avian species richness. Remote Sensing of Environment 195:142–152.

Hunt, M. L., G. A. Blackburn, G. M. Siriwardena, L. Carrasco, and C. S. Rowland. 2022. Using satellite data to assess spatial drivers of bird diversity. Remote Sensing in Ecology and Conservation:1–17.

Hurlbert, A. H., and J. P. Haskell. 2003. The effect of energy and seasonality on avian species richness and community composition. American Naturalist 161:83–97.

Kéry, M., and J. A. Royle. 2016. Applied hierarchical modeling in ecology: analysis of distribution, abundance and species richness in R and BUGS. Elsevier Inc.

Knopf, F. L. 1994. Assemblages on Altered. Studies in Avian Biology:247–257.

Langham, G. M., J. G. Schuetz, T. Distler, C. U. Soykan, and C. Wilsey. 2015. Conservation status of North American birds in the face of future climate change. PLoS ONE 10:1–16.

Michaud, J. S., N. C. Coops, M. E. Andrew, M. A. Wulder, G. S. Brown, and G. J. M. Rickbeil. 2014. Estimating moose (Alces alces) occurrence and abundance from remotely derived environmental indicators. Remote Sensing of Environment 152:190–201.

NABCI. 2016. North American Bird Conservation Initiative. 2016. The State of North America's Birds 2016. Environment and Climate Change Canada: Ottawa, Ontario.

Pavlacky, D. C., P. M. Lukacs, J. A. Blakesley, R. C. Skorkowsky, D. S. Klute, B. A. Hahn, V. J. Dreitz, T. L. George, and D. J. Hanni. 2017. A statistically rigorous sampling design to integrate avian monitoring and management within Bird Conservation Regions. PLoS ONE 12:1–22.

Peer, B. D., and S. G. Sealy. 2004. Correlates of egg rejection in hosts of the Brown-headed Cowbird. The Condor 106:580–599.

Radeloff, V. C., M. Dubinin, N. C. Coops, A. M. Allen, T. M. Brooks, M. K. Clayton, G. C. Costa, C. H. Graham, D. P. Helmers, A. R. Ives, D. Kolesov, A. M. Pidgeon, G. Rapacciuolo, E. Razenkova, N. Suttidate, B. E. Young, L. Zhu, and M. L. Hobi. 2019. The Dynamic Habitat Indices (DHIs) from MODIS and global biodiversity. Remote Sensing of Environment 222:204–214.

Razenkova, E., M. Dubinin, A. M. Pidgeon, M. L. Hobi, L. Zhu, E. V. Bragina, A. M. Allen, M. K. Clayton, L. M. Baskin, N. C. Coops, and V. C. Radeloff. 2023. Abundance patterns of mammals across Russia explained by remotely sensed vegetation productivity and snow indices. Journal of Biogeography 50:932–946.

Razenkova, E., K. E. Lewińska, H. Yin, L. S. Farwell, A. M. Pidgeon, P. Hostert, N. C. Coops, V. Radeloff, and O. C. (n.d.). Medium-resolution Dynamic Habitat Indices from Landsat satellite imagery. in review.

Razenkova, E., V. C. Radeloff, M. Dubinin, E. V Bragina, M. Allen, M. K. Clayton, A. M. Pidgeon, L. M. Baskin, C. Nicholas, and M. L. Hobi. 2020. Vegetation productivity

summarized by the Dynamic Habitat Indices explains patterns of moose abundance across Russia. Scientific Reports 10:1–12.

Reidy, J. L., F. R. Thompson, and S. W. Kendrick. 2014. Breeding bird response to habitat and landscape factors across a gradient of savanna, woodland, and forest in the Missouri Ozarks. Forest Ecology and Management 313:34–46.

Rosenberg, K. V., A. M. Dokter, P. J. Blancher, J. R. Sauer, A. C. Smith, P. A. Smith, J. C. Stanton, A. Panjabi, L. Helft, M. Parr, and P. P. Marra. 2019. Decline of the North American avifauna. Science 366:120–124.

Royle, J. A., D. K. Dawson, and S. Bates. 2004. Modeling abundance effects in distance sampling. Ecology 85:1591–1597.

Salewski, V., and B. Bruderer. 2007. The evolution of bird migration - A synthesis. Naturwissenschaften 94:268–279.

Schlossberg, S. 2006. Abundance and habitat preferences of Gray Vireos (Vireo vicinior) on the Colorado Plateau. Auk 123:33–44.

Shoemaker, C. M., and R. S. Phillips. 2011. Observation of ground roosting by American Crows. Wilson Journal of Ornithology 123:185–187.

Sillett, T. S., R. B. Chandler, J. A. Royle, M. Kéry, and S. . Morrison. 2012. Hierarchical distance-sampling models to estimate population size and habitat-specific abundance of an island endemic. Ecological Applications 22:1997–2006.

Skidmore, A. K., B. O. Oindo, and M. Y. Said. 2003. Biodiversity Assessment by Remote Sensing. Proceedings of the 30th International symposium on remote sensing of the environment: information for risk management and sustainable development:1–4.

Srivastava, D. S., and J. H. Lawton. 1998. Why more productive sites have more species: An experimental test of theory using tree-hole communities. American Naturalist 152:510–529.

Storch, D., E. Bohdalková, and J. Okie. 2018. The more-individuals hypothesis revisited: the role of community abundance in species richness regulation and the productivity–diversity relationship. Ecology Letters 21:920–937.

Suttidate, N., M. L. Hobi, A. M. Pidgeon, P. D. Round, N. C. Coops, D. P. Helmers, N. S. Keuler, M. Dubinin, B. L. Bateman, and V. C. Radeloff. 2019. Tropical bird species richness is strongly associated with patterns of primary productivity captured by the Dynamic Habitat Indices. Remote Sensing of Environment 232:1–10.

Thompson, F., S. Lewis, J. Green, and D. Ewert. 1999. Status of neotropical migrant landbirds in the Midwest: identifying species of management concern. NCASI Technical Bulletin 2:542.

Thompson, W. L. 2002. Towards Reliable Bird Surveys: Accounting for Individuals Present but not Detected. The Auk 119:18–25.

Wilson, H. B., L. N. Joseph, A. L. Moore, and H. P. Possingham. 2011. When should we save the most endangered species? Ecology Letters 14:886–890.

Woiderski, B. J., N. E. Drilling, J. M. Timmer, M. F. McLaren, C. M. White, N. J. Van Lanen, D. C. P. Jr., and R. A. Sparks. 2018. Integrated Monitoring in Bird Conservation Regions (IMBCR): 2017 Field Season Report. Bird Conservancy of the Rockies. Brighton, Colorado, USA.

Wolf, A. T., R. W.Howe, and G. J.Davis. 1995. Detectability of forest birds from stationary points in northern Wisconsin. U.S. Department of Agriculture, Forest Service General Technical Report PSW-GTR-149.

Wright, D. H. 1983. Species-energy theory: an extension of species–area theory. Oikos 41:496–506.

Table 9: List of the bird species in alphabetical order by common name including abbreviation, scientific name, IUCN status and trend, migration strategy, and preferable habitat. LC –least concern, NT- near threatened, VU-vulnerable.

Common name	Abbreviation	Scientific name	IUCN status	IUCN trend	Migration Form	Habitat
American Crow	AMCR	*Corvus brachyrhynchos*	LC	Increasing	Short Distance Migrant	Open Woodland
Baird's Sparrow	BAIS	*Centronyx bairdii*	LC	Stable	Neotropical Migrant	Grasslands
Black-billed Magpie	BBMA	*Pica hudsonia*	LC	Stable	Permanent Resident	Open Woodland
Black-capped Chickadee	BCCH	*Poecile atricapillus*	LC	Increasing	Permanent Resident	Forest
Black-headed Grosbeak	BHGR	*Pheucticus melanocephalus*	LC	Increasing	Neotropical Migrant	Forest
Brewer's Sparrow	BRSP	*Spizella breweri*	LC	Decreasing	Neotropical Migrant	Schrub
Bullock's Oriole	BUOR	*Icterus bullockii*	LC	Stable	Neotropical Migrant	Open Woodland
Chipping Sparrow	CHSP	*Spizella passerina*	LC	Decreasing	Neotropical Migrant	Open Woodland
Common Nighthawk	CONI	*Chordeiles minor*	LC	Decreasing	Neotropical Migrant	Grasslands
Field Sparrow	FISP	*Spizella pusilla*	LC	Decreasing	Short Distance Migrant	Schrub
Grasshopper Sparrow	GRSP	*Ammodramus savannarum*	LC	Decreasing	Neotropical Migrant	Grasslands
Gray Vireo	GRVI	*Vireo vicinior*	LC	Increasing	Neotropical Migrant	Schrub
House Wren	HOWR	*Troglodytes aedon*	LC	Increasing	Neotropical Migrant	Schrub
Lark Bunting	LARB	*Calamospiza melanocorys*	LC	Decreasing	Neotropical Migrant	Grasslands
Loggerhead Shrike	LOSH	*Lanius ludovicianus*	NT	Decreasing	Short Distance Migrant	Open Woodland
Northern Bobwhite	NOBO	*Colinus virginianus*	NT	Decreasing	Permanent Resident	Grasslands

Northern Flicker	NOFL	*Colaptes auratus*	LC	Decreasing	Short Distance Migrant	Open Woodland
Pinyon Jay	PIJA	*Gymnorhinus cyanocephalus*	VU	Decreasing	Permanent Resident	Open Woodland
Virginia's Warbler	VIWA	*Leiothlypis virginiae*	LC	Decreasing	Neotropical Migrant	Open Woodland
Yellow Warbler	YEWA	*Setophaga petechia*	LC	Decreasing	Neotropical Migrant	Open Woodland

Table 10: List of the bird species in alphabetical order by common name including abbreviation, scientific name, IUCN status and trend, migration strategy, and preferable habitat. LC –least concern, NT- near threatened, VU-vulnerable.

Common name	Abbreviation	Scientific name	IUCN status	IUCN trend	Migration Form	Habitat
American Crow	AMCR	*Corvus brachyrhynchos*	LC	Increasing	Short Distance Migrant	Open Woodland
Baird's Sparrow	BAIS	*Centronyx bairdii*	LC	Stable	Neotropical Migrant	Grasslands
Black-billed Magpie	BBMA	*Pica hudsonia*	LC	Stable	Permanent Resident	Open Woodland
Black-capped Chickadee	BCCH	*Poecile atricapillus*	LC	Increasing	Permanent Resident	Forest
Black-headed Grosbeak	BHGR	*Pheucticus melanocephalus*	LC	Increasing	Neotropical Migrant	Forest
Brewer's Sparrow	BRSP	*Spizella breweri*	LC	Decreasing	Neotropical Migrant	Schrub
Bullock's Oriole	BUOR	*Icterus bullockii*	LC	Stable	Neotropical Migrant	Open Woodland
Chipping Sparrow	CHSP	*Spizella passerina*	LC	Decreasing	Neotropical Migrant	Open Woodland
Common Nighthawk	CONI	*Chordeiles minor*	LC	Decreasing	Neotropical Migrant	Grasslands
Field Sparrow	FISP	*Spizella pusilla*	LC	Decreasing	Short Distance Migrant	Schrub
Grasshopper Sparrow	GRSP	*Ammodramus savannarum*	LC	Decreasing	Neotropical Migrant	Grasslands
Gray Vireo	GRVI	*Vireo vicinior*	LC	Increasing	Neotropical Migrant	Schrub
House Wren	HOWR	*Troglodytes aedon*	LC	Increasing	Neotropical Migrant	Schrub
Lark Bunting	LARB	*Calamospiza melanocorys*	LC	Decreasing	Neotropical Migrant	Grasslands
Loggerhead Shrike	LOSH	*Lanius ludovicianus*	NT	Decreasing	Short Distance Migrant	Open Woodland
Northern Bobwhite	NOBO	*Colinus virginianus*	NT	Decreasing	Permanent Resident	Grasslands

Northern Flicker	NOFL	*Colaptes auratus*	LC	Decreasing	Short Distance Migrant	Open Woodland
Pinyon Jay	PIJA	*Gymnorhinus cyanocephalus*	VU	Decreasing	Permanent Resident	Open Woodland
Virginia's Warbler	VIWA	*Leiothlypis virginiae*	LC	Decreasing	Neotropical Migrant	Open Woodland
Yellow Warbler	YEWA	*Setophaga petechia*	LC	Decreasing	Neotropical Migrant	Open Woodland

Table 11: List of the bird species in alphabetical order by common name, Bird Conservation Regions (BCR) regions included into analysis, number of detection species, and the type of distribution for model.

Common name	BCR	Number of detection	Distribution
American Crow	9, 10, 16, 17, 18, 19	5598	NB
Baird's Sparrow	11, 17	1304	NB
Black-billed Magpie	9, 10, 16, 17, 18	6414	NB
Black-capped Chickadee	9, 10, 16, 17, 18	5001	NB
Black-headed Grosbeak	9, 10, 16, 17, 18, 34	5175	Poisson
Brewer's Sparrow	9, 10, 11, 16, 17, 18	37305	NB
Bullock's Oriole	9, 10, 17, 18, 19	983	Poisson
Chipping Sparrow	9, 10, 16, 17, 18, 34	26884	NB
Common Nighthawk	9, 10, 11, 16, 17, 18, 19	4029	Poisson
Field Sparrow	17, 18, 19	4941	NB
Grasshopper Sparrow	9, 10, 11, 17, 18, 19	19412	NB
Gray Vireo	9, 16	645	NB
House Wren	9, 10, 16, 17, 18, 19, 34	16708	NB
Lark Bunting	10, 11, 17, 18	14695	NB
Loggerhead Shrike	9, 10, 17	509	Poisson
Northern Bobwhite	18, 19	1295	NB
Northern Flicker	9, 10, 16, 17, 18, 34	13487	NB
Pinyon Jay	9, 10, 16, 34	1753	NB
Virginia's Warbler	16, 34	2227	NB
Yellow Warbler	9, 10, 11, 16, 17, 18	6902	NB

Table 12: Results of modeling bird abundance using the Poisson and negative-binomial regression. Results are reported for the null model (without either abundance or detection covariates), and the most parsimonious model (i.e., the model with the fewest variables) based on lowest AIC score for bird species in alphabetical order by common name. Estimates, standard error, p-value, and the AIC score are shown for each model. Lowest AIC score are highlighted in bold. Note: for the models that included primary habitat as detection covariates only the first habitat is listed.

Common name	Model	Variable	Estimate	Standard error	p-value	AIC
American Crow	Null model	(Intercept)	-3.56	0.09	0	**7112**
	Top model	(Intercept)	-3.56	0.09	0	7113
		Variation DHI	-0.04	0.05	0.42	
Baird's Sparrow	Null model	(Intercept)	-1.05	0.08	<0.01	5879
	Top model	(Intercept)	-1.06	0.08	<0.01	
		Cumulative DHI	-0.29	0.08	<0.01	**5855**
	Detection	Year	-0.13	0.03	<0.01	
Black-billed Magpie	Null model	(Intercept)	-2.51	0.06	0	14630
	Top model	(Intercept)	-2.52	0.06	0	**14627**
		Minimum DHI	-0.10	0.04	0.02	
Black-capped Chickadee	Null model	(Intercept)	-0.86	0.03	<0.01	28847
	Top model	(Intercept)	-0.86	0.03	<0.01	
		Variation DHI	0.22	0.03	<0.01	**28729**
	Detection	Habitat AS	0.04	0.08	0.62	
Black-headed Grosbeak	Null model	(Intercept)	-1.22	0.03	0	31438
	Top model	(Intercept)	-1.20	0.03	0	
		Minimum DHI	0.04	0.02	<0.01	**31211**
	Detection	Habitat AS	0.68	0.18	<0.01	
Brewer's Sparrow	Null model	(Intercept)	1.23	0.02	0	74388
	Top model	(Intercept)	1.23	0.02	<0.01	
		Variation DHI	0.08	0.02	<0.01	**74358**
	Detection	Habitat AS	-0.05	0.04	0.26	
		Year	-0.01	0.005	0.03	
Bullock's Oriole	Null model	(Intercept)	-2.72	0.07	0	7680
	Top model	(Intercept)	-2.73	0.07	0	
		Cumulative DHI	-0.06	0.04	0.15	7680
		Year	-0.04	0.02	0.09	
Chipping Sparrow	Null model	(Intercept)	1.29	0.02	0	103164
	Top model	(Intercept)	1.29	0.02	<0.01	**103105**

		Minimum DHI	-0.07	0.01	<0.01	
	Detection	Habitat AS	0.00	0.03	0.94	
		Year	0.01	0.004	<0.01	
Common Nighthawk	Null model	(Intercept)	-2.14	0.04	0	18400
	Top model	(Intercept)	-2.14	0.04	0	
		Minimum DHI	-0.11	0.03	<0.01	**18367**
	Detection	Habitat AS	-0.61	0.23	<0.01	
Field Sparrow	Null model	(Intercept)	-1.21	0.05	<0.01	14142
	Top model	(Intercept)	-1.17	0.05	<0.01	
		Minimum DHI	-0.37	0.04	<0.01	**14064**
	Detection	Year	0.10	0.07	0.17	
		Time	0.13	0.09	0.15	
Grasshopper Sparrow	Null model	(Intercept)	1.34	0.02	0	56920
	Top model	(Intercept)	1.31	0.02	<0.01	
		Variation DHI	0.28	0.02	<0.01	**56744**
	Detection	Year	-0.01	0.004	<0.01	
		Time	0.02	0.004	<0.01	
Gray Vireo	Null model	(Intercept)	-1.78	0.09	<0.01	4751
	Top model	(Intercept)	-1.77	0.09	<0.01	**4746**
		Minimum DHI	-0.17	0.08	0.03	
House Wren	Null model	(Intercept)	0.51	0.02	<0.01	58761
	Top model	(Intercept)	0.50	0.02	<0.01	
		Variation DHI	-0.16	0.02	<0.01	**58678**
	Detection	Habitat AS	-0.04	0.05	0.44	
Lark Bunting	Null model	(Intercept)	-0.15	0.03	<0.01	32833
	Top model	(Intercept)	-0.16	0.03	<0.01	**32773**
		Minimum DHI	0.25	0.03	<0.01	
Loggerhead Shrike	Null model	(Intercept)	-3.1	0.09	<0.01	4473
	Top model	(Intercept)	-3.10	0.09	<0.01	**4472**
		Cumulative DHI	0.09	0.05	0.05	
Northern Bobwhite	Null model	(Intercept)	-2.08	0.07	<0.01	3005
	Top model	(Intercept)	-2.28	0.13	<0.01	**3004**
		Variation DHI	-0.23	0.12	0.06	
Northern Flicker	Null model	(Intercept)	-1.06	0.03	0	44039
	Top model	(Intercept)	-1.06	0.03	0	
		Cumulative DHI	0.04	0.02	0.02	**43974**
	Detection	Habitat AS	-0.27	0.54	0.62	
		Year	0.01	0.02	0.52	
Pinyon Jay	Null model	(Intercept)	-2.99	0.10	<0.01	5045
	Top model	(Intercept)	-2.98	0.10	<0.01	**5041**
		Minimum DHI	0.17	0.07	0.02	
Virginia's Warbler	Null model	(Intercept)	0.33	0.05	<0.01	11382
	Top model	(Intercept)	0.32	0.05	<0.01	**11377**
		Variation DHI	0.08	0.03	0.01	
Yellow Warbler	Null model	(Intercept)	-0.50	0.03	<0.01	29445
	Top model	(Intercept)	-0.49	0.03	<0.01	**29401**

		Variation DHI	0.10	0.03	<0.01	
	Detection	Habitat AS	-0.14	0.08	0.06	

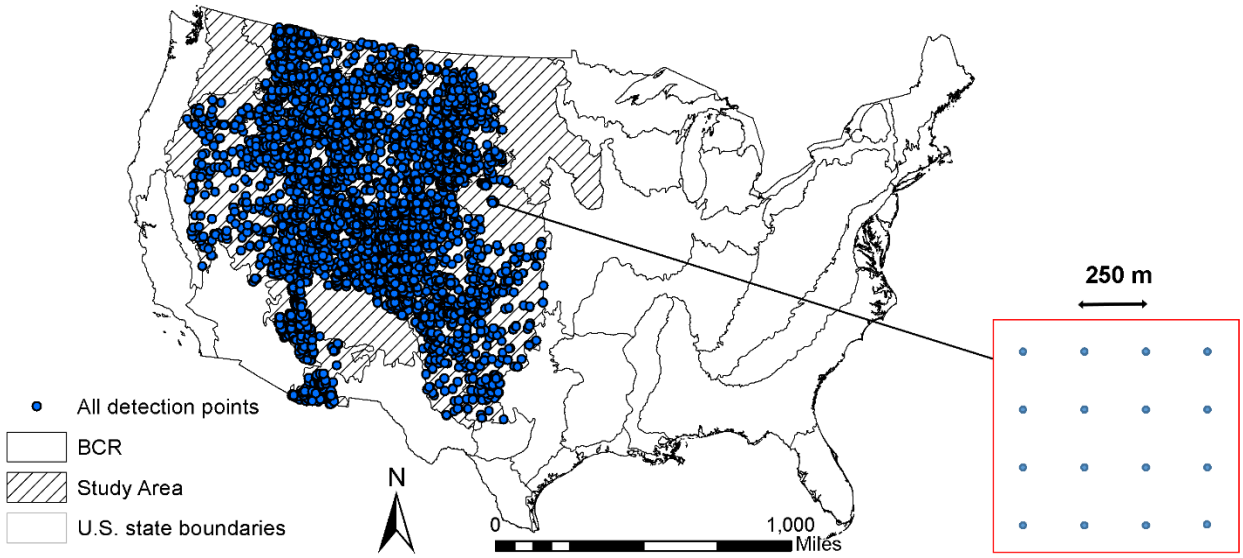

Figure 10: Bird Conservation Regions (BCR) across the conterminous United States. Shaded areas indicate BCRs included in our analysis. All detection points are shown in dark blue, with inset showing a 1-km^2 sampling unit used in the IMBCR design. The projection of the map is Albers Equal Area.

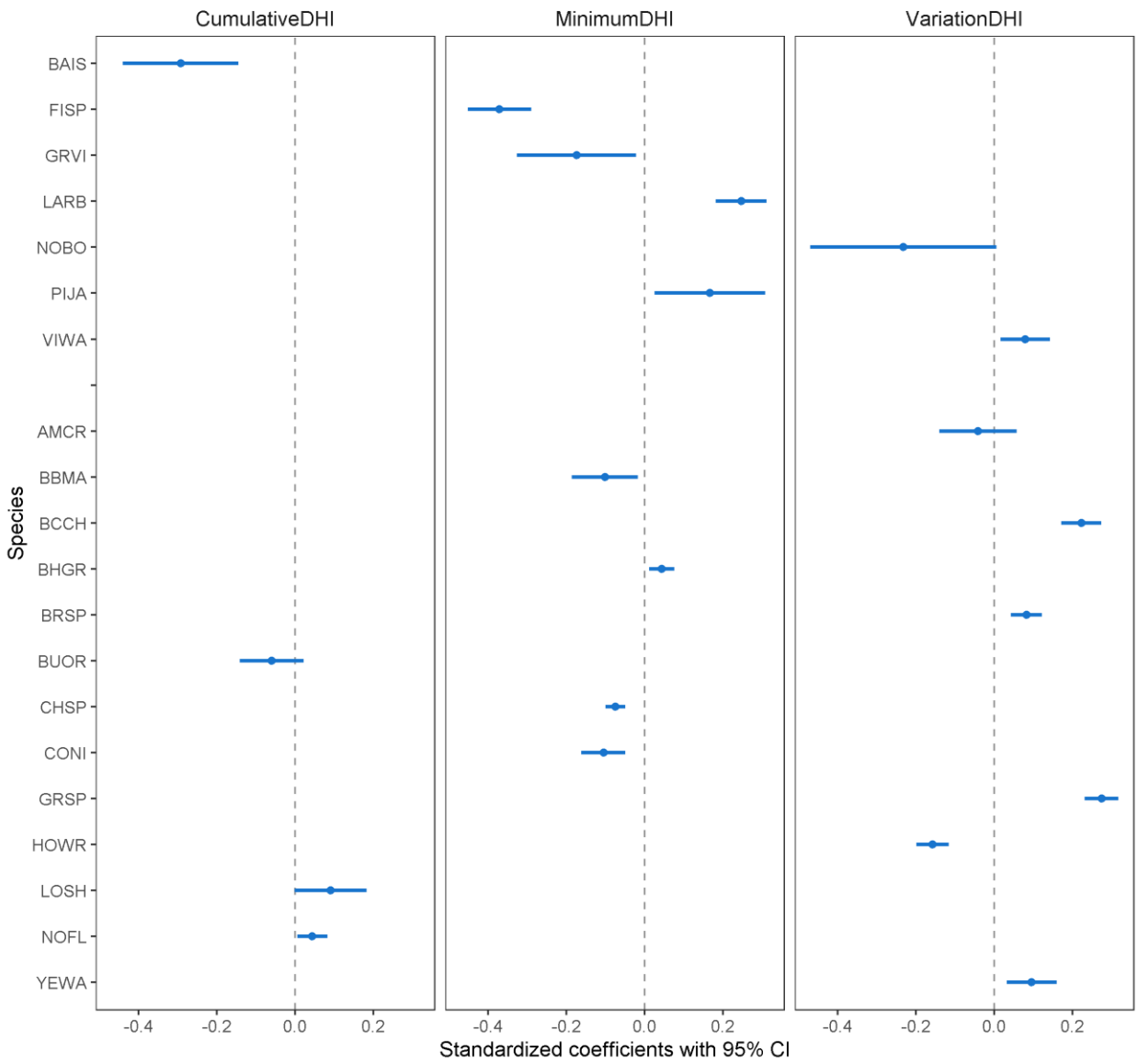

Figure 11: Standardized coefficients with 95% confidence interval for explanatory variables for most parsimonious models for 20 bird species. The species are AMCR - American Crow, BAIS - Baird's Sparrow, BBMA - Black-billed Magpie, BCCH - Black-capped Chickadee, BHGR - Black-headed Grosbeak, BRSP - Brewer's Sparrow, BUOR - Bullock's Oriole, CHSP - Chipping Sparrow, CONI - Common Nighthawk, FISP - Field Sparrow, GRSP - Grasshopper Sparrow, GRVI - Gray Vireo, HOWR - House Wren, LARB - Lark Bunting, LOSH - Loggerhead Shrike,

NOBO - Northern Bobwhite, NOFL - Northern Flicker, PIJA - Pinyon Jay, VIWI - Virginia's Warbler, and YEWA - Yellow Warbler.

Figure 12: Predicted bird abundance for 20 bird species. The species are AMCR - American Crow, BAIS -Baird's Sparrow, BBMA - Black-billed Magpie, BCCH - Black-capped Chickadee, BHGR - Black-headed Grosbeak, BRSP - Brewer's Sparrow, BUOR - Bullock's Oriole, CHSP - Chipping Sparrow, CONI - Common Nighthawk, FISP - Field Sparrow, GRSP - Grasshopper Sparrow, GRVI - Gray Vireo, HOWR - House Wren, LARB - Lark Bunting, LOSH - Loggerhead Shrike, NOBO - Northern Bobwhite, NOFL - Northern Flicker, PIJA - Pinyon Jay, VIWI - Virginia's Warbler, and YEWA - Yellow Warbler.

Predicted abundance
0
2
4
6
8
10
12
14
AMCR
BAIS
BBMA
BCCH
BHGR
BRSP
BUOR
CHSP
CONI
FISP
GRSP
GRVI
HOWR
LARB
LOSH
NOBO
NOFL
PIJA
VIWA
YEWA

Appendix 9: The top five competitive models for which ΔAIC < 4 sorted in order from lowest to highest AIC scores. "+" indicates that this models was selected as the most parsimonious models, "-" indicates that the model was not selected.

Species	Model	Abundance covariates	Detection covariates	AIC	Parsimonious model
American Crow	Model 1	Variation DHI		7113	+
	Model 2	Minimum DHI		7113	-
	Model 3	Cumulative DHI		7114	-
	Model 4	Minimum DHI	Year	7115	-
	Model 5	Variation DHI	Year	7115	-
Baird's Sparrow	Model 1	Cumulative DHI	Year	5855	+
Black-billed Magpie	Model 1	Minimum DHI		14627	+
	Model 2	Minimum DHI	Year	14627	-
	Model 3	Minimum DHI	Habitat	14628	-
	Model 4	Minimum DHI	Time	14629	-
	Model 5	Minimum DHI	Year + Time	14629	-
Black-capped Chickadee	Model 1	Variation DHI	Habitat	28729	+
Black-headed Grosbeak	Model 1	Minimum DHI	Habitat + Time	31211	-
	Model 2	Minimum DHI	Habitat + Time + Year	31213	-
	Model 3	Minimum DHI	Habitat	31213	+
	Model 4	Minimum DHI	Habitat + Year	31214	-
Brewer's Sparrow	Model 1	Variation DHI	Habitat + Year	74358	+
Bullock's Oriole	Model 1	Cum DH	Year	7680	+
Chipping Sparrow	Model 1	Minimum DHI	Habitat + Year	103105	+
	Model 2	Minimum DHI	Habitat + Time + Year	103106	
	Model 3	Cumulative DHI	Habitat + Year	103107	
Common Nighthawk	Model 1	Minimum DHI	Habitat	18367	+
	Model 2	Minimum DHI	Habitat + Time	18369	
	Model 3	Minimum DHI	Habitat + Time + Year	18370	
Field Sparrow	Model 1	Minimum DHI	Year + Time	14064	+
Grasshopper Sparrow	Model 1	Variation DHI	Year + Time	56744	+
Gray Vireo	Model 1	Minimum DHI	Habitat	4746	-
	Model 2	Minimum DHI		4746	+
	Model 3	Minimum DHI	Habitat + Time + Year	4746	-

	Model 4	Minimum DHI	Habitat + Time	4746	-
	Model 5	Variation DHI	Habitat + Year	4748	-
House Wren	Model 1	Variation DHI	Habitat	58678	+
	Model 2	Variation DHI	Habitat + Time	58679	-
	Model 3	Variation DHI	Habitat + Year	58680	-
	Model 4	Variation DHI	Habitat + Time + Year	58681	-
Lark Bunting	Model 1	Minimum DHI		32773	+
	Model 2	Minimum DHI	Year	32775	-
	Model 3	Minimum DHI	Time	32775	-
	Model 4	Minimum DHI	Year + Time	32777	-
Loggerhead Shrike	Model 1	Cumulative DHI		4472	+
	Model 2	Cumulative DHI	Time	4472	-
	Model 3	Cumulative DHI	Year	4474	-
	Model 4	Variation DHI	Time	4474	-
Northern Bobwhite	Model 1	Variation DHI		3004	+
	Model 2	Minimum DHI		3005	-
	Model 3	Variation DHI	Year	3006	-
	Model 4	Variation DHI	Time	3006	-
	Model 5	Cumulative DHI		3006	-
Northern Flicker	Model 1	Cumulative DHI	Habitat + Year	43974	+
Pinyon Jay	Model 1	Minimum DHI		5041	-
	Model 2	Minimum DHI	Time	5043	-
	Model 3	Variation DHI		5044	-
	Model 4	Minimum DHI	Habitat	5045	-
Virginia's Warbler	Model 1	Variation DHI	Time	11377	-
	Model 2	Variation DHI	Year + Time	11378	-
	Model 3	Variation DHI		11378	+
	Model 4	Variation DHI	Year	11379	-
Yellow Warbler	Model 1	Cumulative DHI	Habitat + Time	29401	-
	Model 2	Variation DHI	Habitat + Time + Year	29401	-
	Model 3	Cumulative DHI	Habitat + Time + Year	29402	-
	Model 4	Variation DHI	Habitat	29403	+
	Model 5	Cumulative DHI	Habitat	29403	-

Appendix 10: Results of modeling bird abundance using the Poisson and negative-binomial regression. Results are reported for the parsimonious models that included habitat as detection covariates based on lowest AIC score for bird species in alphabetical order by common name. Estimates, standard error, p-value, and the AIC score are shown for each model. Two-letter code to describe primary habitat at breeding landbird survey point are available below in Table S3.

Common name	Model	Variable	Estimate	Standard error	p-value
Black-capped Chickadee	Top model	(Intercept)	-0.86	0.03	<0.01
		Variation DHI	0.22	0.03	<0.01
	Detection	Habitat AS	0.04	0.08	0.62
		Habitat BU	**0.25**	**0.09**	**0.01**
		Habitat CR	0.12	0.11	0.27
		Habitat DS	0.18	0.13	0.15
		Habitat DW	0.11	0.14	0.43
		Habitat GR	0.10	0.06	0.11
		Habitat II	-0.13	0.11	0.25
		Habitat LP	**0.38**	**0.10**	**<0.01**
		Habitat MC	**0.26**	**0.07**	**<0.01**
		Habitat MM	5.33	NaN	NaN
		Habitat OA	0.00	0.14	1.00
		Habitat PJ	0.03	0.07	0.65
		Habitat PP	**0.20**	**0.07**	**<0.01**
		Habitat RI	**0.22**	**0.08**	**<0.01**
		Habitat SA	**0.23**	**0.06**	**<0.01**
		Habitat SF	**0.15**	**0.08**	**0.05**
		Habitat SH	0.08	0.08	0.27
Black-headed Grosbeak	Top model	(Intercept)	-1.20	0.03	0
		Minimum DHI	0.04	0.02	<0.01
	Detection	**Habitat AS**	**0.68**	**0.18**	**<0.01**
		Habitat BU	0.09	0.11	0.40
		Habitat CR	-0.15	0.11	0.19
		Habitat DS	-0.08	0.12	0.52
		Habitat DW	-0.11	0.16	0.48
		Habitat GR	**-0.15**	**0.07**	**0.03**
		Habitat II	0.33	0.18	0.06
		Habitat LP	-0.06	0.10	0.53
		Habitat MC	0.05	0.08	0.51
		Habitat MM	**0.53**	**0.22**	**0.02**

		Habitat OA	2.00	2.87	0.49
		Habitat PJ	**0.24**	**0.09**	**0.01**
		Habitat PP	0.13	0.08	0.11
		Habitat RI	-0.02	0.08	0.83
		Habitat SA	-0.08	0.07	0.28
		Habitat SF	**0.36**	**0.11**	**<0.01**
		Habitat SH	0.20	0.09	0.04
Brewer's Sparrow	Top model	(Intercept)	1.23	0.02	<0.01
		Variation DHI	0.08	0.02	<0.01
	Detection	Habitat AS	-0.05	0.04	0.26
		Habitat BU	0.00	0.04	0.96
		Habitat CR	0.02	0.05	0.75
		Habitat DS	0.03	0.04	0.47
		Habitat DW	-0.05	0.05	0.32
		Habitat GR	-0.06	0.03	0.04
		Habitat II	0.00	0.06	0.96
		Habitat LP	-0.01	0.04	0.73
		Habitat MC	0.00	0.03	0.91
		Habitat MM	-0.04	0.05	0.40
		Habitat OA	**-0.24**	**0.07**	**<0.01**
		Habitat PJ	-0.05	0.03	0.16
		Habitat PP	**-0.08**	**0.03**	**0.02**
		Habitat RI	0.00	0.03	0.89
		Habitat SA	-0.04	0.03	0.16
		Habitat SF	-0.07	0.04	0.07
		Habitat SH	-0.02	0.03	0.51
		Year	-0.01	0.00	0.03
Chipping Sparrow	Top model	(Intercept)	1.29	0.02	<0.01
		Minimum DHI	-0.07	0.01	<0.01
	Detection	Habitat AS	0.00	0.03	0.94
		Habitat BU	0.05	0.03	0.15
		Habitat CR	-0.02	0.04	0.56
		Habitat DS	0.00	0.04	0.92
		Habitat DW	-0.01	0.05	0.78
		Habitat GR	-0.05	0.02	0.07
		Habitat II	0.05	0.05	0.24
		Habitat LP	0.03	0.03	0.47
		Habitat MC	0.01	0.03	0.70
		Habitat MM	0.00	0.04	0.91
		Habitat OA	0.05	0.04	0.30
		Habitat PJ	0.02	0.03	0.50
		Habitat PP	0.01	0.03	0.64
		Habitat RI	0.00	0.03	0.91
		Habitat SA	-0.04	0.03	0.09

		Habitat SF	0.00	0.03	0.92
		Habitat SH	-0.04	0.03	0.14
		Year	0.01	0.00	0.01
Common Nighthawk	Top model	(Intercept)	-2.14	0.04	0
		Minimum DHI	-0.11	0.03	<0.01
	Detection	**Habitat AS**	**-0.61**	**0.23**	**0.01**
		Habitat BU	-0.40	0.25	0.10
		Habitat CR	**-0.88**	**0.25**	**<0.01**
		Habitat DS	**-0.98**	**0.25**	**<0.01**
		Habitat DW	-0.34	0.35	0.34
		Habitat GR	-0.30	0.21	0.15
		Habitat II	-0.68	0.26	0.01
		Habitat LP	-0.16	0.27	0.57
		Habitat MC	-0.16	0.22	0.47
		Habitat MM	**-0.52**	**0.27**	**0.05**
		Habitat OA	**-0.57**	**0.29**	**0.05**
		Habitat PJ	-0.42	0.22	0.06
		Habitat PP	**-0.43**	**0.21**	**0.05**
		Habitat RI	-0.10	0.24	0.67
		Habitat SA	-0.29	0.21	0.17
		Habitat SF	-0.05	0.27	0.85
		Habitat SH	-0.20	0.23	0.38
House Wren	Top model	(Intercept)	0.50	0.02	<0.01
		Variation DHI	-0.16	0.02	<0.01
	Detection	Habitat AS	-0.04	0.05	0.44
		Habitat BU	-0.01	0.05	0.80
		Habitat CR	**-0.19**	**0.05**	**<0.01**
		Habitat DS	**-0.15**	**0.06**	**0.02**
		Habitat DW	-0.17	0.09	0.07
		Habitat GR	**-0.07**	**0.03**	**0.05**
		Habitat II	-0.14	0.08	0.07
		Habitat LP	**-0.25**	**0.06**	**<0.01**
		Habitat MC	**-0.07**	**0.04**	**0.05**
		Habitat MM	0.00	0.07	0.95
		Habitat OA	-0.03	0.06	0.59
		Habitat PJ	**-0.09**	**0.04**	**0.02**
		Habitat PP	**-0.13**	**0.04**	**<0.01**
		Habitat RI	-0.04	0.04	0.34
		Habitat SA	-0.01	0.03	0.73
		Habitat SF	-0.05	0.04	0.27
		Habitat SH	**-0.12**	**0.04**	**<0.01**
Northern Flicker	Top model	(Intercept)	-1.06	0.03	0
		Cumulative DHI	0.04	0.02	0.02

	Detection	Habitat AS	-0.27	0.54	0.62
		Habitat BU	-0.49	0.52	0.35
		Habitat CR	-0.92	0.50	0.07
		Habitat DS	-0.69	0.52	0.19
		Habitat DW	-0.66	0.57	0.25
		Habitat GR	-0.81	0.48	0.09
		Habitat II	-0.76	0.52	0.14
		Habitat LP	-0.86	0.49	0.08
		Habitat MC	-0.53	0.48	0.28
		Habitat MM	1.26	8.18	0.88
		Habitat OA	0.92	5.35	0.86
		Habitat PJ	-0.23	0.51	0.65
		Habitat PP	-0.81	0.48	0.09
		Habitat RI	-0.57	0.49	0.24
		Habitat SA	-0.88	0.48	0.07
		Habitat SF	-0.52	0.50	0.29
		Habitat SH	-0.73	0.49	0.13
		Year	0.01	0.02	0.52
Yellow Warbler	Top model	(Intercept)	-0.49	0.03	<0.01
		Variation DHI	0.10	0.03	<0.01
	Detection	Habitat AS	-0.14	0.08	0.06
		Habitat BU	0.15	0.09	0.08
		Habitat CR	0.23	0.13	0.08
		Habitat DS	-0.05	0.12	0.71
		Habitat DW	-0.09	0.17	0.60
		Habitat GR	0.07	0.06	0.23
		Habitat II	**-0.23**	**0.11**	**0.03**
		Habitat LP	**-0.25**	**0.07**	**<0.01**
		Habitat MC	0.05	0.06	0.46
		Habitat MM	-0.02	0.11	0.87
		Habitat OA	-0.03	0.14	0.84
		Habitat PJ	-0.03	0.07	0.65
		Habitat PP	0.06	0.07	0.35
		Habitat RI	-0.06	0.07	0.36
		Habitat SA	-0.03	0.06	0.60
		Habitat SF	-0.10	0.07	0.18
		Habitat SH	-0.07	0.07	0.32

Appendix 11: Two-letter code to describe primary habitat at breeding landbird survey point copied from (Blakesley and Timmer 2019).

Two-Letter Code	Habitat Description
AS	Aspen: Overstory dominated by aspen although scattered ponderosa pine or Douglas-fir may be present. The overstory cover should be ≥10% and consist of ≥50% aspen. Aspen stands often have an abundant and diverse shrub layer. Typical shrub species in aspen habitats include snowberry, willow, sagebrush, mountain mahogany, and oak. On occasion there may be no shrub layer. Typically the ground under aspen stands is covered by grasses and forbs.
BU	Burned: Forest habitat where ≥50% of canopy is dead and shows evidence of severe fire scars or where ≥50% of trees have burned and fallen.
CR	Cliff/Rock: Area is dominated by rock and/or generally lacking vegetative cover (e.g., talus slopes, boulder fields, and rocky outcroppings). Areas described as Cliff/Rock should have ≤10% shrub cover and <10% canopy cover. Bare rock should make up ≥20% of the exposed ground cover.
DS	Dry Shrubland: Dry landscape containing shrubs, but lacking a co-dominant grass component. % shrub cover should be ≥10. Shrubs often include sagebrush, greasewood, Fremont mahonia and saltbush. Sagebrush must comprise ≤30% of the shrub composition (see Sage Shrubland). Ground cover layer is typically dominated by bare ground and rock with limited forbs and grasses present. Grass and forbs make up ≤20% of ground cover (see Shrubland).
DW	Habitat consisting of ≥10% canopy cover that is dominated by deciduous species other than Aspen or Oak species. Native deciduous species should comprise ≥50% of the canopy cover and Aspen or Oak spp. must comprise ≤50% of the canopy cover. The 50m radius should not include a permanent or seasonal water source (see Riparian).
GR	Ground cover: Landscape lacking an overstory and significant shrub component. Ground cover is dominated by grasses and perhaps some forbs. Shrub component must be <10% (see Shrubland). The sum of live and dead standing grass must be ≥10%.

II	Forested habitat with ≥10% of the overstory composition dead or sickly - typically referring to pine and spruce bark beetles affecting several species of pine and spruce trees. Canopy cover must be ≥10%.
LP	Lodgepole pine: Habitat consisting of ≥10% canopy cover that is dominated by lodgepole pine. Canopy may have other conifer species or some aspen, but lodgepole pine must comprise ≥50% of the overstory cover. Shrub layer can be conspicuous or nearly absent.
MC	Mixed Conifer: Forested habitat consisting of several species of conifers, such as ponderosa pine, lodgepole pine, Douglas-fir, or spruce/fir spp. If the area is dominated by Douglas-fir, use Mixed Conifer as the primary habitat type. Canopy cover should be ≥10%. Overstory may range from very dense to relatively open. Undergrowth is complex and typically contains deciduous shrubs and/or conifer saplings. Stands with dense overstory may have little or no shrub and ground cover.
MM	Mountain Meadow: Areas with little to no overstory that are surrounded by forests. Elevations should be ≥2,133 m. Soils should be moist to wet with forbs or grass as the dominant ground cover. Canopy cover should be ≤10%. Shrub layer should be ≤10%.
OA	Oak: Habitat dominated by oaks (*Quercus* spp.), often accompanied by juniper, ponderosa pine, pinyon pine, or Chihuahuan Pine. The overstory and shrub cover must sum to ≥10% cover, with oak species making up ≥50% of that cover. In some instances there may be little or no overstory because the Oak species that are present are <3 m high. In southern Arizona this habitat code should be used for Madrean woodlands.
PJ	Pinyon Juniper: Vegetative communities largely influenced by pinyon pine, juniper, or a combination of the two species. The overstory and shrub cover must sum to ≥10%. Semi-arid conditions often produce a relatively short overstory. Juniper tends to dominate at lower elevations while pinyon dominates at higher elevations. Typically, shrub layer includes sagebrush, rabbit brush, oak, or mahogany. Ground cover is usually dominated by grasses with fewer forbs. In some instances there may be little or no overstory because the PJ that is present is <3 m high.
PP	Ponderosa Pine: Areas with ≥5% overstory cover that is made up primarily of ponderosa pine. This habitat often includes other tree types such as fir, pine, and aspen, but ponderosa pine should comprise ≥50% of the overstory layer. Shrub layer relatively open and often includes common juniper, oak, cliffrose, and currants. Ground cover typically dominated by grass species. This code should be used even if there is a significant oak understory.

RI	Riparian: Stands or strips of trees or shrubs near a permanent or seasonal water source. Typical tree and shrub species include cottonwood, box elder, maple, aspen, alder, and willows. Riparian areas are typically discrete habitats, often surrounded by coniferous forest, grassland, shrubland or sagebrush habitat. If riparian habitat is present within the 50-m radius, this should be the primary habitat type.
SA	Sagebrush: Habitat where grasses and shrubs are co-dominant and the shrub cover is ≥10%. Shrub species must consist of ≥30% sagebrush. Typical ground cover is dominated by grasses with limited forbs and bare ground.
SF	Spruce/Fir: Coniferous forest that is dominated by spruce and fir species (typically occurring at elevations ≥2,133 m). Note that Douglas-fir is not a true fir species (see Mixed Conifer). Overstory cover should be ≥10% with spruce and fir species comprising ≥50% of the overstory cover. Variable understory typically includes shrubs and forbs with few grasses.
SH	Shrub: Landscape co-dominated by grass and shrub species. Shrub cover must be ≥10%. Sagebrush must be <30% of shrub layer (see Sage Shrubland). Typical shrub species include ceonothus, manzanita, sage, rabbitbrush, currant, skunkbrush, serviceberry, and plum. Grass and forbs should make up ≥20% of ground cover (see Desert/Semi desert Shrubland).

Appendix 12: Results for goodness-of-fit of the most parsimonious models. The FreemanTukey test statistic and Chi-squared (overdispersion) are reported for the top model for each species. Freeman Tukey test statistics above 0.05 and below 0.95 indicate good model fit, and Chi-squared values below two indicate that there is no overdispersion.

Species	Freeman Tukey	Chi-squared
American Crow	0.51	1.13
Baird's Sparrow	0.45	0.92
Black-billed Magpie	0.48	1.12
Black-capped Chickadee	0.52	1.10
Black-headed Grosbeak	0.11	1.22
Brewer's Sparrow	0.79	0.86
Bullock's Oriole	0.41	1.35
Chipping Sparrow	0.12	0.07
Common Nighthawk	0.35	1.34
Field Sparrow	0.55	1.10
Grasshopper Sparrow	0.75	0.93
House Wren	0.27	1.13
Lark Bunting	0.68	0.92
Loggerhead Shrike	0.55	1.02
Northern Bobwhite	0.60	0.78
Northern Flicker	0.51	1.04
Pinyon Jay	0.52	1.35
Virginia's Warbler	0.48	1.02
Yellow Warbler	0.32	1.19

Appendix 13: The sign of the estimates of the models that included cumulative DHI, minimum DHI, or variation DHI or each species.

Common name	Abbreviation	Cumulative DHI	Minimum DHI	Variation DHI
American Crow	AMCR	-	-	-
Baird's Sparrow	BAIS	-	-	+
Black-billed Magpie	BBMA	-	-	-
Black-capped Chickadee	BCCH	+	-	+
Black-headed Grosbeak	BHGR	+	+	-
Brewer's Sparrow	BRSP	+	-	+
Bullock's Oriole	BUOR	-	-	-
Chipping Sparrow	CHSP	-	-	+
Common Nighthawk	CONI	+	-	+
Field Sparrow	FISP	-	-	+
Grasshopper Sparrow	GRSP	+	-	+
Gray Vireo	GRVI	+	-	+
House Wren	HOWR	+	+	-
Lark Bunting	LARB	+	+	-
Loggerhead Shrike	LOSH	+	+	-
Northern Bobwhite	NOBO	-	+	-
Northern Flicker	NOFL	+	-	+
Pinyon Jay	PIJA	+	+	-
Virginia's Warbler	VIWA	-	-	+
Yellow Warbler	YEWA	+	-	+